Universität Stuttgart

Metal mesh filter systems for small biomass furnaces

A thesis approved by the Faculty of Energy-, Process and Bio-Engineering at the University of Stuttgart to fulfill the requirements for the degree of a Doctor of Engineering Sciences (Dr.-Ing.)

by

Björn Frederik Baumgarten

born in Köln

Main referee:	Univ.-Prof. Dr. techn. Günter Scheffknecht
Co-referee:	Prof. Dr.-Ing Harald Thorwarth

Date of Examination: November 11^{th}, 2022

University of Stuttgart

Institute of Combustion and Power Plant Technology (IFK)

2022

Contents

List of Figures

List of Tables

Nomenclature

Abbrevations

1. BImschV	"Erste Verordnung zur Durchführung des Bundes-Immissionsschutzgesetzes"
COD	chemical oxygen demand
d.b.	dry basis
EA	elemental analysis
IC	ion-exchange chromatography
ICP-OES	inductively coupled plasma optical emission spectroscopy
LHV	lower heating value
P&ID	piping and instrumentation diagram
pH	potential of hydrogen
PID (controller)	proportional–integral–derivative controller
PM	particulate matter
PM2.5	particles that are 2.5 µm or less in diameter
STP	standard conditions, 273.15 K and 1013.2 mbar
VOC	volatile organic content, [mgC/m^3]

Latin letters

a	coefficient
A	filter surface, [m^2]
b	coefficient
c_{dust}	dust concentration in the flue gas [g/m^3]
D	Dust per m^2 filter surface, [g/m^2]
Δp	pressure drop, [Pa]
Q	volumetric flow, [m^3/h]
t	operation time, [min]
t_{max}	maximum operation time, [min]
v	velocity, [m/h]

Kurzfassung

Heizen mit Holz ist eine Möglichkeit, fossile CO_2-Emissionen im Heizsektor zu verringern. Es führt jedoch zu lokalen Emissionen anderer Luftschadstoffe wie Feinstaub. Ein Metallgewebefilter mit wasserbasierter Abreinigung wurde zur Verringerung der Feinstaubemissionen getestet. Es wurden zwei Optionen untersucht: Spülen des Gewebes mit Wasser im Gegenstrom sowie ultraschallunterstützte Reinigung.

Zunächst wurden grundlegende Untersuchungen mit einem manuell betriebenen Prototypen durchgeführt. Der Schwerpunkt der Untersuchungen lag auf den Filterprozessen und dem allgemeinen Verhalten des Metallgewebes. Sekundäre Phänomene wie z. B. Kondensation und Teerbildung, die das Verhalten des Metallgewebes und des Filterkuchens beeinflussen könnten, wurden minimiert. Es wurden Daten zu Regeneration, erreichbarer Staubabscheidung und Standzeit gesammelt.

Auf der Grundlage der Ergebnisse wurde ein automatisierter Prototyp für einen 180-kW-Ofen gebaut, um die Zuverlässigkeit der Regeneration über einen längeren Zeitraum zu demonstrieren und das gesamte System unter realistischen Bedingungen, einschließlich Kondensationsprozessen, zu untersuchen. Die Feuerung wurde sowohl mit konstanter Leistungsabgabe als auch unter Verwendung eines modulierenden Lastprofils mit Zündungen, Stopps und Laständerungen betrieben, was zu Kondensation und Teeremissionen führte.

Es konnte gezeigt werden, dass die Filtration in zwei Stufen abläuft: Zunächst findet eine Oberflächenabscheidung auf dem Gewebe statt, und anschließend eine Tiefenfiltration im Filterkuchen. Der Abscheidegrad lag während der Oberflächenabscheidung unter 50 %, stieg aber während der Tiefenfiltration nach Bildung eines Filterkuchens auf über 95 % an. Der Druckverlust (Δp) des Filters kann mit einer Exponentialfunktion dargestellt werden:

$$\Delta p = a v D^b$$

Δp = Druckverlust [Pa]
a = Faktor, ca. zwischen 12 und 18
v = Gasgeschwindigkeit [m/h]
b = Faktor, ca. zwischen 0,4 und 0,45
D = Staubbeladung [g/m²]

Die Faktoren werden von der Feuerung, der Ausbrandqualität und der Brennstoffqualität bestimmt.
Beide Regenerationsmodi waren erfolgreich, und es konnte gezeigt werden, dass sowohl die Abscheideleistung als auch die Standzeit (bevor eine Regeneration erforderlich war) von der Wahl des Brennstoffs und der Gasgeschwindigkeit abhängen, ohne dass es Anzeichen für eine Verringerung der Standzeit aufgrund von Rückständen oder Teerbildung gab. Bei einer Gasgeschwindigkeit von 33,3 m/h wurde eine Abscheideleistung von bis zu $91 \pm 1\%$ und eine Standzeit von 55 h (Pellets) bzw. 38 h (Hackschnitzel) gemessen. Bei 66,6 m/h sank der Abscheidegrad auf $74 \pm 4\%$ und 12 (Pellets) bzw. 3,4 h (Hackschnitzel) Standzeit.

Der Langzeitbetrieb des automatisierten Prototyps war erfolgreich. Der Filter wurde 419,5 h mit 234 Regenerationen betrieben. Bei Vermeidung einer Partikelanreicherung im Regenerationswasser wurden keine Anzeichen einer unzureichenden Reinigung festgestellt. Des Weiteren führten Kondensation und Teeremissionen zu keinen Problemen bei der Abreinigung. Es konnten keine Unterschiede zwischen den verschiedenen Regenerationsmethoden festgestellt werden. Allerdings ist ein Unteraschallschwinger kostspielig, weshalb die Gegenstromabreinigung vorzuziehen ist.

Über eine gesamte Filtration (einschließlich beider Phasen) konnte ein Abscheidegrad zwischen 80 und 86% erreicht werden.

Zusätzlich wurden die Abfallprodukte, der unlösliche feste Rückstand und das mit dem löslichen Anteil der Partikel beladene Regenerations-

wasser, bewertet. Die im Holz enthaltenen Schwermetalle bildeten bei der Verbrennung überwiegend unlösliche Verbindungen, die zusammen mit anderen wertvollen Metallen in hohen Konzentrationen in der Feststofffraktion verblieben. Bei einem großflächigen Einsatz des Filters sollte die Nutzung der Flugasche im Rahmen von Urban Mining in Betracht gezogen werden. Die flüssige Fraktion kann über das kommunale Abwassersystem entsorgt werden.

Zusammenfassend lässt sich sagen, dass Metallgewebefilter mit Nassregenerierung eine erfolgsversprechende Option darstellen. Der Hauptvorteil gegenüber den derzeitigen Technologien besteht darin, dass die Emissionen während des gesamten Feuerungsbetriebs gefiltert werden können, einschließlich der Zündung und während Laständerungen, wodurch eine 100-prozentige Verfügbarkeit des Filters erreichbar ist.

Abstract

Wood combustion is a way to reduce fossil CO_2 emissions from the heating sector. However, it results in the local emission of other air pollutants such as particulate matter. A metal mesh filter with wet regeneration was tested as a novel option to reduce particulate matter emissions. Two different options were considered: Counter-current flushing of the mesh with water, and ultrasound-assisted cleaning.

First, fundamental research was performed using a manually operated prototype. The main focus of the investigations were the filtering processes and the general behavior of the metal mesh. Secondary phenomena which could influence the behavior of the metal mesh and the filter cake, like condensation and tar generation, were minimized, and data regarding regeneration, potential collection efficiency, and operation time were collected.

Based on this research, an automatic prototype for a 180 kW furnace was built, to demonstrate long-time feasibility and to evaluate the entire system under realistic conditions, including condensation processes. The system's furnace was operated both at stable conditions and using a modulating load profile including ignitions, stops, and changes of load, causing condensation and tar emissions.

During the fundamental research, it could be shown that filtration underwent two stages: First surface separation on the mesh and second depth-filtration in the filter cake. The collection efficiency was below 50% during surface separation, but increased to more than 95% during depth- filtration after a filter cake was formed. The pressure drop (Δp) during the filtration is following an exponential function:

$$\Delta p = a v D^b$$

Δp = Pressure drop [Pa]
a = Coefficient (approx. between 12 and 18)
v = Gas velocity [m/h]
b = Coefficient (approx. between .4 and .45)
D = Dust per m² filter surface [g/m²]

The coefficients depend on the furnace, the quality of the burnout, and the quality of the fuel.

Both regeneration modes were successful, and it could be shown that collection efficiency and operation time (before a regeneration was required) depend on fuel choice and gas velocity, without any signs of decay due to residues or tarring. At a gas velocity of 33.3 m/h, up to 91 ± 1% collection efficiency and 55 h (pellets) or 38 h (wood chips) operation time was measured. At 66.6 m/h, the collection efficiency decreased to 74 ± 4% and 12 h (pellets) / 3.4 h (wood chips) operation time.

Long-time operation of the automatic prototype was successful. The filter was operated for 419.5 h, and 234 regenerations were performed without signs of insufficient cleaning as long as particle enrichment in the regeneration water was avoided. No differences between the different regeneration methods could be observed. Ultrasound cleaning requires an expensive ultrasound generator, thus, counter-current flushing is favorable.

Over an entire filtration (including both phases), a collection efficiency between 80 and 86% could be reached.

Additionally, the waste products, insoluble solid residue and regeneration water loaded with the soluble part of particulate matter, were evaluated. Heavy metals found in wood formed mostly insoluble compounds during combustion, which remained in the solid fraction along with other valuable metals in high concentrations. If the filter would be used on a large scale, the use of the solid fraction for urban mining should be considered. The liquid fraction can be disposed of using the communal wastewater system.

In conclusion, metal mesh filters with wet regeneration are a viable option. The main advantage over current technologies is the ability to filter the emissions during all times of furnace operation, including ignition and while modulating load, enabling a 100% filter availability.

Acknowledgements

Throughout the writing of this dissertation I received a great deal of support and assistance.

First of all, I want to thank my supervisor, Harald Thorwarth, for the opportunity to work on this project, for the valuable scientific and personal input, and his patience while writing the Phd thesis.

Of major importance were the other members of the project consortium my research was part of. Günter Scheffknecht, my supervisor at the University of Stuttgart, deserves a special mentioning. Also, Günter Baumbach, together with whom I held my first presentation at a conference. Also, without the LK Metallwaren GmbH who built the prototypes, this work would not have been possible.

I would like to acknowledge the staff of the lab for their support and help. Especially Peter, who integrated the set-ups and had to deal with my impatience. Carola, who programmed the data acquisition software

and helped with various tasks in the lab. Rainer and Julian for the introduction into ICP-OES analysis and other lab analysis.

Another notable help were the students of the HFR, probably most important of all my bachelor student, Philip, and also all the Hiwis helping out in the workshop and the lab.

Also, I want to thank the other researchers and employees of the HFR for the many enjoyable hours not only during work but also at the events, barbecues etc. outside of working hours.

In addition, I would like to thank my parents for their help, for motivating me, and also for always reading my papers and this thesis first.

Chapter 1

Introduction

Today, energy generation is in a transition phase.

Since industrialization, the majority of energy produced worldwide is generated by burning fossil fuels. While they were – for a long time – cheap and readily available, they come with major drawbacks which were first unknown and then ignored.

During the burning of fossil fuels, the carbon bound in the fuel is liberated as CO_2, which is a greenhouse gas and leads to increasing global temperatures. The first world climate conference already took place in 1979 discussing this matter on a global stage for the first time, but the first stringent action – implementing the Kyoto protocol – wasn't

taken until 1997 [1].

In the following years, awareness for climate change increased – but the necessary measures were also discussed very controversial. Still, in Europe, there is a wide consensus that climate change is real and actions should be taken [2]. In order to reduce fossil CO_2 emissions, the EU introduced a framework, based on which the individual member states created their own laws, aiming to reduce fossil CO_2 emissions. One of the most important EU-wide laws is the Renewable Energy Directive 2009/28/EC, (RED) [3]. Two goals were formulated: 20% of gross final energy consumption and 10% of the energy consumed in the transport sector should be generated from renewable sources.

Based on the RED, the member states formulated national renewable energy action plans. One major pillar to reach the goals of RED is the usage of biomass [4]: In average, 11.7% of the gross final consumption should be generated from biomass, of which 67% are generated by solid biomass [5]. However, burning biomass generates local emissions of VOC, NO_x and particulate matter. Thus, on a local stage, the use of biomass can be problematic and lead to unpleasant smog [6].

These two sides of biomass burning lead to public discussions and are also reflected in the legislative rules.

In the following, the applicable legislative rules will be discussed, as

well as the causes of the emissions and possible technologies to reduce emissions. Last, the motivation for the research done will be discussed.

1.1. Legislative background

In Germany, a variety of laws exist that both favor wood furnaces over furnaces powered by fossil fuels, but also strictly limit emissions.

The main law is the "Gebäudeenergiegesetz" (GEG), which limits how much energy might be required for heating. The limits can either be met by implementing better insulation, or by use of a less CO_2 intensive heating [7]. In addition, a new tax on CO_2 emissions was introduced which further favors the use of wood for heating [8].

On the other hand, there are various laws limiting the emissions of local pollutants. The current limits for small-scale heating furnaces are defined in the 1. BImSchV [9].

The 1. BImSchV has two stages with increasingly strict limits: The first stage applies to furnaces built between March 22, 2010 and December 31, 2014. The second stage applies to furnaces built from 2015. Older furnaces are not regulated by this legislation. The limits depending on the fuel are listed in Table 1.1.

A second instrument used by the German government is subsidies.

Table 1.1.: Emission limits according to 1. BImSchV [9], simplified

Stage	Fuel	Thermal Output $[kW]$	Dust $[g/m^3]$	CO $[g/m^3]$
Stage 1: 22/3/2010 - 31/12/2014	Coal, Peat	4 - 500	0.09	1.0
		> 500	0.09	0.5
	Natural Logs, Wood chips, Wood dust	4 - 500	0.10	1.0
		> 500	0.10	0.5
	Wood briquettes, Pellets	4 - 500	0.06	0.8
		> 500	0.06	0.5
	Waste wood	4 - 100	0.10	0.8
		100 - 500	0.10	0.5
		> 500	0.10	0.3
	Straw, misc	4 - 100	0.10	1.0
Stage 2: 1/1/2015 - today	Coal, Peat, Natural Logs, Wood chips, Wood dust Wood briquettes, Pellets	> 4	0.02	0.4
	Waste wood	30 - 500	0.02	0.4
		> 500	0.02	0.3
	Straw, misc	4 - 100	0.02	0.4

Amount and conditions of the subsidies are specified in the "Bundesförderung für effiziente Gebäude" (BEG) [10, 11]. Different to the 1. BImschV, subsidies are only granted if dust emissions are below 0.015 g/m³. An additional bonus is granted if dust emissions are below 0.0025 g/m³. The basic subsidy is 35%, but using all boni up to 55% can be granted. Thus, the installation of new furnaces with dust emissions higher than 0.015 g/m³ is unlikely, and the subsidies serve as an additional way to limit emissions of new furnaces.

1.2. Technology overview

Burning wood is the oldest technology to generate heat, and is gaining new importance in order to reduce the CO_2 footprint. Modern stoves and furnaces are very different compared to the first fireplaces, and, in general, are able to generate heat in a controlled and safe way, generating much less emissions than their predecessors. However, there still is a major disadvantage: Compared to oil and especially gas furnaces, they generate much more local pollution [12].

On a worldwide scale, the most important pollutant are greenhouse gases, which increase the average temperature around the globe, and lead to an increase of extreme weather incidents [13]. On a local scale, however, other pollutants play a very important role as well. In regards to burning wood, the most important pollutants are particulate matter (fine dust), NO_x, and volatile organic compounds (VOC) [14]. These are emitted in relatively high amounts, which lead to legislative actions (by introducing lower legal limits) and also a negative public opinion on biomass furnaces.

Thus, if wood energy is supposed to play a vital role in reducing greenhouse gas emissions, emissions of local pollutants have to be reduced to an absolute minimum, while still maintaining competitive costs.

1.2.1. Combustion Process

The combustion of biomass is rather complex, as the feedstock is inhomogenous and consists of many different compounds and polymers.

The combustion of solid biomass can be split into two independent processes: The conversion of solid biomass to gases, and the burn-out of the generated gases.

The conversion of solid biomass to gases can be differentiated into three phases as shown in Table 1.2.

Table 1.2.: Conversion of solid biomass

Phase	Temperature	Main products
Drying	< 100 °C	Water vapour, dried solid biomass
Devolatilization	100 - 600 °C	Tar, combustible gases, H_2O, CO_2, Char
Char conversion	> 600 °C	CO_2, CO, Ash

based on [15, 16]

These phases do not occur one after one, but instead, due to the thermal thickness (the particles can be colder inside than outside) of the fuel particles, occur simultaneously [15]. This makes the process increasingly complex.

During drying, unbound water is evaporated first. Next, water bound to cellulose and hemicellulose (as OH^- groups) is evaporated. This step causes shrinkage and cracking. The process is endothermic, thus it slows down the heating process [15].

As the next step, devolatilization or pyrolysis occurs. Devolatilization occurs under slightly oxidizing, while pyrolysis occurs under slightly reducing conditions. However, both may occur in a biomass furnace, so a definite separation is hard.

The volatile parts of biomass are converted into gases. The composition of the gas created depends on the exact composition of the feedstock, the available oxygen, the temperature, and the heating rate. CO, CO_2, CH_4, H_2, light hydrocarbons and tars as well as nitrogenous compounds are generated. Tars and light hydrocarbons react further to other light gases or repolymerize to char depending on the conditions, while the non-volatile compounds form char and ash [15, 17, 18, 19].

As last step, the residual char is converted to CO and CO_2 and small amounts of H_2 and CH_4 during char conversion [15].

After the conversion from solid fuel to gases, the remaining gases are burnt to CO_2 and H_2O in gas phase reactions. Here, sufficient residence time, good mixing and a high temperature is essential to ensure full burnout to avoid the generation of unwanted toxic products [20].

During the combustion process, also a number of unwanted byproducts are created. NO_x is generated mostly from nitrogen bound inside the fuel and liberated during the devolatilization phase, e.g. as HCN. HCN can react further to form NO_x, or get reduced to N_2 [21].

A possible way to reduce the amount of NO_x is air staging: Air is provided in two (or more) stages, the first one being the bed where typically 80% of the stoichiometrically required air is added. Thus, a reducing zone is generated, where a part of the NO_x and its precursors

like HCN are reduced to N_2 [22].

Other byproducts are VOC (volatile organic compounds) and CO. They are formed by incomplete combustion. Incomplete combustion used to be a larger problem in older furnaces, as is shown in Johansen et al [23]. These emissions are nearly eliminated in modern automatic furnaces, and significantly lower in modern stoves compared to older models [24, 25, 26].

1.2.2. Causes of dust generation

One of the pollutants generated by wood furnaces is fine dust. Given its size, it will stay in the atmosphere for a long time before it settles. Still, it is a local pollutant, which will negatively influence the surroundings of a fireplace.

Fine dust is known to cause cancer as well as cardiovascular and respiratory diseases [27, 28]. However, the toxicity is significantly influenced by the composition as shown by Arif et al [29]. Higher content of hydrocarbons, especially tars, lead to increased toxicity, while other compounds like KCl have a low impact.

Basically, two kinds of dust have to be differentiated: Organic dust caused by incomplete combustion, and inorganic dust caused by trace elements of the wood. The first has a considerably higher impact on health and is thus most important to limit [29].

As mentioned in the previous section, incomplete combustion was already reduced drastically, so particles from incomplete combustion are less important.

Inorganic dust stems from trace elements vital for the biomass to grow like potassium, sodium, and zinc as well as chloride and sulfate. These elements are therefore called aerosol-forming elements. Their distribution is not uniform in all parts of the plants, in the bark as well as in thin branches the concentration is higher then in the stem wood [30].

The release of inorganic dust is quite complex: The aerosol-forming elements are liberated from the biomass during combustion. Their main constituent is potassium. Potassium compounds have a low vapour pressure at the temperatures reached during pyrolysis, thus the main release occurs during the char conversion stage [16]. The composition of the potassium gases changes during their passage through the furnace. The majority of the potassium is liberated as KCl or KOH, but while cooling down, the composition changes to KCl and K_2SO_4 [31]. During cooldown, the different compounds start to precipitate. Normally, the compounds precipitated first are Zn-compounds, followed by Na and K. The compounds can either form new particles (Nucleation), or precipitate on existing surfaces. Thus, many particles have a core of Zn, coated in potassium and sodium [32]. The freshly emitted particles have sizes around 50 nm during complete combustion conditions, but during incomplete combustion, the particle size increases to 100 nm and more [32].

There is a strong correlation between the content of aerosol-forming elements and dust emissions [33, 34, 35, 36]. As a useful simplification, the correlation between aerosol-forming elements and dust emissions is linear. Pollex et al. postulated a critical potassium content of 500 - 600 mg/kg (dry basis) in order to comply with the German legal limit for small biomass furnaces [37].

1.2.3. Pollution Control: State of the Art

Primary measures

In the past, one of the major sources of dust was incomplete combustion. Due to the introduction of air staging and Computational Fluid Dynamics (CFD)-aided design of secondary burnout zones, these could be minimized [38, 39]. Especially for automatic furnaces, dust from incomplete combustion can nearly be neglected during stable operation [40].

In contrast, during start-up and stop of the furnaces, incomplete combustion is still a major issue and can add considerably to dust emissions [41].

Currently, the research focuses on the reduction of inorganic dust.

One solution is to limit the amount of aerosol-forming elements in the fuel. As most of the elements can be found in the bark and thin

branches, this means combusting stem wood. However, stem wood is much more expensive, thus, this is not an option for larger furnaces. Still, for small furnaces, it is a viable option. The European standard for pellets (Norm DIN EN ISO 17225-1:2021)[42] sets strict limits on the amount of ash, which are only possible to fulfill using high-quality wood – or sawdust from sawmills and carpenters. As a result, in January 2021, the price for pellets was 236 €/t, while wood chips were considerably cheaper with prices between 79 and 123 €/t [43].

A different option is to limit the release of aerosol-forming elements. There are two different approaches to achieve this: The addition of additives that bind the aerosol-forming elements into the ash, or reduction of the firebed temperature in order to reduce evaporation.

There already was extensive research on additives, and theoretically, it is possible to reduce the amount of dust released drastically. The most common additive is Kaolin, but in theory, there are four different possible groups: Aluminium-silicates-based additives, calcium-based additives, phosphorus-based additives, and other additives [44].

Aluminium-silicate-based additives form potassium aluminium silicates, which are stable at high temperatures and thus bind potassium in the fuel bed [45, 46]. The other groups also bind potassium, but the resulting stable compounds are different: Calcium-based additives form calcium potassium phosphates if a surplus of potassium and phosphate is present in the fuel [47, 48], while phosphate additives form

calcium potassium phosphates if a surplus of potassium and calcium is present [49]. However, there are also notable drawbacks to additive addition: First, it requires additional processing of the fuel, which increases fuel costs. Second, the amount of ash is increased, which might cause problems with the ash removal system of common furnaces. Third, the current pellet standards do not allow additives, as that would increase the ash content [42].

Instead of binding potassium in more stable compounds, cooling of the firebed can also reduce evaporation of the aerosol-forming elements. In some, typically larger, furnaces, grate cooling is already employed but the main reason is to reduce thermal stress of the grate. In small scale, there were two test beds:

Gehrig et al. [50, 51, 52] added a water cooling loop to the burner of a conventional pellet furnace, which resulted in slightly lower firebed temperatures and reduced dust emissions.

Perez-Orozco [53] designed an experimental furnace with cooling of both the bed and the burnout chamber. While their design reduced dust emissions to a large extent, the burnout chamber cooling resulted in incomplete burnout and extensive build-up of tar on the cooled walls.

Secondary measures

Currently, plants with a thermal output in excess of 1 MW already use extensive secondary measures. However, these are still uncommon for smaller furnaces with outputs between 50 kW and 1 MW. In this

range, the usage of high-quality fuel (pellets) is normally too expensive, so they are fueled with wood chips. On the other hand, the investments required for secondary measures are too high.

One exception is the use of cyclones, which are already in use, but only remove coarse particles with an aerodynamic diameter above 10 µm [54].

For removing particulate matter with a diameter below 10 µm, the use of electrostatic precipitators or filtering separators is required.

Electrostatic precipitators are already commercially available [55], and can remove 70 – 80% of the fine dust [56]. However, they come with one important drawback: They can only be operated if the exhaust gas temperature is high enough to avoid dew. Thus, the availability of the electrostatic precipitators depends on the amount of ignitions and on the modulation of the furnace [57].

Filtering separators are also available [58]. One commercial solution consists of ceramic filter candles which (according to the producer) guarantee very low dust concentrations below 3 mg/m^3. A second manufacturer offers fabric filters. On the downside, like electrostatic precipitators they can only be operated at high exhaust temperatures or risk being irrecoverably plugged by tars.

In theory, fabric filters can yield the highest separation efficiencies with over 99%. However, fabric filters as used in large-scale plants combined with jet-pulse cleaning cannot be used due to sparks in the

exhaust gas [54]. As an alternative filter medium, stainless steel meshes can be used. For example, Hartmann et al. [59] used a stainless steel mesh with a jet-pulse cleaning facility for a grain combustion furnace. The collection efficiency was very high with 95-99%, but the removal of the filter cake was only partial using jet-pulses.

Still, a similar solution was commercially available but taken off the market. It required electrical preheating [60], which resulted in very high operational costs. Also, like electrostatic precipitators and ceramic filters, it was impossible to use during start-up. Schiller und Schmid [61] improved cleaning and collection efficiency by adding a precoat to their filter.

Brandelet et al. [62] optimized the temperature required before fabric filters (or mesh filters) can be operated, but the issue remains.

In research are filters that incorporate SCR abatement by adding SCR catalysts to the filter, but these also require sufficient temperatures before they can be used [63].

A different concept was tried by Struschka and Goy [64]: Instead of a jet-pulse cleaning facility, brushes were used to remove the filter cake mechanically. Jet-Pulse cleaning is a relatively simple technology, but it comes with a relevant draw-back: The cleaning pulses are loud, and pressurized air is required whose compressors are also noisy. In household appliances, this can be a problem. The mechanical cleaning was supposed to avoid this problem, but the cleaning was not sufficient.

A second project based on the work by Struschka and Goy was started in 2018, of which the presented research is part of. The project name was "Entwicklung eines kompakten und kostengünstigen Gewebefilters für Biomassekessel – Stufe 2", funded by the Fachagentur für Nachwachsende Rohstoffe, grant number 22019417. The project was a collaborative project of the University of Stuttgart (Fabian Schott, Günter Baumbach, Ulrich Vogt), LK Metallwaren GmbH (Oskar Winkel, Ferdinand Ehard), and the University of Applied Forest Sciences Rottenburg (Björn Baumgarten, Harald Thorwarth). The research part of this thesis was conducted at the University of Applied Forest Sciences Rottenburg.

The aim of the project was to examine different regeneration methods for metal mesh filters with small prototypes able to filter approximately 50 m^3/h flue gas, and a subsequent up-scaling of the more promising option to an automatic prototype for a 180 kW furnace.

The University of Stuttgart tested a metal mesh filter with jet-pulse cleaning, while the University of Applied Forest Sciences Rottenburg tested a water-based regeneration method. The project report is online [65].

The University of Stuttgart could provide insight into the filtering characteristics of a metal mesh with pulse cleaning. In the main filtering phase, the collection efficiency was very high, but during the cleaning pulses, a notable amount of dust passed the filter, and peaks in the dust concentration of the filtered gas could be measured. In addition, it could

be shown that the collection efficiency depends on the fuel and on the pore size of the metal mesh: Using wood pellets, a maximum collection efficiency of 91.3% was reached with 25 µm mesh, 71.6% with 50 µm and 20.7% with 135 µm. With wood chips, 96.4% was reached with 25 µm and 75.4 % with 50 µm [65].

At the University of Applied Forest Sciences Rottenburg, two different regeneration methods were tested: Counter-current flushing of the metal mesh with water, which is to some extent similar to cleaning pulses, but with a different medium. Water is incompressible and has a higher viscosity than air, thus, the force applied to the filter cake is more uniform and also lasts a longer time. The second method was ultra-sound cleaning where the filter cake was removed with the aid of ultrasound. In addition to the mechanical removal, a part of the filter cake is soluble and is dissolved in the cleaning water, facilitating the cleaning.

The results of the University of Applied Forest Sciences Rottenburg, which are presented here, were also published in two research papers [66, 67], which are included in the Appendix. The first publication [66] discusses the research presented in Chapter 3, while the second [67] discusses the research discussed in Chapter 4. The CRedIT author statement of the second publication is valid for both publications: The majority of the work was done by myself, especially the scientific experiments, their design, the evaluation of the experiments, and the writing. LK Metall-

waren GmbH (Ferdinand Ehard) provided the prototypes, while Peter Grammer integrated them into the infrastructure of the Hochschule of Rottenburg and was responsible for the infrastructure of the Hochschule. The design of the filter was done by Oskar Winkel, Günter Baumbach, Ulrich Vogt, Ferdinand Ehard, Harald Thorwarth, and me. The original grant was written by Michael Struschka and Harald Thorwarth. Ulrich Vogt was the overall project leader, while Harald Thorwarth was the responsible for the part at the Hochschule of Rottenburg. Günter Scheffknecht and Harald Thorwarth were my supervisors, and helped with the review and editing of the publications.

1.3. Motivation for the research

As described in the previous Section 1.2.3, the current secondary measurements have a number of issues. Most importantly, they cannot be used when the exhaust gas temperature is below the dew point and condensation might occur. On the other hand, these are also the phases when emissions are highest. Thus, a metal mesh filter with a new regeneration method - using water, by counter-current flushing with or without the aid of ultrasound cleaning, was developed and tested.

The main compounds of ash – chloride and sulfate salts of potassium, sodium and zinc – are soluble in water, which was expected to facilitate the cleaning process. Ultrasound is already in use for many cleaning applications, and is known to be very effective for the removal of small particles [68]. Ultrasound causes cavitation, which results in jets directed

at the surface of objects inside the ultrasonic bath. These mechanically remove particles [69].

Chapter 2

Research Objectives

As discussed in Chapter 1, there are two commercial options to limit particulate matter emissions of furnaces: The use of high quality fuel, or the use of secondary measurements. In this work, a secondary measurement was focused on: A metal mesh filter with an innovative, water-based regeneration method.

There were earlier attempts to use metal mesh filters for biomass furnaces, however, not much theoretical data were published. Approximate gas velocities were stated, but no scientific examination of the influence of the gas velocity was performed and published before. Water-based regeneration was not attempted before, thus no data was available.

As a result, this work was split into two parts:

- Filtering characteristics of a metal mesh
- Evaluation of a filter prototype

In the first part, the main focus is the behaviour of the metal mesh during filtration.

For that, all phenomena which could potentially influence the filtering behaviour of the metal mesh were minimized. Thus, the furnace providing the flue gas for the filter was operated at steady state, and the filter was preheated to avoid condensation. The collection efficiency and the operation time was measured in dependence of the gas velocity and the used fuel, and the necessary parameters to design a larger prototype were determined. Also, the influence of different cleaning mechanisms was tested. As last step, a concept for design and operation of an automated prototype was derived from the knowledge gained.

During evaluation of the filter prototype, a prototype as close as possible to a commercial version was built for a 180 kW furnace, which was operated under realistic conditions with a modulating load cycle.

The main topic is the long-time operation and reliability of the filter under realistic operation conditions. Also phenomena like condensation or unstable flue gas composition including the emission of volatile organic compounds were not excluded.

In addition, different possibilities to reduce costs were tested. This includes the pore size of the metal mesh used, the necessity of ultrasound-

assisted cleaning and prefiltration by a cyclone.

Another important topic were the residues: During operation, the dust is partly dissolved in the regeneration water. Thus, there are two waste products: Regeneration water and solid, insoluble particles. Both were examined and options for disposal were evaluated.

Chapter 3

Filtering characteristics of a metal mesh

The aim of the first part of the work was to prove the general feasibility of a metal mesh for filtering particulate matter from a biomass furnace. Also, the influence of the gas velocity and the type of fuel (high-quality pellets compared to low-quality wood chips) should be examinated. Additionally, the influence of different cleaning mechanisms - ultrasound-assisted cleaning and counter-current cleaning - should be tested.

For this, a manually operated filter prototype was built. As emission source, a furnace able to burn both high-quality pellets and wood chips was used. This way, operation under optimal conditions, with a good burnout quality, low concentrations of dust, and no volatile organic compounds (which could condensate on the filter) in the raw gas and under more challenging conditions with high dust concentrations and volatile organic compounds could be simulated.

To gain further insight, the design of the filter enabled inspection of the metal mesh filter and sampling of the filter cake between each test and regeneration. In general, the regeneration and operation were performed manually, only the control of the gas velocity and the shutdown of the filter upon reaching maximum pressure drop was automated to ensure reproducible test results. The gas velocity is the speed of the gas through the filter surface, and equals the filter surface load:

$$v\,[m/h] = \frac{Q\,[m^3/h]}{A\,[m^2]} \tag{3.1}$$

v = Gas Velocity

Q = Volumetric Flow

A = Filter Surface

Q/A = Surface Load

To achieve the research objectives at this stage, 16 test runs as described in Table 3.1 were evaluated.

Table 3.1.: Experimental runs of the manual prototype

Gas velocity [m/h]	Measurements	Cleaning mode	Fuel
66.6	3	Ultrasound	Pellets
50	3	Ultrasound	Pellets
33.3	1	Ultrasound	Pellets
66.6	3	Counter-current flushing	Wood Chips
50	3	Counter-current flushing	Wood Chips
33.3	3	Counter-current flushing	Wood Chips

3.1. Methods and Materials

Testing of the cleaning concept was performed using a small-scale prototype with manual operation, integrated into a laboratory setup with gas composition and dust concentration measurement before and after filtering.

3.1.1. Filter prototype

The prototype was designed by the project consortium and constructed by LK Metallwaren GmbH.

The design of the filter is shown in Figure 3.1. 15 filter candles surround an ultrasonic transducer in two rings. The filter candles have a surface of 0.08 m^2 each, totaling to 1.2 m^2, and are made of a metal mesh from stainless steel (1.4404) with a mesh size of 25 µm.

As ultrasound transducer, a rod transducer (SONOPUSH MONO SPM 1500 25-495 VA, Weber Ultrasonics) with a power of 1500 W was used.

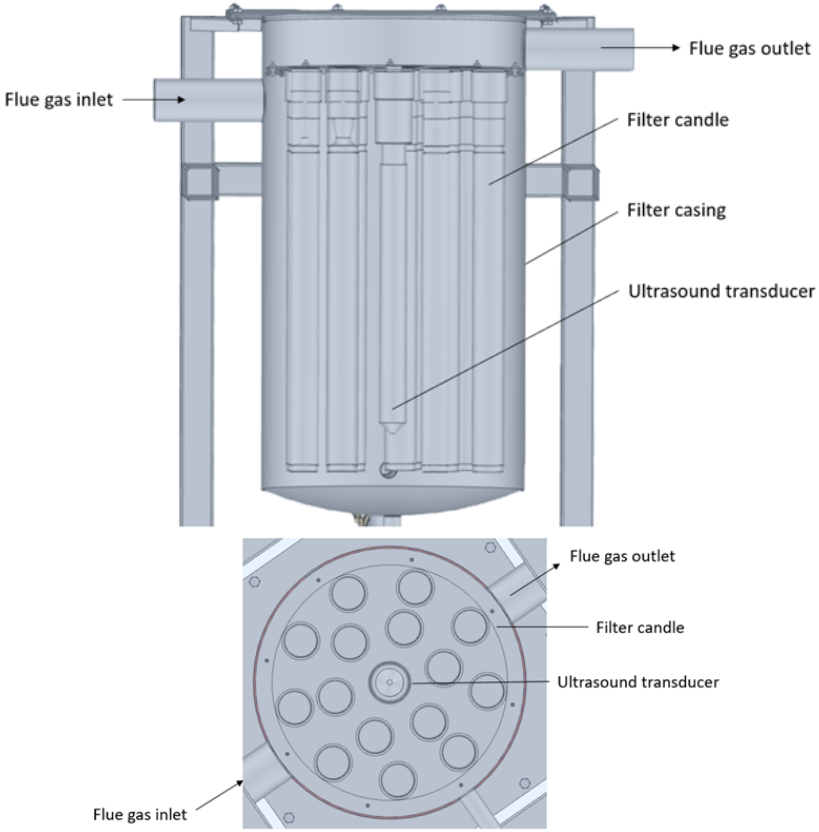

Figure 3.1.: Construction of the manual prototype.

To avoid condensation, the filter was equipped with an 800 W barrel heater (Freek, custom build).

During operation, the flue gas entered the filter using the flue gas inlet on the left, entered the casing, and was filtered while flowing from the outside to the inside of the filter candles, producing a filter cake on the outside of the candles. The filtered gas then left the filter via the flue gas outlet.

Before cleaning, the filter candles were inspected and a sample of the filter cake was taken for chemical analysis by removing the top plate and lifting the filter candles out of the filter casing.

There were two possible modes of cleaning:

For ultrasound cleaning, the filter casing was filled with water, and ultrasound was applied for 15 min.

For counter-current cleaning, the top plate was removed, and the candles were flushed manually using a water hose. That way, the water flowed from the inside of the filter candles to the outside and removed the filter cake on the outside of the filter elements.

3.1.2. Experimental setup

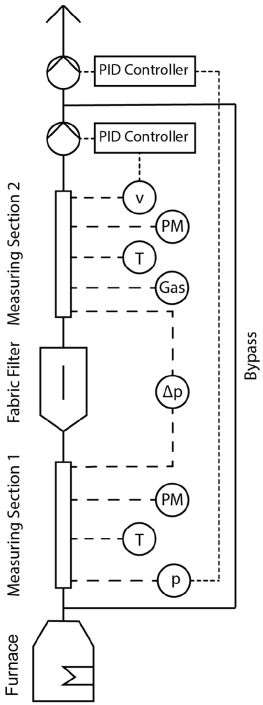

Figure 3.2.: Experimental set-up manual prototype

The filter was integrated into an experimental setup according to DIN SPEC 33999 [70]. The P&ID diagram is shown in Figure 3.2.

A commercial moving grate boiler (KWB Multifire II) was chosen which can combust both pellets and wood chips. The thermal output of the boiler was 50 kW. Given the scale of the filter, the furnace was operated at 50% load. With this setting about 100 m^3/h flue gas with an oxygen concentration of 9.5% was produced.

Using a side channel blower (Airtech ASC0080-1MT400-6), a partial stream of the flue gas was sucked through the filter. The remaining flue gas bypassed the filter using an open bypass to ensure nominal conditions for the furnace. The relative pressure behind the furnace was regulated using a blower and set to −12 Pa.

Up- and downstream of the filter, a measuring section was added. An overview of the used instruments is given in Table 3.2. The measuring

sections were designed in accordance to DIN SPEC 33999 [70] and VDI 2066 [71].

Particulate matter concentration, temperature, gas composition, and differential pressure over the filter were measured. The downstream measuring section also contained a calorimetric flow meter (SEIKOM RLSW8AL) to control the side channel blower.

The barrel heater was controlled with a Pt100 thermoelement inside of the filter housing. Process control and data logging were performed using two ADIT Profimessage modules (Delphin).

3.1.3. Gaseous analysis

PM measurement was performed under isokinetic conditions according to VDI 2066 [71] before and after the filter.

Plane quartz fiber filters (47 mm diameter, Munktell MG 160) were used on both sides, while an additional pre-filtration with plugged glass wool (extra-fine, Karl Hech GmbH & Co KG) was performed before the filter if the measurement time exceeded 1 hour to avoid overloading of the plane fiber filters. The gas volume of the measured gas was determined after cooling to room temperature and drying of the gas with a gas meter.

Before the measurement, the PM filters and glass wool were pretreated at 200°C for one hour before the measurement and at 180 °C before weighting. They were cooled down overnight using a desiccator and weighted in a climate-controlled room with a laboratory scale (Sartorius

CPA 124S, readability 0.1 mg).

The gaseous flue gas composition was logged continuously using an ABB modular measuring solution downstream of the filter. As described in table Table 3.2, the modular measuring tower measured CO, NO, CO_2, SO_2, O_2 and VOC (volatile organic compounds). The position was chosen in order to monitor the tightness of the setup, however, VOC measurements might be influenced by the low temperatures in the duct and the filter, especially during the start and the stop of the filter. Before measurement, the flue gas sample passed through a condenser (ABB), thus, the gas concentrations are for dry gas.

All values were corrected to standard temperature and pressure (STP, 273.15 K and 1013.2 mbar).

Table 3.2.: Measuring Equipment for the manual prototype

Parameter	Measuring principle	Instrument	Measuring range	Unit
Total dust	Gravimetry	Plane Filter plugged glass wool	20 (*) 1000 (*)	mg
O_2	Paramagnetism	ABB Magnos 206	0 - 25	vol-%
CO_2	IR photometry	ABB Uras 206	0 - 20	vol-%
CO	IR photometry	ABB Uras 206	0 - 1000 0 - 20000	ppmv
NO	IR photometry	ABB Uras 206	0 - 408	ppmv
CO	IR photometry	ABB Uras 206	0 - 6220	ppmv
VOC	Flame ionization	ABB Fidas 24	0 - 100	mgC/m³
T	Thermoelectricity	Thermoelements Type K	-100 - 1370	°C
v	Calorimetry	Seikom RLSW8AL V8 LCD	0.1 - 10	m/s
Δp	Differential pressure	thermokon DPT 2500	0 - 1000 0 - 2500	Pa

(*): Maximum load at the end of the measuring period

3.1.4. Chemical analysis

The fuels and ashes produced were analyzed. Sampling and preparation were conducted according to DIN EN 14778 [72] and 14780 [73]. All samples were dried at 105 °C for at least 24 h and milled to 0.25 mm grain size using a Fritsch Pulverisette 19 (Rotor: hardened steel blades, fixed knives: tungsten carbide) before analysis.

For the determination of the ash content, 1 g milled sample was heated in a furnace (AAF 11/18, Carbolite) according to EN ISO 18125:2017 [74].

For the calorific value of the fuels, 1 g milled sample was pressed into a pellet and combusted in a calorimeter (C 6000, IKA). Ash samples were treated differently: 100 mg of ash were combusted with the aid of a combustion bag (IKA) and 250 mg paraffin oil (IKA). The water from combustion was diluted to 50 ml with bi-distilled water for determination of the chloride and sulfate. For the measurement, an IC (ion-exchange chromatograph, 883 Basic IC plus, Metrohm) was used as described in EN ISO 16994:2016 [75].

Ultimate analysis was performed using a vario MACRO cube (Elementar). For fuels, 40 mg milled sample was wrapped into zinc foil (Elementar) and pressed into a tablet, while for ash, 20 mg ash and 60 mg of WO_3 (Elementar) and zinc foil were used.

Chemical analysis of trace elements was performed using an ICP-OES (Inductively Coupled Plasma Optical Emission Spectroscopy, Spectroblue FMX 26, Spectro) after microwave digestion. For digestion, 0.4 g of milled wood or 0.1 g of ash was oxidized using 1 ml of 30% H_2O_2 (for Synthesis, Roth), and dissolved in 4 ml 69% HNO_3 (Rotipuran Supra, Roth) and 9 ml 35% HCl (Rotipuran Supra, Roth). The digestion was performed using a Multiwave GO (Anton Paar) microwave with a ramp program: The total time in the microwave was 80 min at 175 °C, and 5 min at 185 °C. After the digestion was complete, the sample was diluted to 50 ml with bi-distilled water and the analysis was performed using the ICP-OES.

3.1.5. Measurement Procedure

During commissioning, it became apparent that condensation reduced the measured dust concentration after the filter to a high degree. Since only the collection efficiency of the filter should be measured, additional measures were introduced to avoid this problem.

The filter was preheated overnight. Additionally, during the startup of the furnace, the piping was preheated by blowing hot air through the piping and filter. With these measures, temperatures above 80 °C could be ensured in the measurement sections and the filter before starting the measurements.

The experiments were started after the pre-heating measures were

complete and the furnace was operating for at least two hours at 50% power output to ensure stable combustion conditions during the entire test run. During the test run, the desired gas flow was maintained using a PID-controlled side channel blower. Once the pressure drop reached 2000 Pa, the side channel blower automatically shut down.

During the entire period, the experimental data was logged in 1 s steps by Profimessage Modules. Dust sampling was performed following the scheme in Table 3.3.

Table 3.3.: Sample times during test runs

	Sample Time	Time between samples
1st sample	15 min	10 min
2nd to 4th sample	30 min	10 min
5th sample	1 h	10 min
6th to 7th sample	4 h	10 min
Night	-	over night
Additional samples	2x 4 h, afterwards pause over night	10 min / over night

Before the reported experiments, 10 tests were performed using ultrasound cleaning and pellets, but with inappropriate measures to avoid condensation. This led to an increased collection efficiency, thus these measurements could not be evaluated. During the last run using pellets and ultrasound cleaning, the boiler encountered an error and went into emergency shutdown. Tar deposits inside the boiler from the malfunction caused a change in the emission characteristics of the boiler, thus, no additional runs were possible.

The maximum measurement time during the testing using wood chips and counter-current flushing was limited to 12 hours. Technical limitations of the fuel feeding system required the manual refilling of wood chips every 30 min, making automated experiments overnight impossible.

3.2. Results

3.2.1. Fuel properties and raw gas quality

The behavior of the metal mesh should be tested both with a high-quality fuel with low content of aerosol-forming elements, and a low-quality fuel containing a high amount of aerosol-forming elements. In order to do so, the furnace was operated during the first experiments with commercial pellets obtained from Scharr Wärme. For the later experiments, low-quality wood chips obtained from a local supplier were used. Wood chips larger than 32 mm were removed by sieving to avoid plugging of the furnace's screw. To confirm the desired quality of the fuels, both were analyzed as described in Section 3.1.4.

As shown in Table 3.4, the pellets fulfill the requirements for EN plus [76] and DIN plus A1 [77] certification. The amount of aerosol-forming compounds (K, Na, Zn, Cl, and S) was low with a total of 561.4 mg/kg. As intended, the wood chips contained much more aerosol-forming elements with 2384.7 mg/kg.

Table 3.4.: Fuel composition, manual prototype

		Pellets				Wood chips				Instrument
Water content[b]		6.5			%	16.0			%	Drying Oven
Ash content[b]	d.b.	0.3			%	2.1			%	Ash oven
LHV[b]	d.b.	18789	±	6	J/g	18327	±	5	J/g	Calorimeter
C[a]	d.b.	500.8	±	4.3	g/kg	489.6	±	2.0	g/kg	EA
H[a]	d.b.	65.2	±	0.6	g/kg	61.7	±	0.5	g/kg	EA
N[a]	d.b.	0.8	±	0.1	g/kg	2.7	±	0.2	g/kg	EA
O[a]	d.b.	432.6			g/kg	446.0			g/kg	EA
Cl[a]	d.b.	2.7	±	0.2	mg/kg	5.9	±	0.3	mg/kg	IC
S[a]	d.b.	4.8	±	0.2	mg/kg	17.7	±	0.3	mg/kg	IC
Ca[a]	d.b.	941	±	12	mg/kg	7297	±	320	mg/kg	ICP-OES
K[a]	d.b.	537	±	7.8	mg/kg	2247	±	76	mg/kg	ICP-OES
Na[a]	d.b.	3.3	±	1.7	mg/kg	88.1	±	0.9	mg/kg	ICP-OES
Zn[a]	d.b.	13.6	±	1.9	mg/kg	26.0	±	0.9	mg/kg	ICP-OES

d.b.: Dry basis. Average ± Standard deviation. [a]: 6 Measurements. [b]: 3 Measurements.

Gaseous emissions of the boiler were measured for two reasons: To assess the combustion quality and to measure a potential gas leakage of the setup. No gas leakage could be measured, as the deviation between the data measured by the lambda sensor of the furnace and the measured oxygen content was below 1% and within 1.5% of the nominal oxygen content of the furnace (9.5%).

The quality of the combustion was - as intended - depending on the used fuel.

With pellets, combustion was very good, with low levels of dust and hydrocarbons as shown in Figure 3.3. Dust concentration was 7 mg/m³ (corrected to 13% O_2, STP), VOC was mostly below the detection limit and the CO concentration was 53 mg/m³. NO_x concentration was 68 mg/m³.

In contrast to the low emissions with pellets, the emissions were higher during the combustion of wood chips and above the legal limits of the 1. BImschV [9]. The dust concentration was 0.049 g/m³ (limit: 0.02 g/m³) during wood chip combustion, VOC concentration was 49 mg/m³, CO concentration was 1.8 g/m³ (limit: 0.4 g/m³), and NO_x concentration was 113 mg/m³.

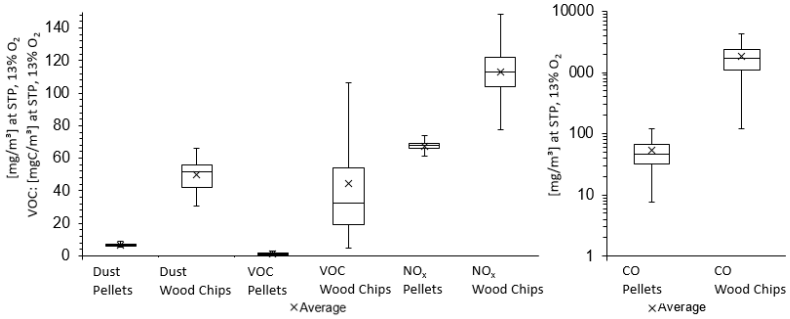

Figure 3.3.: Raw gas composition during Pellet and Wood Chip combustion. X: Average. Whiskers: Minimum/maximum value. Box: First quartile, median and third quartile

3.2.2. Dust collection efficiency

In general, assuming constant flow the dust collection efficiency can be defined as

$$E = c_{Dust,in} - c_{Dust,out} / c_{Dust,in} * 100 \qquad (3.2)$$

$E =$ Collection Efficiency

$c_{Dust,in}$ = Dust concentration at the inlet, $[g/m^2]$

$c_{Dust,out}$ = Dust concentration at the outlet, $[g/m^2]$

Averaged pressure drop and dust collection efficiencies are displayed in Figures 3.4 to 3.6. Each figure shows the averaged results for pellet and wood chips combustion. During the experiments at 33.3 m/h flow, the experiments had to be stopped before the maximum pressure drop of 2000 Pa was reached.

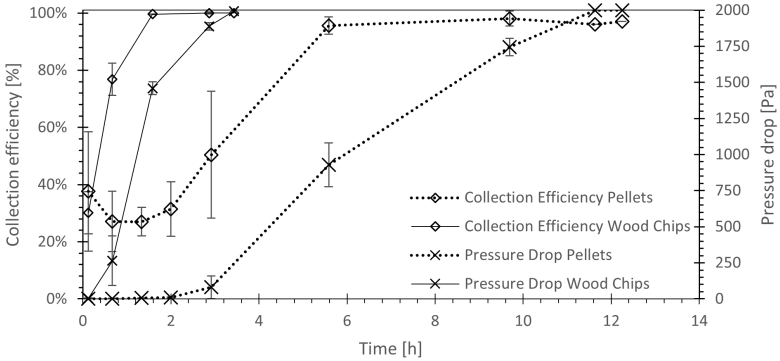

Figure 3.4.: Collection efficiency and pressure drop for Pellet and Wood Chip combustion at 66.6 m/h flow velocity. Averaged curves from 3 measurements. Error bars equal standard deviation.

The main difference between the different curves is the total duration, thus, Figure 3.7 shows one curve for discussion in detail.

The filtration can be separated into two different phases:

Phase 1 is characterized by low collection efficiency and low pressure drop.

Phase 2 is characterized by a high collection efficiency, and an increase

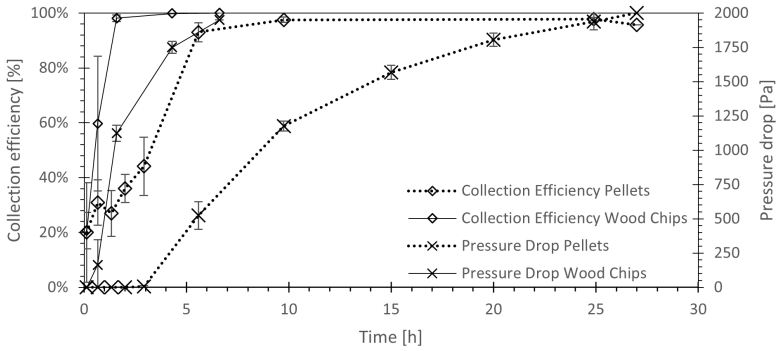

Figure 3.5.: Collection efficiency and pressure drop for Pellet and Wood Chip combustion at 50 m/h flow velocity. Averaged curves from 3 measurements. Error bars equal standard deviation.

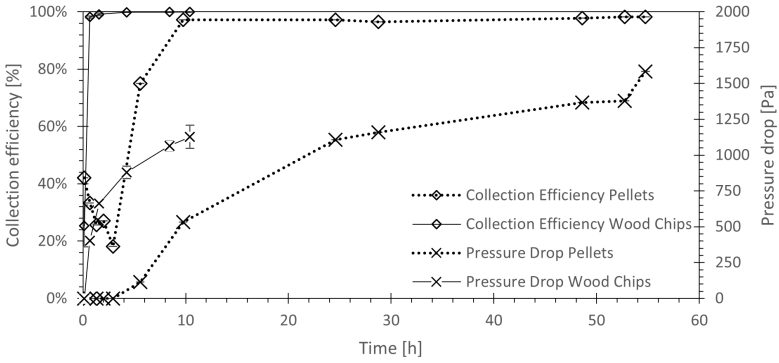

Figure 3.6.: Collection efficiency and pressure drop for Pellet and Wood Chip combustion at 33.3 m/h flow velocity. Averaged curve from 3 measurements for wood chip combustion, single run for pellet combustion. Error bars equal standard deviation.

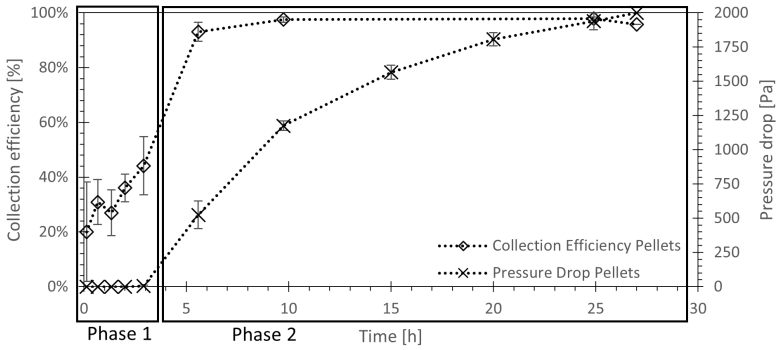

Figure 3.7.: Filtration phases during the experiments at 50 m/h. Averaged curve from 3 measurements for pellet combustion. Error Bars equal standard deviation.

in pressure drop over time, until the maximum pressure drop of 2000 Pa is reached and the experiment is stopped.

During Phase 2, the collection efficiency is close to 100%. The measured raw gas concentrations were extremely low and within the detection limit of the method, at 0 - 0.3 mg/m³ (corrected to 13% O_2, STP). Separation efficiencies exceeded 98%. In Table 3.5, the average time for the phases and the overall separation efficiencies are displayed for all fuels and flow velocities.

With decreasing flow, Phase 2 prolongs in comparison to Phase 1, resulting in higher overall collection efficiency.

Table 3.5.: Duration of the phases and overall collection efficiency

Gas velocity $[m/h]$	Phase 1 $[h]$	Phase 2 $[h]$	Collection Efficiency[d] $[\%]$	Pressure Drop $[Pa]$
Pellets				
66.6[b]	1.8 ± 0.6	9.9 ± 0.5	75 ± 4	2000
50.0[b]	3.1 ± 0.5	22.0 ± 3.0	86 ± 1	2000
33.3[c]	4.7	49.3	84	1585
Wood Chips				
66.6[b]	0.45±0.1	3.0 ± 0.5	83 ± 1	2000
50.0[b]	0.58±0.2	5.5 ± 3.0	86 ± 3	2000
33.3[b]	0.35±0.1	10.0 ± 0.1	91 ± 1	1190 - 1266

Average ± Standard deviation. [b]: 3 Measurements. [c]: 1 Measurement. [d]: including both phases

3.2.3. Regeneration

Potential signs of an incomplete regeneration are an increase in residual pressure after the regeneration is completed, decreasing operation time, or visible remains of filter cake.

None of these signs could be observed at any test run.

No residual pressure drop could be measured during the campaign. Also, the operation time before the maximum pressure drop was reached was only dependent on the gas velocity and the used fuel. Measurements were repeated three times for one case (e.g. 50 m/h gas velocity and pellets). The operation time was in all cases constant for all three measurements. On optical inspection, as depicted in Figure 3.8, no filter cake remains could be detected after regeneration.

Figure 3.8.: Metal mesh filter before and after cleaning

During the entire testing period, including cases of furnace maloperation, the mesh was cleaned using either the ultrasound method or by counter-current flushing with water. During commissioning, another 10 runs with ultrasound-assisted cleaning were performed, amounting to a total count of regenerations of 26.

3.2.4. Chemical analysis of fly ash

Before regeneration, ash samples were scraped off the candles and analyzed. The results can be found in Table 3.6.

Carbon content is 18.97 wt-% in pellet ash and 2.31 wt-% in wood chip ash. The main constituents of the ash are aerosol-forming compounds. Potassium represents 47.8 wt-% of pellet ash and 41.9 wt-% of wood chip ash. Chloride (14.7 and 25.8 wt-%) and Sulphur (4.8 wt-% and 4.9 wt-%) are inorganic compounds with the second and third largest share. Another important aerosol-forming compound is zinc with 3.24 and 3.77 wt-%.

Table 3.6.: Ash composition, manual prototype

		Pellet Ash				Wood Chip Ash				Instrument
C[a]	d.b.	18.97	±	1.40	wt-%	2.31	±	0.20	wt-%	EA
H[a]	d.b.	0.47	±	0.03	wt-%	0.36	±	0.01	wt-%	EA
N[a]	d.b.	0.08	±	0.01	wt-%	0.27	±	0.02	wt-%	EA
Cl[a]	d.b.	14.7	±	0.2	wt-%	25.8	±	2.9	wt-%	IC
S[a]	d.b.	4.8	±	1.2	wt-%	4.9	±	0.8	wt-%	IC
Ca[a]	d.b.	1.54	±	0.02	wt-%	0.41	±	0.01	wt-%	ICP-OES
K[a]	d.b.	47.83	±	2.54	wt-%	41.95	±	0.79	wt-%	ICP-OES
Na[a]	d.b.	0.32	±	0.01	wt-%	0.67	±	0.02	wt-%	ICP-OES
Zn[a]	d.b.	3.24	±	0.11	wt-%	3.77	±	0.08	wt-%	ICP-OES

d.b.: Dry basis. Average ± Standard deviation. [a]: 6 Measurements.

3.3. Discussion

3.3.1. Flue gas composition

The burning of pellets resulted in a relatively clean flue gas, which was already below legal limits. In contrast, during the combustion of wood chips, the emissions were elevated and emission limits were surpassed.

This resulted in two very different flue gas streams which pose different challenges to the filter.

Using pellets, the dust loading is already low with 7 mg/m^3, and the initial buildup of a filter cake might be inhibited.

With wood chips, the dust loading is much higher at 49 mg/m^3, which facilitates the build-up of a filter cake. However, volatile organic compounds are present, which might lead to a sticky filter cake and thus regeneration might be more problematic compared to pellet combustion. The high concentration of CO (1.8 g/m^3) and presence of VOC indicate incomplete combustion.

The used wood chips did not fulfill the furnace's requirement for fuel, most notably they were sieved to 32 mm maximum size instead of 16 mm. Due to the small grate of the furnace, this leads to unstable conditions during combustion. Wood chips from forest residue contain a high amount of bark, and thus a high amount of aerosol-forming elements as confirmed by chemical analysis.

In general, the flue gas temperature at the outlet of the boiler was in the range of 80 °C. Thus, condensation of water and tar is possible, however, at the concentrations measured, unlikely.

Dust measurements were difficult, especially during pellet combustion. Already before filtering, concentrations were low, with around 7 mg/m³. Downstream of the filter, the concentration was below 1 mg/m³. This resulted in problems during the gravimetric measurement of the dust concentration: The loading of the plane filters used for gravimetric measurement was less than a microgram of dust downstream of the filter. Thus, the standard deviation of the measurements of the dust concentration was high. During the combustion of wood chips, the problem of deviation was less apparent as the concentrations were higher.

3.3.2. Dust collection efficiency

A total of 16 runs were performed to evaluate the dust collection efficiency of the filter. As shown in Figure 3.7, the filtration has to be divided into two phases, which has major implications on the dust collection efficiency. As criterion to differentiate between the phases, the pressure drop can be used: As soon as the pressure drop increases, phase 2 starts. During the first phase, a filter cake has yet to accumulate, and only filtration at the surface of the mesh is possible. Compared to the majority of the fine dust particles (diameter according to literature: 50-100 nm), the

pores are much larger with 22 µm. Thus, only the biggest particles are retained and the collection efficiency is low until a filter cake is covering the entire surface of the metal mesh. During this phase, no pressure drop could be measured.

Once a filter cake was formed, the second phase started, during which the retention of particulate matter is nearly complete. Instead of surface filtration, deep filtration in the filter cake is the main mode of filtration in this phase. The pressure drop increases with the accumulation of the filter cake until the maximum pressure drop is reached.

The division of the filtering into two phases has a meaningful impact on how the collection efficiency has to be evaluated. The first phase should not be neglected, as it has a major impact on the overall collection efficiency. Thus, the collection efficiency has to be averaged over an entire filtration process for evaluation. Considering only the high efficiency during the second phase results in impressive numbers, which are, however, not representative for the entire period. During the second phase, collection efficiencies exceeding 99% are common, but for the total process, the collection efficiency is between 75 and 91% depending on fuel and gas velocity.

In general, the collection efficiency increases when the gas velocity is decreased, as the second phase is prolonged compared to the first phase.

The behavior of the first phase is ambigous. It could be expected that

a constant amount of dust needs to accumulate on the filter surface until a filter cake has formed, which would result in a constant amount of dust passing through the filter during the first stage. However, as shown in Figure 3.9, this is not the case. The amount of dust passing the filter was calculated from the gas velocity, multiplied by the dust loading of the raw gas and the collection efficiency measured. The variety in the amount of dust passing through the filter is quite high, and no trend can be observed. Still, it can be assumed that about 0.5 g of dust will pass through a square meter of the filter before a sufficient filter cake has built up.

During the first phase, in some cases, the dust collection efficiency seems to decrease in the first minutes. This effect is most likely caused by condensation at the very beginning of the filtration. During commissioning, the filter and the piping were not preheated, and the observed effect was stronger. Thus, a barrel heater was installed to preheat the filter casing, and the measurement procedure was adjusted to include preheating.

3.3.3. Pressure drop modelling during depth filtration

In contrast to the first phase, the results of the second phase were very reproducible. The measured separation efficiencies were very high, during pellet combustion 98 ± 2% were measured, during wood chip combustion 99.5 ± 0.8%. The error is in absolute numbers similar, but due to higher dust concentrations caused by wood chip combustion the relative

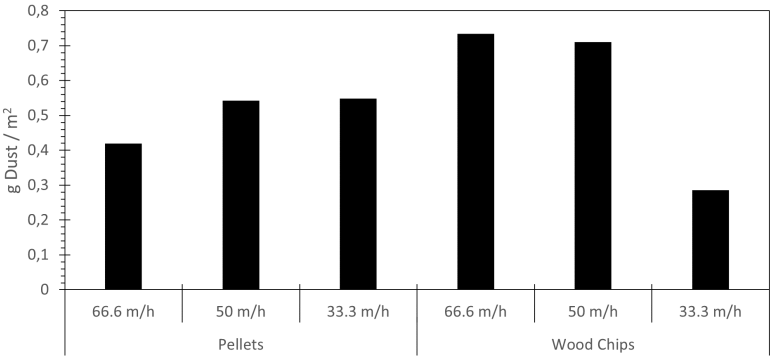

Figure 3.9.: Amount of dust passing the filter before a filter cake is accumulated

error is smaller. Due to the measurement uncertainty, negative dust concentrations were measured in the filtered gas.

As shown in Figures 3.4 to 3.6, the pressure drop follows an exponential slope. Thus, the behavior of the pressure drop during the second phase can be described with a mathematical function.

Given the pressure drop increases linearly with gas velocity, all measurements were normalized to 50 m/h by a linear approach (as an example, for a gas velocity of 33.3 m/h, the pressure drop was multiplied by 50/33.3). The normalized data for both fuels is plotted in Figure 3.10.

The pressure drop per g of dust is significantly lower for dust from wood chip combustion compared to pellet combustion. Using the plot,

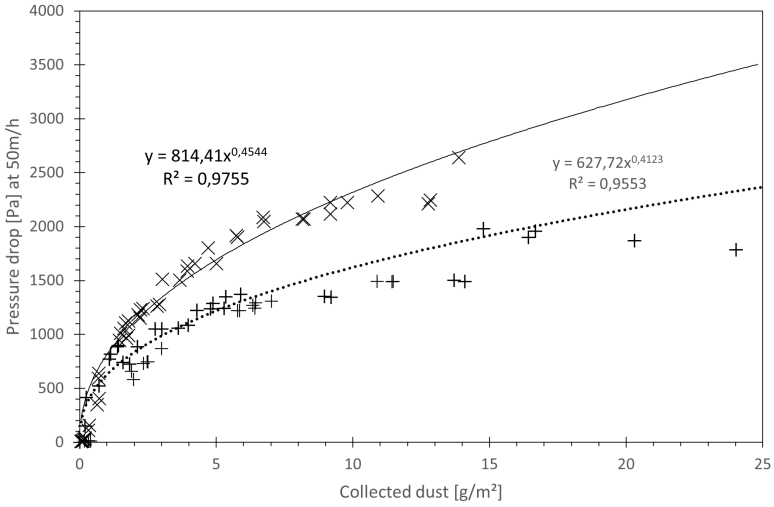

Figure 3.10.: Model functions of the pressure drop. Solid line: pellets, dotted line: wood chips. Each cross marks an individual measurement. For the regression curve, values below 500 Pa were ignored

the coefficients of a normalized model function of the form

$$\Delta p = a_n D^b \tag{3.3}$$

$\Delta p =$ Pressure drop [Pa]

$a_n, b =$ Coefficients

$D =$ Dust per m² filter surface [g/m²]

were calculated using a least square approach. All measurements above 500 Pa pressure were used. The coefficients were a_n = 814.41, b =

0.4544 for pellet combustion and a_n = 627.72, b = 0.4125 for wood chip combustion.

Without the normalization, the general function is:

$$\Delta p = a v D^b \tag{3.4}$$

Δp = Pressure drop [Pa]
a, b = Coefficients
v = Gas velocity [m/h]
D = Dust per m² filter surface [g/m²]

In this case, a is 16,28 for pellets and 12,55 for wood chips.

Using this data, it is possible to approximate the operation time in dependence of the gas velocity and dust concentration by replacing D with c_{Dust}*v*t if the collection efficiency of the second, depth-filtration phase is approximated to 100%:

$$t_{max} = \left[\frac{\Delta p_{max}}{(a c_{dust} v^2)^b} \right]^{\frac{1}{b}} \tag{3.5}$$

t_{max} = maximum operation time [h]
Δp_{max} = maximum pressure drop [a]
a, b = Coefficients from least square approximation
v = Gas velocity [m/h]

c_{dust} = Dust concentration in the flue gas [g/m³]

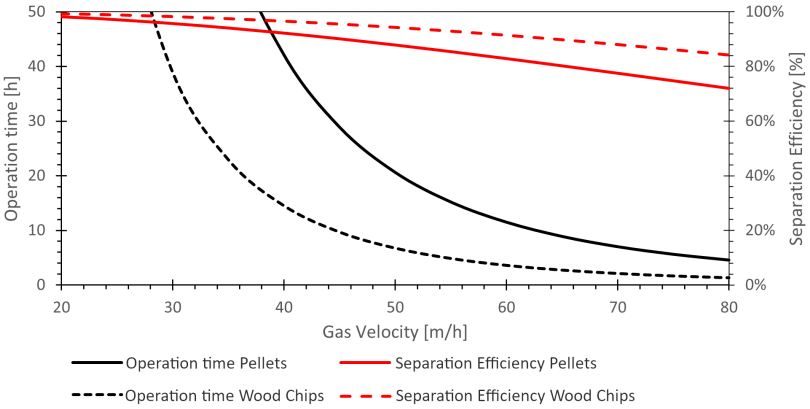

Figure 3.11.: Operation time and effective collection efficiency dependent on the gas velocity through the filter

The result is plotted in Figure 3.11. In addition, it is also possible to calculate theoretical effective separation efficiencies (including the build-up of the filter cake and the following deep-filtration) using the average collection efficiencies of the phases. For phase 1, it was assumed that 0.5 g of dust would pass 1 m² of filter surface until a sufficient filter cake is built up.

3.3.4. Regeneration

For regeneration, two different cleaning modes were attempted which are fundamentally different.

Ultrasound cleaning and counter-current cleaning use different cleaning mechanisms which have different implications on cleaning:

In an ultrasonic bath, cavitation bubbles cause small jets directed at any immersed surfaces. These remove particles on the surface, and since cavitation is induced in the entire bath, the cleaning is uniform. At the used frequency, the ultrasound cannot penetrate the mesh, which could in theory cause issues if dust is deposited inside the mesh.

Counter-current cleaning is less uniform, as the water flows through the candle and removes the filter cake mechanically due to a pressure gradient over the mesh. In theory, it would be possible that only a small part of the filter cake gets removed at the bottom of the candle where the pressure is highest due to hydrostatic effects, and afterwards, the required pressure gradient is not reached anymore.

In addition to the mechanical forces, most compounds of the dust are soluble, which further facilitates cleaning.

Both cleaning methods proved to be sufficient. The filter cake was removed completely from the entire surface, without any spots or patches which were not cleaned. The usage of additives was not necessary, and thus not evaluated. Tap water without surfactants provided a sufficient cleaning.

3.3.5. Fly ash composition

The fly ash composition is largely as expected from literature data. The main constituents are aerosol-forming compounds, followed by carbon. It is, however, important to note that there is considerably more carbon in fly ash from pellet combustion than in fly ash from wood chip combustion. Gaseous emission measurements would indicate the opposite, as volatile organic compounds were only detectable during wood chip combustion.

However, it is also important that only the relative amount of carbon is higher. The absolute concentration in the flue gas is 1.2 mgC/m^3 for pellet combustion and 1.1 mgC/m^3 for wood chip combustion. This is an indication that the generation of carbon-containing compounds in the dust is independent of the amount of aerosol-forming compounds and to a certain extent from the combustion quality.

The measured carbon is likely carbonates of inorganic compounds, e.g. potassium carbonate is a very possible candidate. With the used instruments, a differentiation between carbonates and oils or tars is not possible. This would also mean that generated organic compounds will not condense inside of the fabric filter, and thus pass the filter.

3.3.6. Design of an commercial filter

Based on the results, it is possible to outline a general design and concept for a commercial filter.

The filter needs to be regenerated periodically. During the regenera-

tion, no filtering is possible. Thus, it is required to either shut the filter down or to use multiple filters which are operated in parallel.

For pellet furnaces, the use of a single module with a gas velocity of 30 - 40 m/h leads to an operation time of multiple days, or even weeks, between regenerations. Thus, the use of a single module should be possible, and to regenerate the filter during shutdowns of the furnace.

For bigger wood chip furnaces, regenerations are more frequent and thus a single module is less viable. Instead, three (or more) modules should be used, which can be regenerated one after another. For this to work, the gas velocity of all modules combined should also be limited to 30 - 40 m/h.

3.4. Conclusions

The research done using the manual prototype gave important insight into the behavior of a metal mesh filter during filtration. Most importantly, it could be shown that both ultrasonic and counter-current cleaning remove the filter cake reliably.

It could also be shown that the filtering has to be divided into two phases: Build-up of the filter cake, followed by depth filtration in the filter cake. During the build-up of the filter cake, collection efficiency is low, while particle retention is nearly complete during depth filtration. Since the ratio of both phases depends on the gas velocity, the gas velocity is not only an important variable to influence the operation time, but

also to adjust the collection efficiency.

Also, it was possible to obtain functions for the pressure drop, operation time, and collection efficiency which can be used for designing larger and automated filters.

Chapter 4

Evaluation of a filter prototype

While the focus of previous research was to evaluate the general feasibility as well as the theoretical behavior of the filter mesh, the following research focused on practical aspects of the operation.

The most important aspects for a successful commercial application are high reliability and low costs. Thus, long-time experiments were conducted. Also, the residues – regeneration water and solid, insoluble residues – were analyzed and possible ways of disposal assessed. Additionally, possibilities to simplify the filter design were examined. The option with the biggest economic impact is to use counter-current

flushing instead of ultrasound, but also the choice of the mesh and the use of prefiltration by a cyclone are further possibilities.

The most challenging step of the process is regeneration. While the results from the metal mesh testing were promising, long-time stability was not sufficiently tested. Also, process control had to be evaluated.

4.1. Material and Methods

A new, automated prototype was built for a 180 kW boiler. Since both regeneration methods proved to be feasible, the filter consisted of two modules: One with ultrasound cleaning and one with counter-current cleaning.

Since the main focus was the reliability of the regeneration, the filter was designed to be regenerated more often than would be recommended for a commercial application. In addition to the filter modules, the filter prototype also included a programmable logic controller to automate the process and four measuring sections (one upstream and one downstream of each filter module), a regeneration water reservoir and a blower as shown in Figure 4.1.

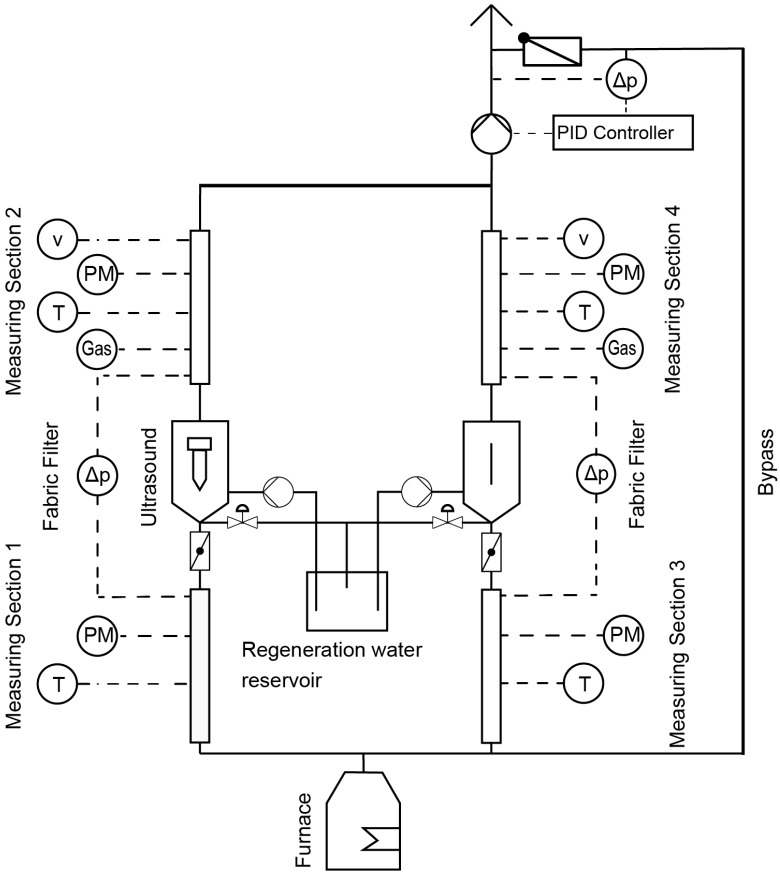

Figure 4.1.: P&ID of the automated prototype

4.1.1. Filter modules

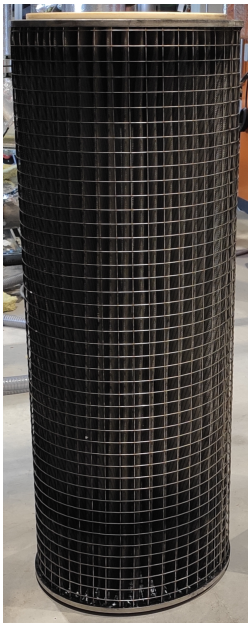

Figure 4.2.: Filter cartridge

Compared to the previous filter, the most important change of the filter modules was the use of folded filter cartridges as shown in Figure 4.2 instead of filter candles. By folding, the surface area can be increased to 5 m^2 per module without increasing the required space. To evaluate the influence of pore size, cartridges with a pore size of 22 µm and 60 µm were used. Both types of cartridges were made from V2A steel (1.4301), and the meshes were plain weave meshes.

The ultrasound transducer (SONOPUSH® MONO HD, 2000 W, Weber Ultrasonics) was moved inside the cartridge, which meant only one, relatively big cartridge was used per module.

The flow of the flue gas was reversed: During operation, the flue gas entered the filter on top, flowed through the filter cartridge from the inside to the outside, so the filter cake accumulated on the inside of the module. Thus, it could be removed by ultrasound. The design and operation scheme is shown in Figure 4.3.

Similar to the previous prototype, there was a bypass which connects

the furnace directly to the chimney, ensuring save operation. During filtering, an additional flue gas fan was used to direct flow through the filters. To avoid recirculating of filtered gas when all of the flue gas was filtered, the bypass was equipped with a check-valve. A PID controller was used to create a Δp of 20 Pa over the check-valve to ensure filtering of the entire flow.

Alternatively, it was possible to couple the controller to one of the volumetric flow meters and filter a defined volumetric flow in one module.

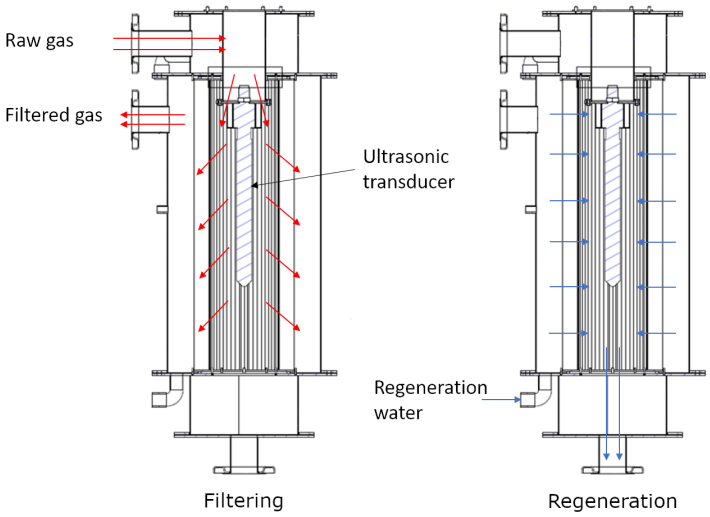

Figure 4.3.: Scheme and operation of the automated prototype. Left: Filtering operation. Right: Regeneration.

The filter cartridge has seals on the top and bottom and was clamped between the upper and the lower part of the housing. The filter housing

consists of stainless steel (V2A).

For the ultrasound module, an additional holder for the ultrasound transducer was added. Also, the ultrasound generator had to be cooled by an additional cooling coil to limit the temperature of the generator. According to the producer, the ultrasound generator should not be subjected to temperatures above 100 °C, or the piezoelectric compounds of the generator might lose their piezoelectric properties. For the cooling circuit, a cooling water pump and a cooling water reservoir were added to the frame of the filter.

To regenerate the filter, the filter is flooded with water via the outer compartment and flows through the mesh in opposite direction compared to the earlier flue gas flow.

For counter-current cleaning, the filter was first filled with water to the top. Then, the water valve was opened and the water flowed back into the regeneration reservoir. Since the water pipe had an 80 mm diameter, this process was quick and high flow rates were achieved, which is important for the cleaning. The cleaning process was repeated once.

For ultrasound-assisted cleaning, the filter was filled with water, and ultrasound was applied for 5 min. No repetition of the cleaning process was done.

4.1.2. Experimental Set-up

The filter modules described in the previous chapter were integrated into an experimental setup. The P&ID can be found in Figure 4.1.

For flue gas generation, a 180 kW wood chip boiler (Schmidt UTSR 180) was used. The boiler is a modified version of the commercial unit, with additional temperature measurement in the grate, in the burnout zone, additional sampling ports above the firebed, and in the burnout zone for gas sampling, and exhaust gas recirculation.

For the experiment, the boiler was set to an oxygen concentration of the exhaust gas of 8.5% at full load and 10% at 30% load. Primary air was set to a fixed amount depending on the thermal output, while secondary and tertiary air was controlled by a lambda sensor. Exhaust gas recirculation was set to dilute the primary air by a ratio of approximately 80 : 20 (fresh air : recirculated flue gas). Secondary and tertiary air were not diluted.

Cooling water at 75 °C was provided by the infrastructure of the University of Applied Sciences Rottenburg, which also measured the thermal output.

The measurement sections were designed according to DIN EN 33999 [70] with a diameter of 150 mm. To avoid turbulence, the suggested distances between measuring ports were used. As result, the measuring sections were large, and the total height exceeded 4 m. The list of

instruments can be found in Table 3.2.

4.1.3. Gaseous analysis

Particulate matter concentration was measured before and after the filter during test runs.

For accurate and repeatable measurements, sampling was started once a volumetric flow was registered inside of the measuring section after the filter, and stopped when the blower was shut down. Thus, the average particulate matter concentration during the entire filtration process was measured.

To account for the different dust concentrations and measuring times compared to the earlier experiments, some changes were implemented to the sampling described in Section 3.1.3: Before and after the filter, plane quartz filters and plugged extra-fine glass wool for prefiltration were used.

The gaseous flue gas composition was logged continuously using an ABB modular measuring solution downstream of the filter, which was already described in Section 3.1.3. The position was chosen to monitor the tightness of the setup, however, VOC measurements might be influenced by low temperatures in the duct and filter, causing condensation and thereby too low values. This is especially problematic during the start and stop of the filter, as the temperatures are lower during these phases,

and condensation of water was observed. As described in Table 3.2, the modular measuring tower measured CO, NO, CO_2, SO_2, O_2 and VOC. Before measurement, the flue gas sample passed through a condenser (ABB), thus, the gas concentrations are for dry gas.

All values were corrected to standard temperature and pressure (STP).

4.1.4. Chemical analysis of the fuel, ashes, and regeneration water

The fuel was obtained from one distributor, but due to the volume, three different batches had to be used for the tests. The fuel arrived in a roll-off container, of which samples were taken from different spots and heights.

During operation, different waste products were generated: Regeneration water, an insoluble solid residue that accumulated at the bottom of the regeneration water reservoir, and bottom ash from the furnace. Samples were taken from the regeneration water and the solid residue during the exchange of the regeneration water, and also a sample of the bottom ash was taken.

In addition, a sample was taken directly from the filter cake after decommissioning of the filter.

Chemical analysis was performed as described in Section 3.1.4.

Additionally, the regeneration water was analyzed directly using the ICP-OES without digestion as the sample was already a liquid. pH was measured using a pH meter (Mettler Toledo FE20) and chemical oxygen demand (COD) was measured using a rapid test kit (Macherey-Nagel, Nanocolor CSB 40 and CSB 160).

4.2. Filter testing

To prove the reliability of the regeneration, the filter was operated using a load cycle which was intended to be close to real operation. Additionally, the filter was operated at fixed volumetric flows during operation at full load to evaluate design options.

4.2.1. Long time operation

As discussed in the introduction, modulating load is common during the operation of a boiler, and also starts and stops occur. Thus, a cycle was designed to include load modulation and re-ignition of the furnace. It is shown in Figure 4.4. The cycle is eight hours long and is repeated three times per day. The furnace is operated at thermal outputs between 30 and 100% before shutting down for one hour after which ignition is required. The desired thermal output was transferred to the boiler using a LabVIEW-programme with a MODBUS interface, which was also used to log the experimental data.

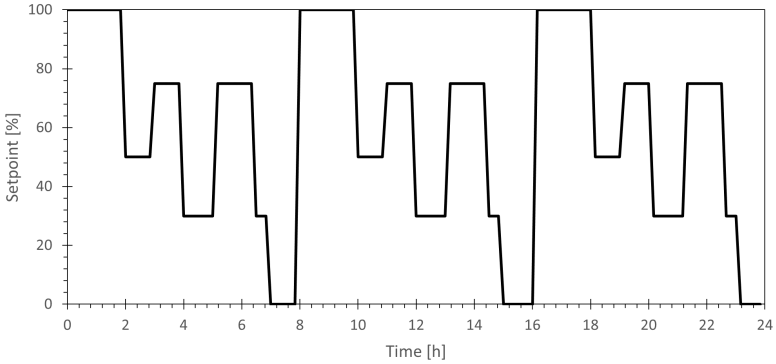

Figure 4.4.: Load cycle of the furnace

The filter was operated during all times, also during start and stop phases.

4.2.2. Design Simplification

The following design options were tested:

- Use of a metal mesh with 22 µm or 60 µm opening
- Use of ultrasound cleaning
- Use of a cyclone as a prefilter

To examine the influence of different metal meshes, the cartridge of the ultrasound module was exchanged with a 22 µm cartridge, while the 60 µm cartridge in the second module which was already used in the previous experiments was kept.

Different to the previous measurements, only one module was used at a time, and a constant volume flow was used during the entire experiment. The furnace was operated at full load, to ensure reproducible conditions for the design optimisation. As will be discussed in more detail in Section 4.3.2, the initial design did not account for thermal expansion which led to internal leakages of unfiltered flue gas into the filtered gas compartment. Thus the construction had to be changed. Instead of clamping between two metal surfaces, a sleeve with a radial seal was used on the top, so that there was sufficient room for thermal expansion. A schematic display of the solution is shown in Figure 4.5.

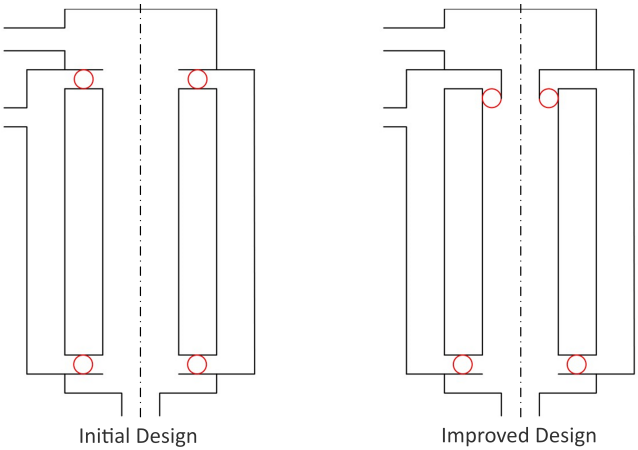

Figure 4.5.: Gasket scheme of the prototype. Left: Initial design. Right: Improved design, with a sleeve to allow thermal expansion.

The new design required a change in the mode of operation, as gas

cannot pass through the wet metal mesh. To avoid the usage of electric heating, the modules were dried with flue gas as shown in Figure 4.6.

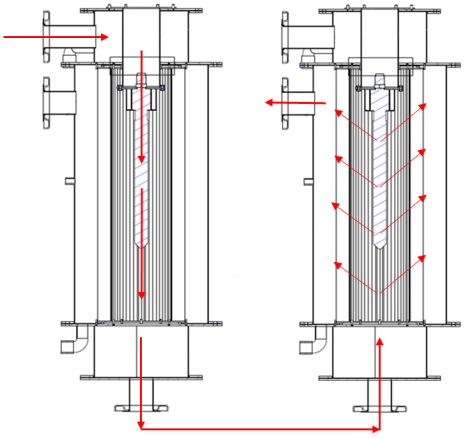

Figure 4.6.: Drying of the improved filter. Left: Wet filter, right: Dry filter.

Instead of dividing the flue gas and filtering of a partial stream in both filters, the entire flow was passed through the inside of the wet filter and passed into the second, dry filter using the water pipe. In the second filter, the flue gas was filtered and left via the outlet to the flue gas fan and chimney. To achieve this, both water valves were opened and the valve between the dry filter and the furnace was closed.

4.3. Results

4.3.1. Fuel properties and raw gas quality

Commercial wood chips were used for the operation tests. This way, a realistic quality of the fuel was ensured. Three containers were required.

Table 4.1.: Fuel composition, automatic prototype

		Batch I	Batch II	Batch III
Water content[b]		38.7 %	29.3 %	35.07 %
Ash content[b]	d.b.	1.4 ± 0.1 %	2.0 ± 0.2 %	0.7 ± 0.1 %
LHV[b]	d.b.	18482 ± 32 J/g	18600 ± 14 J/g	18516 ± 15 J/g
C[a]	d.b.	491 ± 3 g/kg	496 ± 3 k/kg	485 ± 3 g/kg
H[a]	d.b.	64.4 ± 0.9 g/kg	64.8 ± 0.6 k/kg	64.1 ± 0.9 g/kg
N[a]	d.b.	2.2 ± 0.1 g/kg	2.7 ± 0.2 k/kg	0.9 ± 0.2 g/kg
O[a]	d.b.	437.2 g/kg	430.3 g/kg	446.9 g/kg
Cl[a]	d.b.	58.6 ± 1.1 mg/kg	52.3 ± 1.9 mg/kg	57.7 ± 2.3 mg/kg
S[a]	d.b.	33.5 ± 12 mg/kg	94.6 ± 47.4 mg/kg	38.4 ± 13.0 mg/kg
Ca[a]	d.b.	3488 ± 71 mg/kg	4479 ± 93 mg/kg	2048 ± 6 mg/kg
K[a]	d.b.	1785 ± 14 mg/kg	1814 ± 28 mg/kg	1115 ± 4 mg/kg
Na[a]	d.b.	29 ± 3 mg/kg	46 ± 1 mg/kg	188 ± 10 mg/kg
Zn[a]	d.b.	12 ± 2 mg/kg	30 ± 2 mg/kg	18 ± 4 mg/kg

d.b.: Dry basis. Average ± Standard deviation. [a]: 6 Measurements. [b]: 3 Measurements.

The quality of the wood chips varied as shown in Table 4.1. For dust generation, two values are especially important: The water content, as it may cause incomplete combustion if it is too high, and the amount of aerosol-forming compounds (K, Na, Zn, Cl, S). The water content and content of aerosol-forming compounds of Batch I were high, while Batch II had a lower water content and Batch III a lower content of aerosol-forming compounds.

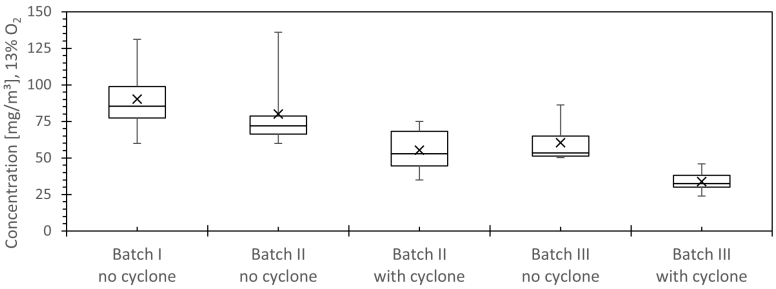

Figure 4.7.: Raw gas particulate matter concentration. X: average. Whiskers: minimum/-maximum value. Box: first quartile, median and third quartile

The different amounts of aerosol-forming compounds and water affects the raw gas particulate matter concentrations downstream the boiler, as shown in Figure 4.7.

Modulating load had a major influence on the raw gas composition. The programmed load cycle included large, instantaneous changes of the power output (compare: Figure 4.4), but the boiler software limits the rate of changes to reduce emissions. The resulting internal setpoint, thermal output, and flue gas temperature before the filter is shown in Figure 4.8. Due to the large thermal mass of the furnace, the recorded output is following the internal setpoint with a delay. The change in flue gas temperature has an additional delay. During shutdowns of the boiler, the flue gas temperature decreases to less than 70 °C, which should result in the formation of condensate. Also, short decreases in temperature can be observed during regeneration of the filter, as the gas

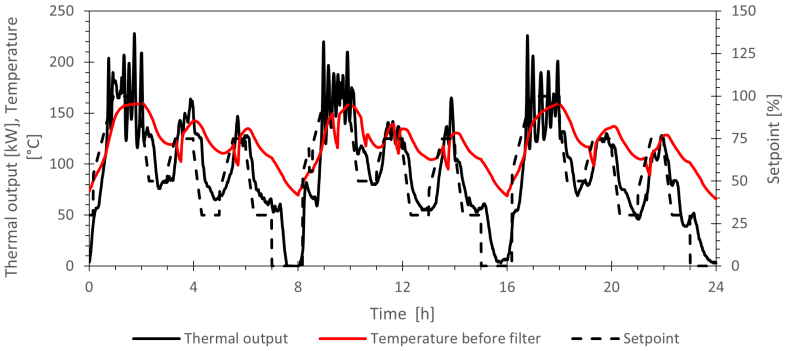

Figure 4.8.: Thermal output and flue gas temperature during modulating load. 8/4/2020, fuel: Batch I

is stagnant in the measuring section (e.g. at 03:15).

The resulting gas composition is shown in Figure 4.9. CO emissions depend on the load (and previous load history) of the furnace. During ignition, but also during stop and at low power settings, the CO emissions are increased. The highest value was measured while the boiler was in standby with 2022 mg/m³, while the average CO emission was 391 mg/m³. During re-ignition of the furnace, VOC emissions were measured in some cases. Oxygen content was close to nominal value only at full load.

Stable load conditions as shown in Figure 4.10 lead to lower emissions. CO emissions never exceeded 400 mg/m³, with an average of 94 mg/m³. The oxygen concentration was much more stable and close to the setpoint. Over time, the O_2 concentration slowly increased. No VOC emissions

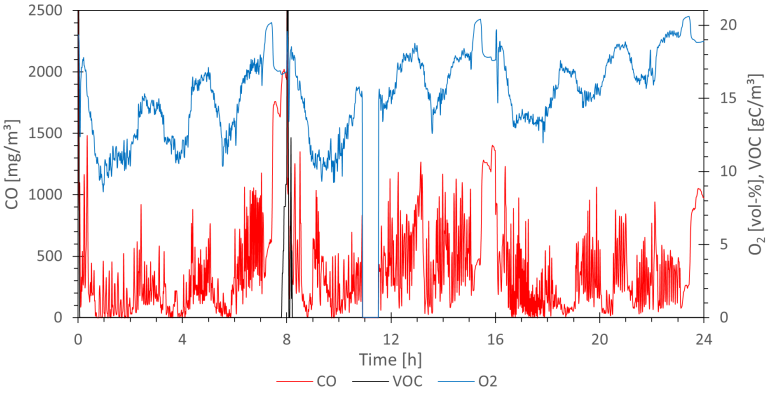

Figure 4.9.: Flue gas composition during modulating load. 8/4/2020, fuel: Batch I

were measured during stable conditions.

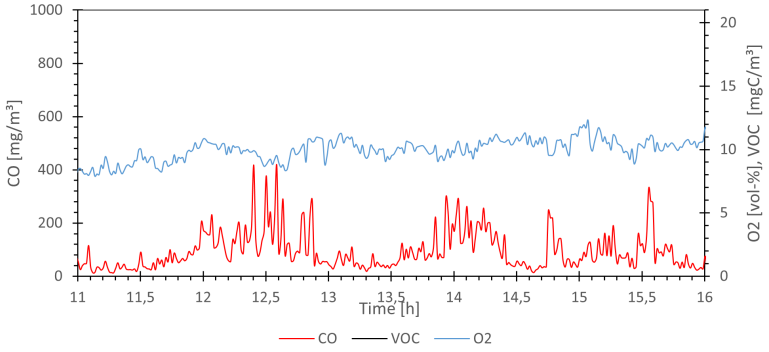

Figure 4.10.: Flue gas composition during stable load (100%). 19/08/2020, fuel: Batch III

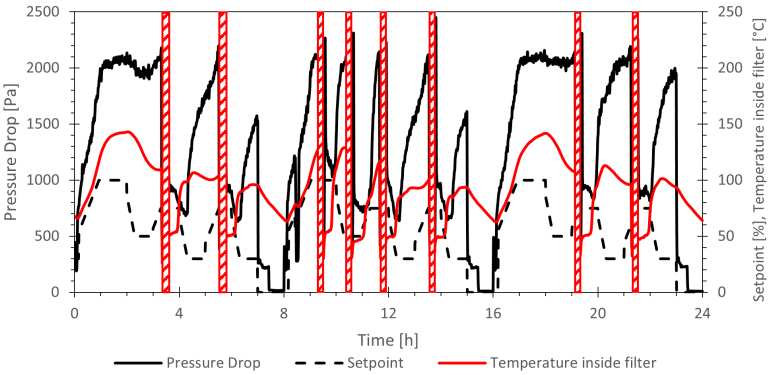

Figure 4.11.: Long-time measurements of the 8/4/2020. Red boxes: regeneration. Fuel: batch I

4.3.2. Long time operation

In Figure 4.11, pressure drop, the temperature inside the filter, and thermal output is displayed for a day of operation. Regenerations are marked with red boxes. During the first 8 hour cycle, two regenerations were required, during the second four regenerations, and during the last cycle of the day, two regenerations were necessary.

After each regeneration, the pressure drop is very high for a short period. While the filters are still wet after regeneration, no flue gas can pass through the filter, resulting in the elevated pressure drop observed. After drying, a minimal pressure drop could be observed at around 700 to 1000 Pa. At a medium gas velocity (200 m^3/h per unit resulting in 40 m/h), a pressure drop of 300 Pa was caused by the piping and the remaining pressure drop was caused by the metal mesh.

In general, the regenerations were successful and no differences regarding regeneration could be recorded between the different modules. As particles accumulated in the regeneration water, the residual pressure drop increased which led to more frequent regenerations as shown in Figure 4.12.

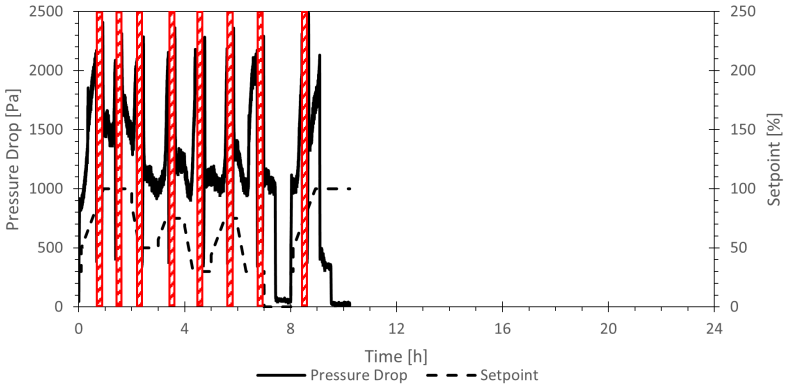

Figure 4.12.: Effect of particle enrichment in the regeneration water. Operation of the filter was stopped at 9:45 due to short regeneration intervals. Same scale as Figure 4.11 for illustration. Red boxes: regeneration. Measured on 26/2/2020. Fuel: batch I

A mud-like layer of insoluble particles was present at this stage in the regeneration water reservoir, and since the water flowed quickly back into the regeneration water reservoir, a portion of it was suspended in the bulk water. Settlement of the suspended particles was slow, so particles were pumped into the filter during the next regeneration. A secondary filter cake formed on the outside of the filter mesh, causing an

additional pressure drop. Estimated from the concentration of potassium in the liquid phase, about 1.35 kg/m³ solid residue was suspended in the regeneration water.

After replacement of the regeneration water, the time between regeneration returned to the previous values for one to two weeks of operation. However, the used water from the first regeneration was heavily contaminated with particles.

During the entirety of the trials, no additional, manual cleaning was required. Only the automated cleaning protocol was used.

During commissioning and during operation testing, collection efficiency was measured. A selection of the measurements is given in Table 4.2.

Table 4.2.: Separation Efficiencies during commissioning and long time operation

	Fuel	Raw gas concentration $[mg/m]$	Filtered gas concentration $[mg/m]$	Separation efficiency [%]	Operation time $[h]$	
Commission 12.2.	Batch I	170 ± 17	35.8 ± 8.3	79	0.9	2
Commission 13.2.	Batch I	123	22.7	82	0.9	1
Full Load 17.2.	Batch I	111 ± 13	30.1 ± 6	73	1.2	3
Full Load 24.2.	Batch I	77 ± 44	32.5 ± 22	58	1.6	3
Full Load 11.3	Batch I	83 ± 25	31.3 ± 63	63	1.2	5
Full Load 12.3.	Batch I	90 ± 6	19.6 ± 4	78	1.2	4
Half Load 13.3.	Batch I	87 ± 17	23.9 ± 20	73	1.7	3
modulating 9.4.	Batch I	93 ± 15	27.9 ± 8	70	-	3

The collection efficiency was lower as expected based on the results from the smaller filter. Inspection of the inside of the filter revealed that

the filter cartridges were compressed, and a gap had formed between the gasket and metal surface. Thus, a portion of the gas could bypass the metal mesh and enter the filtered gas compartment without being filtered.

4.3.3. Design simplification

Before the tests for design simplification, the gasket design was improved as described in Section 4.2.2 to obtain reliable values for the collection efficiency.

Mesh size

During the evaluation of different mesh sizes, values for the collection efficiency in dependence of the gas flow velocity were obtained as shown in Table 4.3.

During the first runs, the gaskets were not leaking which resulted in higher separation efficiencies of up to 87% for both filters. During the later runs, small leakages were registered which resulted in lower

Table 4.3.: Collection efficiency with improved gasket design and different mesh sizes

Volumetric Flow $[m/h]$	Mesh Size $[\mu m]$	Fuel	Raw gas concentration $[mg/m]$	Filtered gas concentration $[mg/m]$	Separation efficiency [%]	Operation time $[h]$
250	60	Batch II	51.1 ± 4	9.3 ± 0.5	82 ± 2	1.2
250	22	Batch II	45.7 ± 3	8.7 ± 1.9	81 ± 4	1.2
200	60	Batch II	52.9 ± 15	6.2 ± 0.7	87 ± 4	3.5
200	22	Batch III	31.9 ± 5	4.4 ± 0.6	86 ± 5	1.2
150	60	Batch III	38.7 ± 6	7.3 ± 0.3	81 ± 3	3.2
150	22	Batch III	30.6 ± 1	6.2 ± 0.6	80 ± 3	3.2

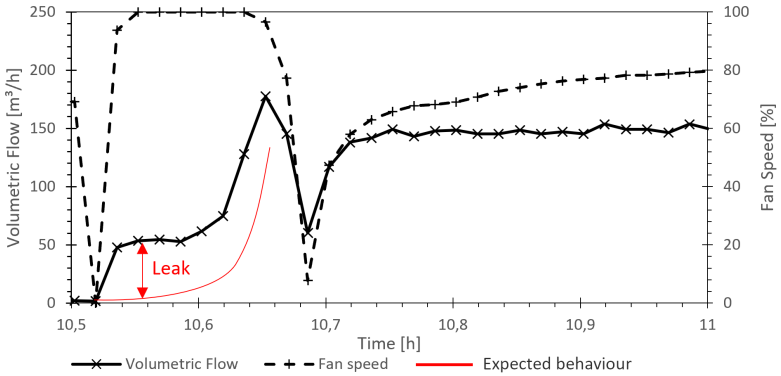

Figure 4.13.: Expected and real behaviour of the filter during drying. The difference between expected and real development of the volumetric flow is caused by a leak.

collection efficiency.

Figure 4.13 shows the expected behavior of the filter in comparison to the recorded behavior during drying.

As explained in Section 4.2.2, flue gas cannot pass through wet filters. Thus, the filter was dried by passing flue gas through the inside. If the filter would be tight, no flow should be registered during the beginning of the drying process. Instead, a small flow of 50 m³/h was registered. After the required flow passed through the filter around 10.65 h, the drying process was stopped and normal filtering started. The flue gas fan automatically stopped whenever no gas flaps were open, thus, the fan speed reduces during the switch to normal operation. Both modules had similar leak flows, thus, the measurements are still comparable.

Use of ultrasound

In general, one module was used with and one without ultrasound cleaning. The results of both modules are similar when it comes to regeneration. Still, this might also be caused by differences in the modules. Thus, additional test runs were performed: Six subsequent runs were performed without the use of ultrasound cleaning, before re-enabling ultrasound cleaning and conducting an additional run after ultrasound cleaning. The operation time for all runs was constant. The results are shown in Table 4.4.

Table 4.4.: Effect of the use of ultrasound transducer and cyclone

	Raw gas concentration $[mg/m^3]$	Filtered gas concentration $[mg/m^3]$	Separation efficiency [%]	Operation time $[h]$
no Ultrasound	28.2 ± 4	4.6 ± 3	84 ± 2	2.0 ± 0.2
Ultrasound	27.8	6.2	78	2.0
Cyclone	33.9 ± 3	4.4 ± 1	87 ± 1	2.3 ± 0.1
no Cyclone	62.4 ± 17	8.0 ± 3	86 ± 3	1.2 ± 0.3

Pre-separation by a cyclone

The furnace is equipped with a built-in multi-cyclone. To evaluate its influence on the fabric filter, the filter was operated three times with and three times without cyclone. The collection efficiency is almost equal in both cases, but the raw gas concentration (and thus also the filtered gas concentration) was nearly twice as high without the cyclone. Operation time slightly decreased as shown in Table 4.4.

4.3.4. Waste products

During operation, the dust which is removed from the flue gas is partly dissolved by the regeneration water. This leads to a liquid and a solid waste fraction, which must be separated and disposed of.

Insoluble compounds form a black mud, which accumulates at the bottom of the regeneration water reservoir but is also suspended in the water. Three samples were taken and analyzed as shown in Table 4.5.

Table 4.5.: Solid Waste products

	Solid Residue
C $[g/kg]$	269.0 ± 48
H $[g/kg]$	16.6 ± 2.7
N $[g/kg]$	10.2 ± 2.3
Cl $[g/kg]$	0.2 ± 0.06
S $[g/kg]$	1.5 ± 0.1
Ca $[g/kg]$	169.4 ± 10
Fe $[g/kg]$	26.7 ± 7.5
K $[g/kg]$	12.9 ± 1.1
Al $[g/kg]$	11.2 ± 1.7
Mg $[g/kg]$	8.9 ± 0.5
Zn $[g/kg]$	8.7 ± 0.5
Cu $[g/kg]$	2.2 ± 1.4
Mn $[g/kg]$	2.9 ± 0.1
Pb $[g/kg]$	0.4 ± 0.05
Cr $[g/kg]$	0.3 ± 0.08

Table 4.6.: Liquid waste products

	Liquid Residue	Limit
pH	6.4 - 7.6	
CSB $[mgO_2/l]$	< 83	
K $[mg/l]$	< 1210	
Sulfates $[mg/l]$	< 989	
Chlorides $[mg/l]$	< 169	
Cr $[mg/l]$	< 0.095	0.5
Cu $[mg/l]$	< 0.0552	0.5
Ni $[mg/l]$	< 0.0225	0.5
Pb $[mg/l]$	< 0.0015	0.1
Zn $[mg/l]$	< 0.69	

Limits according to the German waste water ordinance [78]

The easiest and cheapest way to dispose of the regeneration water is to dispose of it into the municipal wastewater system. For that, legal limits are given in the wastewater ordinance [78]. Five samples of the

regeneration water were analyzed. The highest value measured and the corresponding legal limit is shown in Table 4.6.

4.4. Discussion

4.4.1. Fuel properties and raw gas quality

The choice of fuel has a big economic impact. Thus, most furnaces will use the cheapest fuel available, which quite often means low quality and high content of aerosol-forming compounds.

To reflect this, the cheapest fuel available was used during the test runs.

Pollex et al. [37] stated that the potassium content should not be higher than 500 mg/kg if the dust concentration should not surpass the legal limits. The measured potassium content of the fuel used was two to four times higher, which subsequently led to dust concentrations between 34.0 and 90.1 mg/m³ in the raw gas, as expected surpassing the legal limit of 0.02 g/m³.

The emissions depend primarily on the fuel, but it can also be seen that pre-filtration by the built-in cyclone can reduce the amount of dust in raw gas: During combustion of Batch II, the cyclone reduces gas emissions from 80.1 to 55.3 mg/m³, and during combustion of Batch III dust emissions are reduced from 60.3 to 34.0 mg/m³. However, the cyclone only removes coarse particles, and not the dangerous particles of PM2.5

and below.

Modulating load leads to much higher gaseous emissions, which indicate high particulate emissions during start-up and while changing load.

At stable load, the control of the combustion air was very good, resulting in stable conditions and lower gaseous emissions.

Compared to the experiments during the metal mesh testing where wood chips were burned, the gaseous emissions of CO and VOC were lower (see: Figure 3.3 for the 50 kW furnace, Figure 4.7 for the 180 kW furnace). Still, the raw dust emissions of the 50 kW furnace were comparable to the 180 kW furnace. The 50 kW furnace has a built-in fly dust separator which is supposed to work like a cyclone, and the average dust emissions were 49 mg/m³. During the combustion of Batch II, the 180 kW furnace emitted 55.3 mg/m³ when using a cyclone. The filter was supposed to be tested at all realistic conditions, so the differences in the furnaces are desirable but limit comparability of the different experiments.

4.4.2. Long time operation

The biggest risk for the commercialization of the filter would be insufficient long-time reliability of the regeneration. Thus, during the design of the experiments, a special focus was set to regeneration. The filter was deliberately designed small, so the operation time is short and many

regenerations have to be performed during the experiments. During 419.5 h of operation, 234 regenerations were performed. In a real application, a much longer time between regenerations would be chosen, of approximately 12 h. Thus, 234 regenerations correspond to 2808 h of real operation.

The main advantage of this filter concept is that it can be used at all times, also during ignition and during modulating load. To prove this, the filter was used whenever the furnace was operated. The filter was also used during the warm-up phase before trials under stable conditions were performed.

In other works, negative effects could be measured after a few regenerations (e.g. Schiller and Schmid [61]: 18 regenerations). Still, longer trials over multiple heating periods should be conducted in the future.

Judging from the results, the most problematic phases for regeneration are the ignition and the time directly after a regeneration when the filter is still wet and cold from the regeneration. As shown in Figure 4.9, high emissions of CO and VOC occur during ignition, with exhaust gas temperatures below 70 °C. Under these circumstances, condensation of both water and partially burned hydrocarbons must be expected.

During regeneration, the filter is filled with water, and the surfaces are cooled down to the temperature of the water. Thus, condensation of hydrocarbons which might be present in the exhaust gas is possible after the regeneration as well.

Still, all regenerations were successful as shown in Table 4.4 – regardless of the employed regeneration technique. No differences between ultrasound-assisted cleaning and counter-current flushing could be observed. The filter was only cleaned using the automatic cleaning protocol.

During the majority of the operation testing, the gaskets inside the filter were not tight. Still, the main focus of the trials was to prove the reliability of the cleaning, which could be achieved.

However, it could be shown that the simple settling of the insoluble part of the filter cake is not sufficient.

With increasing particle load in the water, an increasing share of particles was suspended in the water. This led to an increasing residual pressure drop. The effect was reversible, after replacement of the regeneration water the initial residual pressure drop was reached again. Still, the regeneration water had to be replaced weekly, resulting in increased water consumption.

Thus, a more advanced particle separation technology must be implemented to remove the suspended particles from the regeneration water and limit water consumption.

4.4.3. collection efficiency

During the evaluation of the metal mesh (Chapter 3), a collection efficiency of around 80 – 90% was reached. During the operation test, this could not be repeated. The main issue was the gasket concept, as the

thermal expansion was not taken into account. This led to an increasing deformation of the filter cartridge and an increasing leak flow, where flue gas bypassed the filter directly into the filtered gas chamber. Thus, the collection efficiency decreased to less than 70%.

After solving the issue with the manifold as described in Section 4.2.2, collection efficiency of up to 87% was measured. This is in line with the results from the proof of concept.

4.4.4. Design Simplification

Mesh size

Changing the mesh size potentially influences the collection efficiency as discussed in section Section 1.2.3. On the other hand, it also influences the pressure drop and operation time. Thus, two different mesh sizes were tested, but no differences could be observed in Table 4.3. The difference in behavior might be caused by a different particle size distribution, or by the different regeneration method.

However, the higher mesh size is more durable due to the bigger threads used. Thus, using a 60 µm mesh instead of 22 µm is the better choice.

Ultrasound assistance

The ultrasound technology increases the total costs of the metal mesh filter considerably. The ultrasound transducer and generator itself are expensive, but also the transducer may not be subjected to temperatures

exceeding 100 °C or the piezoelectric compounds will degrade. Thus, an additional cooling circuit was necessary, complicating the design and requiring additional machinery and control.

During the operation test, no advantage could be observed. Also, during tests in the ultrasound module with and without ultrasound support, no difference was recorded (Table 4.4). Thus, no ultrasound should be used in a commercial version as it only adds costs without benefits.

Pre-filtration by a cyclone

The 180 kW furnace, like many other furnaces with a power output exceeding 100 kW, has a built-in multi-cyclone. It reduces the raw gas dust concentration by removing coarse particles, but it also causes an additional pressure drop. According to Gaderer et al. [54], the pressure drop can be up to 1500 Pa. The cyclone of the used furnace reduced the dust concentration by approximately 50%. During the tests, the collection efficiency of the fabric filter remains equal. However, it was shown in the proof of concept that the collection efficiency can be increased by increasing the filter surface. Thus, it is recommended to remove the cyclone, or in case of a new furnace order a furnace without a cyclone, and instead increase the filter surface to account for the increase in dust concentration.

Energy consumption is, in general, significant. Assuming a flue gas stream of about 700 m^3/h, 1.05 kW is required to overcome the pressure drop of a cyclone and 1.4 kW for the fabric filter. Thus, removing the cyclone is important to limit energy use.

4.4.5. Waste products

In general, ashes from wood combustion contain several toxic elements, in particular chromium, copper, manganese, lead, iron, and nickel.

Depending on the furnace and its specific configuration regarding particulate matter precipitation, some ash fractions have to be disposed of as hazardous materials, which can invoke additional costs. This is discussed in more detail in [79]. With the metal mesh filter system, the ash is suspended in water, which causes the formation of two fractions: The regeneration water with soluble compounds, and a slurry of insoluble compounds.

Most of the toxic compounds form oxides, salts, or carbonates with low solubility, thus the concentration of toxic elements in the liquid fraction is low. According to the measurements, the liquid fraction can be disposed into the municipal wastewater system as shown in Table 4.6. If more contaminated fuels are used, new measurements have to be performed to re-evaluate the liquid fraction.

On the other hand, the solid fraction contains trace elements and heavy metals in high concentrations. The intermediate solution would be to dispose of it as hazardous material like current fly ash. Due to the dissolution of the soluble compounds, the amount of hazardous material produced is lower and costs can be reduced. However, the content of valuable metals is very high, and in long term, a better solution than disposal should be aimed for.

4.5. Conclusion

The main objectives of this stage could be completed. Automation was successful and reliable. The automated cleaning worked satisfactorily, however, treatment of the regeneration water has to be changed. It is required to introduce a method to automatically remove the insoluble particles in the regeneration water before it is reused. For this, solutions are already commercially available and need to be added to the filter system. Also, it was shown that thermal expansion must be taken into consideration during construction, and the current design has to be improved to compensate for it.

Chapter 5

Evaluation of the Research

Overall, the development of a filter system was successful. Only small improvements are required to change the prototype for operation testing into a commercial product. During the first stage, it could be proven that water-based regeneration is feasible, that high separation efficiencies can be achieved and parameters for scaling were defined. During the second stage, an operation concept was successfully tested and it was shown that counter-current cleaning without the aid of ultrasound is sufficient for reliable cleaning.

5.1. Required Improvements

There are two main points which need to be improved: Solid particles have to be removed from the regeneration water using an appropriate, automated method. The design (especially the gasket design) needs to account for thermal expansion. A possible solution for this is discussed in Section 4.2.2.

5.2. Possible Implementation

With the results of both parts of the research, it is possible to determine the requirements for the installation of a filter, and also to propose a design.

In general, two different designs are possible as already discussed in Section 3.3.6: A single module for small furnaces with low dust concentrations (e.g. pellet boilers) and a filtering system of three or more modules for bigger furnaces.

It was proven that ultrasound cleaning is not necessary for regeneration. Since ultrasound cleaning greatly increases complexity, only counter-current flushing should be used. Also, instead of using cyclones that increase the overall pressure drop, the filter surface should be increased to account for the potential higher dust loading of the raw gas.

Using a single module has a significant drawback: The filter can only be regenerated when the furnace is off. However, for pellet furnaces, the time between regeneration is so long that this should not be an issue. Still, the regeneration has to be integrated into the software of a furnace, so retrofitting might be problematic.

Given the low frequency of regenerations, it is probably advisable to not reuse the regeneration water and instead dispose of it immediately. This way, the design can be greatly simplified. Instead of multiple pumps, flaps, and valves, the filter only requires two valves for water. For regeneration, the furnace is shut down, the filter is filled with tap water, and then the water is disposed of directly into the municipal wastewater system.

For drying, electrical heating will be the cheapest solution. Given the long time between regenerations, the energy required should not make a big difference, and a simple heating coil should be sufficient.

Using folded meshes, very compact filters can be built. A very straightforward option would be to attach the module directly to the furnace, with a folded but otherwise plane filter covering the entire side of the existing furnace.

For bigger furnaces or furnaces with a high dust loading, it is more advisable to use multiple modules, which can be regenerated subsequently. This implies that the filter can be operated 24/7, and no changes to the furnace control are necessary. Thus, this is also an option for existing furnaces.

The design would be close to the design of the prototype used in Chapter 4. However, to enable operation during regeneration, the gas velocity has to be reduced to 30 - 40 m/h to provide the necessary reserves while one filter module is being regenerated. Also, a technical solution for exchanging the regeneration water and removing the solid residue before reuse has to be added.

Chapter 6

Summary

In this work, a water-based regeneration was first attempted for a metal mesh filter for biomass furnaces - and developed close to a commercial stage.

As the first step, a proof of concept was attempted with a small, manual prototype. Initially, it was assumed that ultrasound assistance is required to remove the filter cake from the mesh. However, it was discovered that simple counter-current flushing can reliably remove the filter cake. The regeneration was by far more successful than expected, and regeneration was complete during the entire testing period.

In addition to the proof of concept for the regeneration method, the

filtering process was examined. It could be shown that the filtering process has to be divided into two phases:

First, no filter cake is present, and surface filtration is the main mode of filtration. In this phase, the collection efficiency is between 30 and 70%.

Second, a filter cake has accumulated, and the main mode of filtration thus is depth filtration. The pressure drop is increasing following an exponential function of $t^{0,4}$ to $t^{0,45}$, and collection efficiency is almost complete.

As a result, effective collection efficiency depends on the ratio between both phases. Lowering gas velocity greatly increases the duration of the second phase due to the exponential slope, thereby increasing collection efficiency.

Other than the gas velocity, also the fuel has a major influence on the operation time and collection efficiency. The amount of aerosol-forming elements influences the amount of dust in the raw gas, but that is not the only effect. When comparing the dust deposited onto the filter mesh and the pressure drop, still differences are observed between different fuels.

After completion of the trial with the manual prototype, a new, automated prototype was built to confirm the long-time feasibility of the concept.

The prototype was operated during all phases of furnace operation, and the results are promising. Removal of the filter cake was reliable both with the ultrasound-assisted cleaning mode and with counter-current flushing. This is a major advantage compared to the current particulate matter abatement technologies, as these can only be used if the exhaust gas temperature is above the dew point.

Two issues occurred with the prototype: The gasket design did not account for the thermal expansion of the filter cartridges, and thus had to be changed. Also, the insoluble parts of the dust did not settle in the regeneration water tank and formed a secondary filter cake on the clean gas side of the mesh which led to an increasing residual pressure drop. Changing the regeneration water resolved this issue, but for a commercial model, the removal of the solid residue and replacement of the regeneration water has to be automated.

Apart from these setbacks, the results are promising. Given the difference in complexity and cost, counter-current flushing is the preferred option for a commercial version of the filter.

It could also be shown that the use of a cyclone is not advisable due to its inherent pressure drop, and instead, the filter surface should be increased accordingly during the design of the filter. Also, no difference could be measured between using a pore size of 22 and 60 µm, thus, it is recommended to use the larger pore size due to the increased mechanical stability.

APPENDIX

A.1. Filtering characteristics of a metal mesh

A.1.1. Scientific publication

Biomass Conversion and Biorefinery
https://doi.org/10.1007/s13399-020-00959-9

ORIGINAL ARTICLE

Novel metal mesh filter using water-based regeneration for small-scale biomass boilers

Björn Baumgarten[1] · Peter Grammer[1] · Ferdinand Ehard[2] · Oskar Winkel[3] · Ulrich Vogt[4] · Günter Baumbach[4] · Günter Scheffknecht[4] · Harald Thorwarth[1]

Received: 15 April 2020 / Revised: 11 August 2020 / Accepted: 13 August 2020

Abstract

Particulate matter emissions are a key issue of modern biomass boilers. A novel gas cleaning method using a metal mesh filter combined with water-based cleaning was developed and tested. The filter was tested batch-wise. Flue gas of a commercial 50-kW boiler was filtered until a pressure drop of 2000 Pa was reached. Afterwards, the filter was regenerated. The initial prototype used ultrasound in order to remove the filter cake from the filter candles. Regeneration was complete and, even after boiler malfunctions producing tar, the filter cake could still be removed. Given the good results, a second cleaning mode, flushing the filter candles with water, was tested. The results were as good as with ultrasonic cleaning. Peak mass collection efficiency was very high with 98 ± 2% (burning wood pellets). However, directly after cleaning, the first layer of filter cake has to be developed. In this initial phase, collection efficiency is low. Service time until maximum pressure drop was reached depended on the gas velocity. Using pellets as fuel, at a gas velocity of 66.6 m/h, 12-h service time was reached and 4.1 g dust was collected per square meter filter surface, while at 33.3 m/h, service time increased to 55 h and collected dust to 13.9 g/m^2. Using low-quality wood chips, the raw gas dust loading was much higher but also the maximum loading of the filter was higher with 13.3 to 28.9 g dust separated per square meter. Still, the service time decreased to 3.4 respective 38 h. Peak collection efficiency increased to 99.5 ± 0.8%. The overall collection efficiency including the buildup of the filter cake depends on the gas velocity and fuel. It ranges from 74 ± 4 to 91 ± 1%. The feasibility of the filter concept could be proven, and further development towards a commercial application is in progress. Metal mesh filters with countercurrent cleaning showed a high potential given their simple and robust design, as well as high collection efficiency.

Keywords Biomass combustion · Particulate matter · Particulate matter filter · Ultrasound cleaning · Emission control · Baghouse filter · Ultrafine dust

1 Introduction

Combustion of biomass, in particular wood, is a traditional way of heating, which is gaining new importance given the climate change and that the world strives to reduce CO_2 emissions. However, during the combustion of biomass, a variety of pollutants are emitted. In order to be a viable alternative to other heat sources, emissions have to be restricted. Modern boilers already implement a variety of primary measures to minimize emissions [1]. These are able to reduce gaseous emissions like CO and NO_x to a minimum and ensure good burnout and thus efficiency of boilers. However, in addition to gases, particulate emissions occur. Particulate matter is linked to respiratory diseases, cardiovascular effects, and cancer [2, 3]. Especially very small particles (< PM1), with a high content of polycyclic aromatic hydrocarbons, are proven to cause

Electronic supplementary material The online version of this article (https://doi.org/10.1007/s13399-020-00959-9) contains supplementary material, which is available to authorized users.

✉ Björn Baumgarten
baumgarten@hs-rottenburg.de

[1] University of Applied Sciences Rottenburg, Schadenweilerhof, 72 108 Rottenburg am Neckar, Germany

[2] LK Metallwaren GmbH, Am Falbenholzweg 36, 91126 Schwabach, Germany

[3] Oskar Winkel Filtertechnik, Kaiser-Wilhelm-Ring 30, 92224 Amberg, Germany

[4] University of Stuttgart, Pfaffenwaldring 23, 70569 Stuttgart, Germany

Published online: 29 August 2020

cytotoxic and genotoxic responses [4]. In legislation, demanding limits of fine particle emissions are established. In Germany, the limit for household furnaces is 0.02 g/m^3 dust (STP, 13% O_2) [5]. In order to meet these, primary measures are not sufficient and cannot guarantee compliance with the legal limits under realistic operation conditions [6]. Especially modulating load and lower fuel quality cause violations of the limits. Starts and stops contribute considerably to total emissions but are not taken into consideration in legislation [7].

Dust from biomass plants mostly consist of salts of potassium, sodium or zinc, and chloride or sulfate. These are referred to as aerosol forming elements. Even though the release mechanisms are quite complex [8–12], there is a strong correlation between the content of aerosol forming elements and dust emissions [13–16]. As such, there were various attempts to limit the dust generation by binding of the aerosol forming elements, either by addition of additives like kaolin, which should bind primarily potassium in the grate ash [17–22], or alternatively by fire bed cooling to avoid evaporation [23]. Addition of kaolin proved to be effective; however, it requires additional processing of fuel and increases the ash content of the fuels, which implies additional costs for fuel and disposal of ashes. If the emission limit shall be reached without using additives and using common furnaces, a critical potassium content of about 500–600 mg/kg (dry basis) is assumed [24].

If low quality, cheap fuel with high potassium content is supposed to be burned; cleaning of flue gas is necessary in order to meet legislatory limits under realistic conditions.

In general, there are three main technologies in use to reduce the particle load of flue gas.

1. Cyclones are used to reduce coarse particle load in a variety of boilers; however, they are only effective for particles larger than 10 μm [25].
2. Electrostatic precipitators (ESP) are used in large-scale power plants. Currently, they are getting introduced to the small-scale market, and first models are available. Commercial ESPs for small furnaces can remove up to 80% of the particles [26]. The collection efficiency of ESPs depends on particle size. Most effective is removal of particles bigger than 3 μm and between 50 nm and 0.1 μm. Between 0.03 and 0.2 μm, a local minimum exists due to a change of the charging mechanism. Particles smaller than 50 nm pass ESPs nearly entirely [27–29]. Thus, the legally requested limits are met, but the most dangerous particles remain in the exhaust gas.
3. Fabric filters are used in large-scale plants and have proven their capability to effectively collect all particles, including the finest particles smaller than 50 nm [1]. However, they exhibit a higher pressure drop, thus requiring additional ventilation and power. In addition, fabric filters are traditionally made of textile fabric, which is inflammable. Fabric filters need to be cleaned periodically, as pressure drop increases over time. This requires a periodic regeneration, which is usually realized using jet pulses [1]. Jet pulse use a short pulse of pressurized air, which creates a backflow in the filter as well as a mechanical movement, which removes the filter cake [30].

For small biomass plants (up to 1 MW), the standard procedure of using textile fabric and jet pulse was not commercially realized so far. While inflammable textile fabric filters are state of the art in large combustion plants, they cannot be used in small biomass combustion plants due to the danger of flying sparks in flue gas without the use of a cyclone [1]. As alternative, filters made of stainless-steel mesh was suggested to be used instead, but jet-pulse cleaning of these is problematic. As example, Hartmann et al. [31] used a fabric filter made of stainless-steel mesh with a jet-pulse cleaning facility for a grain combustion furnace. Collection efficiency was excellent with 95–99%, but the pulses cleaned only parts of the filter while the filter cake remained present on the rest of the surface.

Still, similar metal mesh filters with jet-pulse cleaning were available for furnaces with a thermal output of 100 to 740 kW. While a number of filters is still in use, they are not produced anymore. In order to avoid condensation, the filter is electrically preheated before ignition of the furnace. Schwabl et al. [32] worked on an improvement for these. During their work, Schwabl et al. developed a formula for the dust concentration in the exhaust gas. It is only indirectly dependent on the raw gas content, instead, it depends on the maximum pressure drop, the frequency of cleaning, the pressure of the jet-pulse, and the gas velocity [32].

Schiller and Schmid [33] pre-coated a fabric filter with coarse particles. The particulate matter was filtered in the top layers of the pre-coat, while the lower layers of pre-coat facilitated cleaning by separating the potentially sticky particles from the textile. Also, due to the pre-coating, particle slip until a filter cake is built up was avoided. However, the applying and recycling of the pre-coat requires additional machinery and thereby costs.

Struschka and Goy [34] developed a filter based on a stainless-steel mesh and brushes to remove the filter cake mechanically. While jet-pulse cleaning is a technology that is relatively easy to adapt, it comes with drawbacks: It requires pressurized air, and the cleaning pulses are relatively loud. While this is unproblematic for larger furnaces, it is not acceptable for small plants installed in the basement of houses. The mechanical cleaning was meant to avoid these issues, but the cleaning was not sufficient. Based on his work, a new solution was developed, which integrates an ultrasonic bath to clean the metal mesh. Ultrasound is already in widespread use for cleaning applications [35]. The main mode of cleaning is the formation of jets directed at the surface of objects

emerged in the ultrasonic bath, which effectively removes particles [36]. Further contributing to a good cleaning result is the solubility of the main ash compounds in water—chloride and sulfate salts of potassium, sodium, calcium, and zinc [37–39].

In the current work, a metal mesh filter with ultrasonic-assisted water cleaning prototype was tested with regard to regeneration feasibility, pressure drop development, and viable air velocity in order to assess the viability of ultrasound assisted regeneration for a commercial application. For a successful introduction into the market, not only the collection efficiency but also economics have to be taken into consideration. As such, additional tests were carried out using only countercurrent flushing instead of ultrasound cleaning, removing the need for an expensive ultrasound transducer. Ultrasound facilitates the cleaning process by generating jets, which mechanically remove particles at the surface of the filter immersed in the ultrasonic bath; however, it also generates noise, which might impact adaption of the technology. As long as regeneration is efficient without the use of ultrasound, it is advisable not to use it.

2 Methods and material

2.1 Fabric filter

The fabric filter (mesh size 25 μm) consists of stainless steel. The steel fabric is supported by a mesh and welded to form filter candles. In the filter housing, 15 filter candles (0.08 m^2 filter surface each) in two rings surround the ultrasound rod transducer (SONOPUSH MONO SPM1500/25-495 VA, Weber Ultrasonics). The combined filter area is 1.2 m^2. For cleaning, the filter house can be filled with water, and ultrasonic cleaning can be performed. The construction is shown in Figs. 1 and 2. To avoid condensation during operation, the filter house is heated using an 800-W barrel heater (Freek, custom build).

2.2 Pellet and ash analysis

All samples were taken and prepared according to DIN EN 14778 [40] and 14780 [41]. Ash content was analyzed according to EN ISO 18122:2016 [42] by heating 1 g milled samples (< 0.25 mm) in a furnace (AAF 11/18, Carbolite). Moisture content was analyzed according to EN ISO 18134-2:2017 [43] by drying 300 g pellets or wood chips for 24 h at 105 °C.

The calorific value of the pellets and ash was determined according to EN ISO 18125:2017 by milling to 0.25 mm, pressing a pellet of around 1 g, and combustion in a calorimeter (C 6000, IKA).

The ash was also combusted using the calorimeter in order to analyze the chloride and sulfur content. A total of 100 mg of ash was combusted with the aid of a combustion bag and 250 mg paraffin oil.

The combustion water from calorimetry was diluted with bi-distilled water to 50 ml, and the content of chloride and sulfur was measured using an IC (883 Basic IC plus, Metrohm) as described in EN ISO 16994:2016-12 [44].

For ultimate analysis, 40 mg milled fuel sample was wrapped into zinc foil, pressed into a tablet, and analyzed using a vario MACRO cube (Elementar). For ash, 20 mg of ash and 60 mg of WO_3 (Elementar) and zinc foil were pressed into a tablet.

Further chemical analysis was performed using an ICP-OES (Spectroblue FMX 26, Spectro) after microwave digestion using HCl, HNO_3, and H_2O_2 following a routine developed by Tejada et al. [38].

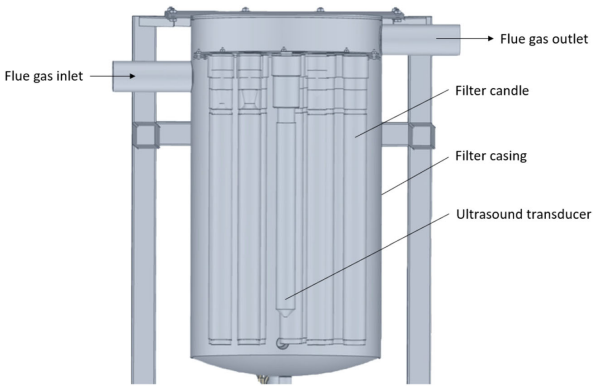

Fig. 1 Design of the filter with ultrasonic rod and 15 filter candles

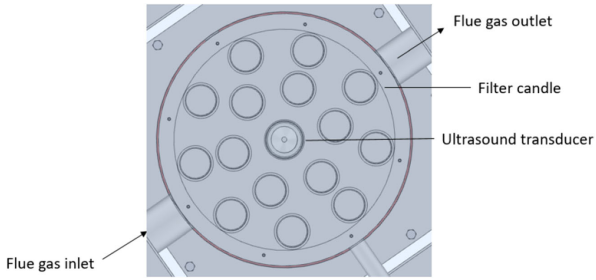

Fig. 2 Top view of the filter prototype

2.3 Pellets and wood chips

For the combustion tests, pellets were purchased from Scharr Wärme, while wood chips were purchased from Maschinenring Sulz GmbH. They were analyzed as described.

The results shown in Table 1 prove compliance with the relevant standards (EN plus A1 [45], DIN plus) and high quality of the pellets, with low amounts of aerosol-forming compounds (K, Na, Zn, S, Cl). Wood chips contain more aerosol-forming compounds.

2.4 Operation test

The filter was tested under standardized conditions. To achieve standardized conditions, an experimental setup was designed similar to DIN SPEC 33999 [46]. As emission source, a commercial moving grate boiler (KWB Multifire) was used. Its nominal thermal output is 50 kW; however, for the experiments, it was set to 50% load. At this setting, around 100 m^3/h flue gas is produced with a nominal O_2 concentration of 9.5%. The design of the setup is depicted in Fig. 3.

In order to ensure normal operation of the boiler, a bypass allows free passage of the flue gas. Measurement data logging and process control was realized using Profimessage modules (2x ADIT) from Delphin. Using a side channel blower (Airtech ASC0080-1MT400-6) controlled via a software PID and a calorimetric flow meter (SEIKOM RLSW8AL), the filter was exposed to a defined volumetric flow between 40 and 80 m^3/h, equaling 33.3 to 66.6 m/h.

Temperature logging was performed upstream and downstream the filter using Type K thermocouples, a Pt100 integrated into the barrel heater, and a Pt100 installed close to the ultrasound generator inside the filter housing, which is used to control the barrel heater.

Gas analysis was performed with a modular tower from ABB Ltd. (CO, NO, CO_2, SO_2: Uras 26, O_2: Magnos 206, VOC: Fidas 24).

PM measurement was conducted according to VDI-2066 [47] before and after the filter using plane quartz fiber filters

Table 1 Analysis of the fuels

		Pellets	Wood chips	Instrument
Water content		6.54%	15.96%	Drying oven
Ash content	d.b.	0.3%	2.11%	Ash oven
Lower heating value	d.b.	18789 ± 6 J/g	18327 ± 5 J/g	Calorimeter
C	d.b.	500.8 ± 4.3 g/kg	489.6 ± 2.0 g/kg	Elemental analyzer
H	d.b.	65.2 ± 0.6 g/kg	61.7 ± 0.5 g/kg	Elemental analyzer
N	d.b.	0.8 ± 0.1 g/kg	2.7 ± 0.2 g/kg	Elemental analyzer
O	d.b.	432.6 g/kg	446.0 g/kg	Calculated by difference
Cl	d.b.	2.7 ± 0.2 mg/kg	5.9 ± 0.3 mg/kg	IC
S	d.b.	4.8 ± 0.2 mg/kg	17.7 ± 4.3 mg/kg	IC
Ca	d.b.	941 ± 12 mg/kg	7297 ± 320 mg/kg	ICP-OES
K	d.b.	537 ± 7.8 mg/kg	2247 ± 76 mg/kg	ICP-OES
Na	d.b.	3.3 ± 1.7 mg/kg	88.1 ± 0.9 mg/kg	ICP-OES
Zn	d.b.	13.6 ± 1.9 mg/kg	26 ± 0.9 mg/kg	ICP-OES

d.b. concentrations on dry basis

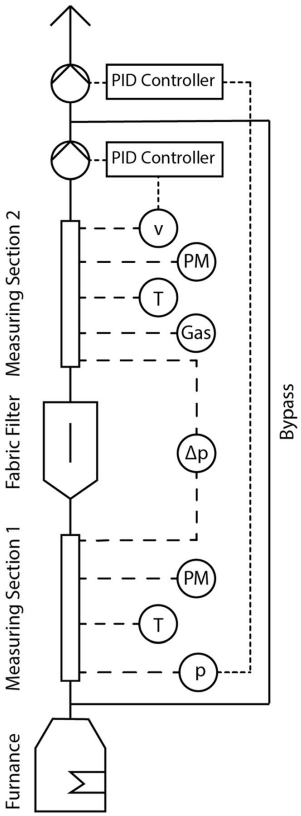

Fig. 3 Experimental set-up

(47-mm diameter, Munktell MG 160). For the raw gas, additional pre-filtration with plugged extra-fine glass wool (Karl Hecht GmbH & CO KG) was required if the measurement exceeded 1 h. The PM filters and the glass wool were thermally treated at 200 °C before and 180 °C after measurement for 1 h. After cooldown overnight using a desiccator, they were weighted in a climate-controlled room (Sartorius CPA 124S, readability 0.1 mg).

2.5 Measurement procedure

The filter house was preheated overnight. The boiler was started 2 h prior start of filtering in order to achieve steady state operation. Once filtering was started, PM sampling was performed as shown in Table 2 to account for the decreasing PM loading in the clean gas.

Once the pressure drop reached 2000 Pa, the side channel blower was automatically shut down. Cleaning was performed by filling the filter house with water and applying ultrasound at 25 kHz and 1500 W power for 15 min. Alternatively, the filter candles were flushed with water by removing the top of the filter case and flushing the candles individually using a water hose.

In total, 7 test runs were carried out using ultrasonic cleaning as shown in Table 3: Three out of those with a gas velocity relative to the filter surface of 66.6 m/h, three with 50 m/h, and one with 33.3 m/h. During the run with 33.3 m/h, the boiler encountered an error and went into emergency shutdown. Tar deposits inside of the boiler from the shutdown changed the behavior of the boiler; thus, later runs are not directly comparable. It was attempted to perform a second run with 33.3 m/h; however, pressure drop increased more slowly. After a full week of operation, the pressure drop was still below 1300 Pa. Given the different behavior and limited amount of pellets available, no further tests were performed.

For cleaning by flushing the filter with water, 9 test runs were conducted, 3 at each gas velocity. Due to technical issues, it was impossible to run the boiler without supervision as the wood chips had to be refilled every 30 min. Thus, the maximum measurement time was 12 h.

3 Results

Measurements of the gas concentrations were performed to measure the quality of combustion and to control gas leakage of the filter. The deviation between the lambda sensor of the furnace and the measured oxygen content was below 1% and within 1.5% of the nominal oxygen content of the furnace (9.5%). In Fig. 4, gas concentrations of dust, CO, NO_x, and VOC emissions of the furnace are displayed. In general, emissions from pellet combustion were much lower compared with emissions from wood chip combustion. The average dust concentrations were very low, with about 7 mg/m^3 (corrected to 13% O_2, STP) during pellet combustion and 49 mg/m^3 during wood chip combustion. CO was 53 mg/m^3 for pellets but 1838 mg/m^3 for wood chips. VOC was mostly below the detection limit during pellet combustion but at 45 mg/m^3 during wood chip combustion. Average NO_x concentrations were 68 mg/m^3 with pellets and 113 mg/m^3 with wood chips.

Pressure drop and dust collection efficiency are displayed in Figs. 5, 6, and 7 for flow velocities of 66, 50, and 33 m/h. In general, the process consists of two phases: In the first phase, the pressure drop is very low and collection efficiency is small. In the second phase, the collection efficiency increases rapidly to over 95%, while the pressure drop increases continuously until the filter is shut down at 2000 Pa. The main difference between the different gas velocities is the time until the maximum pressure drop is reached, while the general

Table 2 PM sampling scheme

	Sample time	Pause between samples
1st sample	15 min	10 min
2nd to 4th sample	30 min	10 min
5th sample	1 h	10 min
6th to 7th sample	4 h	10 min
Night	–	Pause overnight
Additional samples	2× 4 h, afterwards pause overnight	10 min/overnight

behavior is identical. During the runs with 33 m/h with wood chips, the maximum pressure drop of 2000 Pa was not reached within the maximum operation time possible with our setup. The time until a pressure drop could be detected depends both on fuel quality and on gas velocity.

The average duration of the two phases, the overall collection efficiency, and the maximum pressure drop are summarized for each gas velocity in Table 4. The figures as well as the table show that the second phase is prolonged if the gas velocity is reduced; thus, overall collection efficiency increases from 75 to 84% in case of pellets and from 83 to 91% in case of wood chips. The dependence of the first phase on gas velocity is inconsistent. It increases during reduction from 66.6 to 50 m/h; however, the effect of further reduction is much smaller in case of pellets; in the case of wood chips, it is reverted; and the buildup phase is shorter at 33.3 m/h then 50 m/h. It is important to note that the maximum pressure drop of 2000 Pa was not reached during the runs with 33.3 m/h gas velocity, so the overall efficiency would be higher.

In all cases, the regeneration led to a complete removal of the filter cake. This is depicted in Fig. 8. The pressure drop was reduced to zero, and there was no trend to shorter operation times. The filter was never regenerated using other methods than the mentioned ultrasound cleaning or flushing with water.

Deposited fly ash samples from pellet as well as wood chip combustion were taken from the filter and were chemically analyzed. The results can be found in Table 5. Main constituents of both ashes are potassium salts, with concentrations of 47.8 wt-% (pellets) and 41.9 wt-% (wood chips). Chloride concentrations amount to 14.7 wt-% and 25.8 wt-% and sulfur to 4.8 and 4.9 wt-%. Wood chip ash contains much less chloride but approximately the same amount of sulfur as pellet ash. The carbon content is relatively low with 19.0 and 2.3 wt-%. Another important constituent is zinc with 3.2 wt-% and 3.7 wt-%. The calcium content is also low with concentrations of 1.5 and 0.4 wt-%.

Table 3 Experimental runs

Gas velocity (m/h)	Repetitions	Cleaning mode	Fuel
66.6	3	Ultrasound	Pellets
50	3	Ultrasound	Pellets
33.3	1	Ultrasound	Pellets
66.6	3	Countercurrent flushing	Wood chips
50	3	Countercurrent flushing	Wood chips
33	3	Countercurrent flushing	Wood chips

4 Discussion

Gas analysis was done primarily to monitor the tightness of the setup, especially at high pressure drops. The deviation between measured O_2 concentration and nominal O_2 concentration is within measurement error of the probes; thus, dilution effects by false air are negligible.

Additionally, CO, VOC, and NO_x emissions were monitored. CO and VOC can be used to control combustion quality; given the very low emissions observed with pellets (in case of VOC below detection limit), complete combustion can be assumed. CO and VOC emissions were significantly higher during wood chip combustion, indicating incomplete combustion. Still, CO emissions were well within German legal limits (average: 0.18 g/m^3, the limit is 0.4 g/m^3). In order to assess the regeneration of the filter under suboptimal conditions, wood chips of low quality (forest residue) were used. They do not fulfil all requirements of the boiler manufacturer; most notably, they were sieved to 32 mm maximum size instead of 16 mm maximum size. Given the wood chips are from forest residue, they are rich in bark and therefore aerosol forming elements as shown by the chemical analysis, resulting in the observed higher emissions.

Temperature measurements showed low gas temperatures in the range of 80 °C. Normally, at this low temperature, there is a risk of tar condensation. However, given no or only small concentrations of VOC were detected during normal boiler operation, no noticeable tar condensation should occur.

Measurement of the dust concentrations in the filtered gas was difficult. The boiler already emits very low amounts of around 7 mg/m^3 using pellets. This can be accounted to the low amounts of potassium and other aerosol forming elements in the pellets. As a result, the plane filters used during

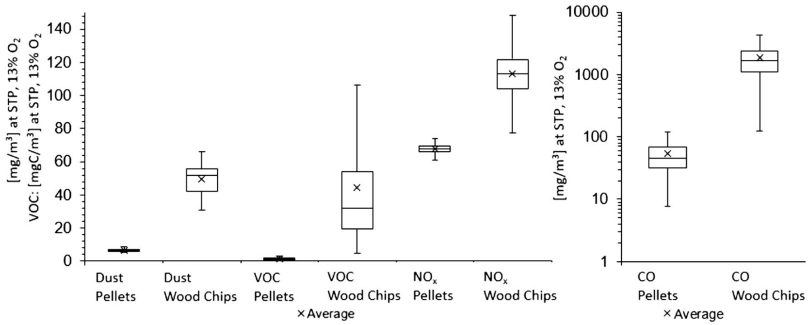

Fig. 4 Gas emissions of the KWB Multifire during operation with pellets and wood chips at 50% load (factory settings) over the course of an entire test run

gravimetric measurement of the dust concentration in the filtered gas were loaded with less than a microgram of dust, leading to a high standard deviation.

With wood chips, the boiler emits 49 mg/m^3 at standard conditions (13% O_2), which is caused by the much higher amount of aerosol forming elements.

Two different phases can be identified in the pressure drop curves: During the first phase, the filter cake is accumulating, the collection efficiency is low, and a pressure drop cannot be measured. The collection efficiency during the first phase seems to decrease in the first minutes. This effect is most likely caused by condensation. During commissioning of the prototype, it was tested without preheating. There, the observed effect was much stronger. Even if it increases apparent collection efficiency, the collection efficiency of a metal mesh filter should be examined and not the effect of condensation on dust emissions. Thus, a barrel heater was purchased and installed. From an engineering point of view, it is not necessary and should not be added to a commercial version since it adds additional costs.

Once the filter cake is established, the second phase begins and the collection efficiency increases up to values close to 100%. While the pressure drop continuously increases, it follows an exponential slope.

The filter captured over 95% of the particulate emissions in the second phase. Given the low clean gas dust concentrations, the measured weight difference of the dust samples was below 1 mg after 4 h. The readability of the scale is 0.1 mg. As a result, the measurement of the peak separation efficiency of pellets is relatively inaccurate with 98 ± 2%. Since the raw gas concentrations during wood chip combustion are much higher, the separation efficiency could be calculated with more precision to 99.5 ± 0.8%. Due to the measurement uncertainty, in some cases, negative dust concentrations were measured in the cleaned gas.

Overall collection efficiency is lower than the separation efficiency during the second phase, as significant penetration of the filter occurs during buildup of the filter cake. With decreasing gas velocity, the share of the filtering phase increases drastically. As such, the overall collection efficiency increases with decreasing gas velocity. Unfortunately, it was not possible to run the setup long enough to reach 2000 Pa pressure drop during the runs with low gas velocity. Still, the overall collection efficiency reached 91% with wood chips

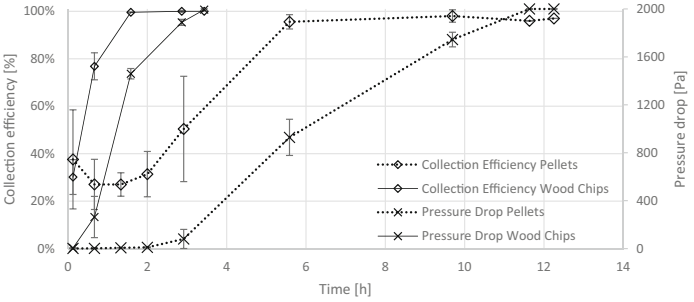

Fig. 5 Pressure drop and collection efficiency of the metal mesh filter. Average of 3 runs at 66 m/h flow velocity. Error bars equal standard deviation

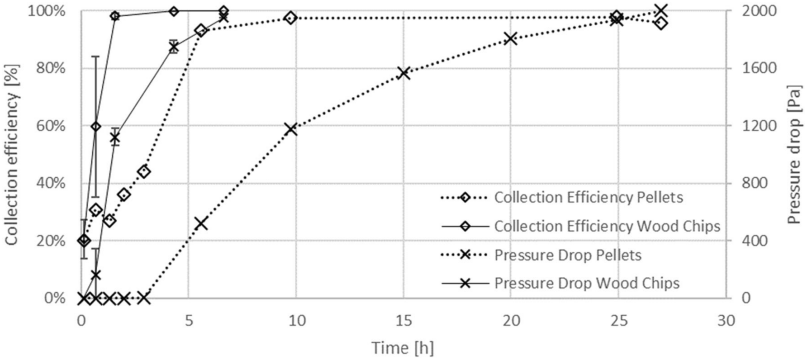

Fig. 6 Pressure drop and collection efficiency of the metal mesh filter. Average of 3 runs at 50 m/h. Error bars equal standard deviation

and 84% with pellets at the lowest gas velocity of 33.3 m/h. Pellet overall collection efficiency during the run with 50 m/h was higher with 86% compared with the run at 33 m/h, but that is most likely due to the early stop of the test at 1585 Pa instead of 2000 Pa.

The influence of the gas velocity on filter cake buildup is inconsistent. For pellets, the 24% decrease in gas velocity from 66.6 to 50 m/h resulted in an increase of 72% in time until a filter cake was established, while the 33% decrease from 50 to 33.3 m/h resulted only in an increase of 51%.

For wood chips, the decrease from 66.6 to 50 m/h led to a 28.8% increase of the duration of the first phase, while the decrease from 50 to 33.3 m/h led to a decrease of 39.6%. In fact, the buildup phase was shorter with a gas velocity of 33.3 m/h then with 66.6 m/h. The exact reason for this behavior cannot be determined using the existing data. Potential causes might be electrostatic forces or diffusion playing a bigger role at lower velocities.

In order to compare the results of the different measurements, they were normalized. Given the pressure drop increases linearly with velocity, the pressure drop of all measurements was normalized to 50 m/h using a linear approach (e.g., if the velocity was 60 m/h, the pressure drop was multiplied by 50/60). From the data of all runs excluding pressure drops below 500 Pa, a model function of the form

$$p = a\,D^b$$

with D being the collected dust per square meter and a and b being coefficients, was calculated for each fuel using the least square approach. In general, the pressure drop with wood chips was lower than with pellets. The coefficients were a = 814.41 and b = 0.4544 for pellets and a = 627.72 and b = 0.4125 for wood chips. The function and all measurements for comparison are displayed in Fig. 9. Based on that, it is possible to approximate the operation time in dependence of

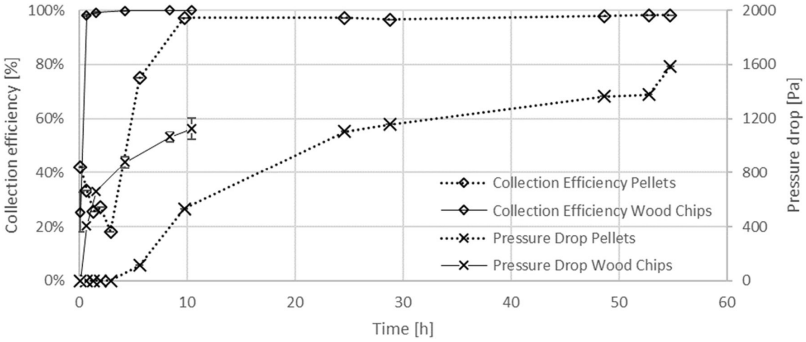

Fig. 7 Pressure drop and collection efficiency of the metal mesh filter. Single run at 33 m/h for pellets and average of 3 runs for wood chips

Table 4 Duration of the phases and overall collection efficiency

	Phase 1	Phase 2	Overall collection efficiency	Maximum pressure drop
m/h	(h)	(h)	(%)	(Pa)
Pellets				
66.6	1.8 ± 0.6	9.9 ± 0.5	75 ± 4	2000
50	3.1 ± 0.5	22.0 ± 3.0	86 ± 1	2000
33.3	4.7	49.3	84	1585
Wood chips				
66.6	0.45 ± 0.1	3.0 ± 0.1	83 ± 1	2000
50	0.58 ± 0.15	5.5 ± 0.4	86 ± 3	2000
33.3	0.35 ± 0.05	10 ± 0.1	91 ± 1	1190–1266

the gas velocity and dust concentration in the flue gas by replacing D with $c_{Dust} * v$ and introducing a linear correction factor for the gas velocity v/50 m/h:

$$t_{max} = \frac{p_{max}}{\left(a\, c_{Dust}\, \frac{v^2}{50\frac{m}{h}}\right)^b}$$

t_{max} maximum operation time (h)
p_{max} maximum pressure drop (Pa)
a, b coefficients from least square approximation
v gas velocity (m/h)
c_{Dust} dust concentration in the flue gas (g/m^3)

Using an average raw gas dust concentration of 7 mg/m^3 for pellets and 49 mg/m^3 for wood chips, the operation time until 2000 Pa pressure drop is reached is displayed in Fig. 10. Using the data, it is possible to determine the optimum filter surface. Depending on the cleaning mode (e.g., shutdown of the furnace and then cleaning or using multiple filters in parallel, which are cleaned one after another enabling continuous operation), the required surface is different.

The composition of the particles is mostly as expected. Given the low concentration of CO and VOC in flue gases, the carbon content is low. While the relative content of carbon in the pellet ash is higher than in the wood chip ash, the absolute concentration in the flue gas is approximately 1.2 mg/m^3, while the concentration in the flue gas from wood chip combustion is approximately 1.1 mg/m^3. This indicates that the generation of dust with compounds incorporating carbon is independent from the amount of aerosol-forming elements and approximately equal for both fuels even though the combustion quality of the wood chips is not as good. However, it is also important to note that not all of the carbon found in dust has to originate from incomplete combustion but can also occur as carbonates of the inorganic compounds like potassium.

In general, the volatile elements (potassium, zinc, sulfur, chloride, sodium) can be found in the fly ash as expected. The biggest constituent is potassium with 47.8 (pellets) and 41.9% (wood chips), followed by chlorine and sulfur.

A more detailed analysis can be found in the supporting information including all elements with a concentration of

Fig. 8 Metal mesh filter before and after cleaning

Table 5 Fly ash composition

	Pellet ash (wt-%)	Wood chip ash (wt-%)	Instrument
C	18.97 ± 1.40	2.31 ± 0.20	Elemental analyzer
H	0.47 ± 0.03	0.36 ± 0.01	Elemental analyzer
N	0.22 ± 0.05	2.56 ± 0.01	Elemental analyzer
Cl	14.7 ± 1.3	25.8 ± 2.9	IC
S	4.8 ± 1.2	4.9 ± 0.8	IC
Ca	1.54 ± 0.02	0.41 ± 0.01	ICP-OES
K	47.83 ± 2.54	41.95 ± 0.79	ICP-OES
Na	0.32 ± 0.01	0.67 ± 0.02	ICP-OES
Zn	3.24 ± 0.11	3.77 ± 0.08	ICP-OES

Elemental concentrations on dry basis

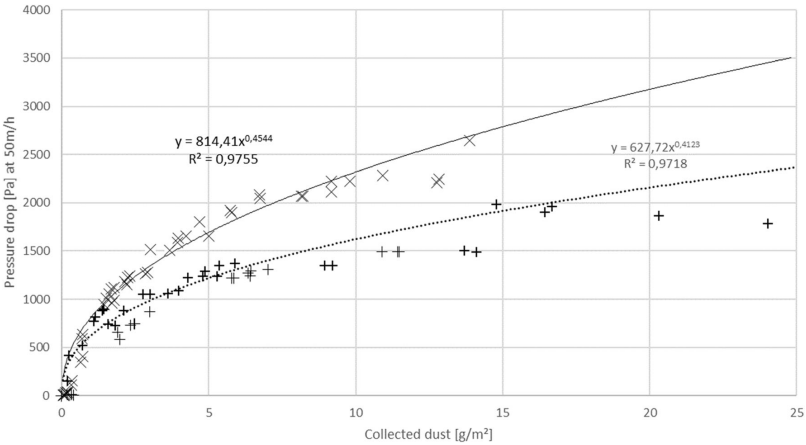

Fig. 9 Model functions of the pressure drop. Solid line: pellets, dotted line: wood chips. Each cross marks an individual measurement. For the regression curve, values below 500 Pa were ignored

more than 500 mg/kg (wood chips: more than 100 mg/kg) in the fly ash.

Cleaning of the filter was expected to be the biggest issue of this work. Instead, the ultrasonic cleaning procedure was successful in all cases. Even after maloperations of the boiler, which caused tar formation, the standard cleaning procedure was sufficient and no additives were required. Given that regeneration by ultrasound cleaning was successful for the first batch of experiments, during the second set of experiments, with the more challenging fuel quality, the filters were only flushed with water and no ultrasound bath was used. It was impossible to detect any efficiency differences between the different cleaning modes, even though the cleaning mechanism of ultrasound and flushing with water are very different. In an ultrasonic bath, cavitation bubbles generate small jets of water directed to the surface and removing any particles as described by Chahine et al [36]. These occur in the entire bath, resulting in a uniform cleaning. At the used frequency, the ultrasound waves cannot penetrate the mesh; however, as the filter cake is on the outside of the candles, that is not necessary.

Cleaning using water is not uniform, as the water flows through the candle. Potentially, it is possible that only parts of the filter cake are removed and the water starts flowing

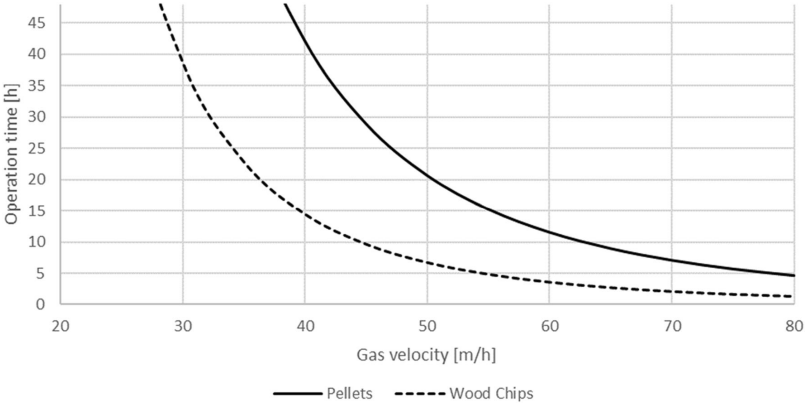

Fig. 10 Operation time until 2000 Pa pressure drop dependent on the gas velocity through the filter

through the already cleaned part of the candle, while the rest of the filter cake remains.

Still, both cleaning modes achieved the same cleaning effect. No residual pressure drop could be recorded after regeneration of the filter. In the supplementary information, the results from the individual test runs in chronological order can be found. No negative trend of the operation time could be recorded during the repetitions at the same gas velocity. Optical inspection of the filter indicates complete removal of the filter cake in all cases. Since it was possible to remove the filter cake after tar generation, the filter can most likely be used during start and stop of the filter. Given that these are phases with very high emissions, that is a major advantage.

Compared with traditional jet-pulse cleaning, the behavior of the filter is different. As discussed by Dittler [30], Hartmann et al. [31], and Schiller and Schmid [33], jet-pulse cleaning results in a residual pressure drop after cleaning. For example, during the experiments of Schiller and Schmid, the residual pressure drop was about 400 Pa. Also, Hartmann et al. reported a residual filter cake after cleaning. In contrast, cleaning using water removes the entire filter cake, resulting in no residual pressure drop. It is also to be noted that, after each cleaning pulse, a considerable amount of dust passes jet-pulse filters, similar to the first phase described here in which the filter cake has to build up. Schwabl et al. [32] state that the separation efficiency of a fabric filter cleaned by jet-pulse depend mostly on the maximum pressure drop, the pressure of the jet-pulse, gas velocity, and cleaning frequency. This is also true for water cleaning; similar to their findings, the separation efficiency increases with lower gas velocity and cleaning frequency, while it improves with a higher maximum pressure drop due to the prolonged phase of filtering.

Another major difference is the resistance against condensation of water or tar. The filter designs discussed by other researchers all require either preheating or a bypass in order to avoid condensation, as condensation would permanently block the filters. During the experiments reported in the present paper, the filter was also preheated in order to avoid the influence of condensation on separation efficiency but not for operational problems. In a commercial application, no preheating is necessary as the cleaning is based on water. Due to the additional mass, which has to be heated up during the start, condensation might occur for a longer time in the exhaust system. Thus, it is necessary to use an appropriate chimney that will not corrode.

5 Conclusion

As shown by the results, fabric filters offer a possibility to limit particulate matter emissions of biomass plants to an absolute minimum and a regeneration using water is feasible. In order to avoid flammability, the application of a metal mesh proved to be feasible. Collection efficiencies exceeding 95% are reached once a filter cake is established. Regeneration using simple flushing is a viable, reliable solution and resulted in a reproducible cleaning without any signs of decay. Flushing of the filter is silent, enabling the use in small household furnaces. It was also possible to demonstrate a nonlinear relationship between gas velocity and time until regeneration of the filter is necessary.

During the buildup phase, penetration of the filter is significant. Thus, the buildup phase has to be limited. A possible option is to decrease the gas velocity and thereby exploiting the nonlinear relationship between gas velocity and pressure drop buildup.

Further research with different biomass is necessary in order to explore the potential of metal mesh filters under more realistic conditions including startups and modulating load. A 3-month test is planned for beginning of 2020 with a commercial prototype. The commercial prototype consists of two modules, thus enabling continuous gas cleaning while one module is regenerated. If very high separation efficiencies are required, another option would be to operate both filters in line directly after cleaning. This would negate the particle slip during build-up of the filter cake but requires additional effort. The commercial prototype is fully automated and, different compared with the current setup, can be used to determine costs. If cleaning without ultrasound proves to be viable over a long period of time, metal mesh filters might be a cost-efficient way to reduce particulate matter emissions to an absolute minimum including start and stop of furnaces. Also, it is required to assess whether an extensive treatment process of the water is required before it can be disposed into the municipal wastewater system.

Author contributions The manuscript was written through contributions of all authors. All authors have given approval to the final version of the manuscript.

Funding Open Access funding provided by Projekt DEAL. The Fachagentur Nachwachsende Rohstoffe (FNR), fund grant number 22019417, funds the project.

References

1. Gaderer M (2016) Abgasreinigung. In: Kaltschmitt M, Hartmann H, Hofbauer H (eds) Energie aus Biomasse, 3., aktualisierte Aufl. 2016. Springer Berlin Heidelberg; Imprint: Springer Vieweg, Berlin, Heidelberg, pp 936–972
2. Lewtas J (2007) Air pollution combustion emissions: characterization of causative agents and mechanisms associated with cancer, reproductive, and cardiovascular effects. Mutat Res 636(1-3):95–133. https://doi.org/10.1016/j.mrrev.2007.08.003
3. Torres-Duque C, Maldonado D, Pérez-Padilla R et al (2008) Biomass fuels and respiratory diseases: a review of the evidence. Proc Am Thorac Soc 5(5):577–590. https://doi.org/10.1513/pats.200707-100RP
4. Arif AT, Maschowski C, Garra P, Garcia-Käufer M, Petithory T, Trouvé G, Dieterlen A, Mersch-Sundermann V, Khanaqa P, Nazarenko I, Gminski R, Gieré R (1994) (2017) Cytotoxic and genotoxic responses of human lung cells to combustion smoke particles of Miscanthus straw, softwood and beech wood chips. Atmos Environ 163:138–154. https://doi.org/10.1016/j.atmosenv.2017.05.019
5. (2019) Erste Verordnung zur Durchführung des Bundes-Immissionsschutzgesetzes (Verordnung über kleine und mittlere Feuerungsanlagen - 1. BImSchV): 1. BImSchV
6. Win KM, Persson T, Bales C (2012) Particles and gaseous emissions from realistic operation of residential wood pellet heating systems. Atmos Environ 59:320–327. https://doi.org/10.1016/j.atmosenv.2012.05.016
7. Schmidl C, Luisser M, Padouvas E, Lasselsberger L, Rzaca M, Ramirez-Santa Cruz C, Handler M, Peng G, Bauer H, Puxbaum H (2011) Particulate and gaseous emissions from manually and automatically fired small scale combustion systems. Atmos Environ 45(39):7443–7454. https://doi.org/10.1016/j.atmosenv.2011.05.006
8. Fatehi H, Li ZS, Bai XS, Aldén M (2017) Modeling of alkali metal release during biomass pyrolysis. Proc Combust Inst 36(2):2243–2251. https://doi.org/10.1016/j.proci.2016.06.079
9. Jokiniemi JK, Lazaridis M, Lehtinen KEJ, Kauppinen EI (1994) Numerical simulation of vapour-aerosol dynamics in combustion processes. J Aerosol Sci 25(3):429–446
10. Lind T, Kauppinen EI, Hokkinen J, Jokiniemi JK, Orjala M, Aurela M, Hillamo R (2006) Effect of chlorine and sulfur on fine particle formation in pilot-scale CFBC of biomass. Energy Fuel 20(1):61–68. https://doi.org/10.1021/ef050122i
11. Fagerström J, Steinvall E, Boström D, Boman C (2016) Alkali transformation during single pellet combustion of soft wood and wheat straw. Fuel Process Technol 143:204–212. https://doi.org/10.1016/j.fuproc.2015.11.016
12. Sippula O, Lind T, Jokiniemi J (2008) Effects of chlorine and sulphur on particle formation in wood combustion performed in a laboratory scale reactor. Fuel 87(12):2425–2436. https://doi.org/10.1016/j.fuel.2008.02.004
13. Olave RJ, Forbes EGA, Johnston CR, Relf J (2017) Particulate and gaseous emissions from different wood fuels during combustion in a small-scale biomass heating system. Atmos Environ 157:49–58. https://doi.org/10.1016/j.atmosenv.2017.03.003
14. Sommersacher P, Brunner T, Obernberger I (2012) Fuel indexes: a novel method for the evaluation of relevant combustion properties of new biomass fuels. Energy Fuel 26(1):380–390. https://doi.org/10.1021/ef201282y
15. Sippula O, Hytönen K, Tissari J, Raunemaa T, Jokiniemi J (2007) Effect of wood fuel on the emissions from a top-feed pellet stove. Energy Fuel 21(2):1151–1160. https://doi.org/10.1021/ef060286e
16. Lamberg H, Tissari J, Jokiniemi J, Sippula O (2013) Fine particle and gaseous emissions from a small-scale boiler fueled by pellets of various raw materials. Energy Fuel 27(11):7044–7053. https://doi.org/10.1021/ef401267t
17. Tran K-Q, Iisa K, Steenari B-M, Lindqvist O (2005) A kinetic study of gaseous alkali capture by kaolin in the fixed bed reactor equipped with an alkali detector. Fuel 84(2-3):169–175. https://doi.org/10.1016/j.fuel.2004.08.019
18. Sommersacher P, Brunner T, Obernberger I, Kienzl N, Kanzian W (2013) Application of novel and advanced fuel characterization tools for the combustion related characterization of different wood/kaolin and straw/kaolin mixtures. Energy Fuel 27(9):5192–5206. https://doi.org/10.1021/ef400400n
19. Bäfver LS, Rönnbäck M, Leckner B, Claesson F, Tullin C (2009) Particle emission from combustion of oat grain and its potential reduction by addition of limestone or kaolin. Fuel Process Technol 90(3):353–359. https://doi.org/10.1016/j.fuproc.2008.10.006
20. Carroll JP, Finnan JM (2015) The use of additives and fuel blending to reduce emissions from the combustion of agricultural fuels in small scale boilers. Biosyst Eng 129:127–133. https://doi.org/10.1016/j.biosystemseng.2014.10.001
21. Gehrig M, Wöhler M, Pelz S, Steinbrink J, Thorwarth H (2019) Kaolin as additive in wood pellet combustion with several mixtures of spruce and short-rotation-coppice willow and its influence on emissions and ashes. Fuel 235:610–616. https://doi.org/10.1016/j.fuel.2018.08.028
22. Gollmer C, Höfer I, Harms D, Kaltschmitt M (2019) Potential additives for small-scale wood chip combustion – laboratory-scale estimation of the possible inorganic particulate matter reduction potential. Fuel 254:115695. https://doi.org/10.1016/j.fuel.2019.115695
23. Gehrig M, Pelz S, Jaeger D, Hofmeister G, Groll A, Thorwarth H, Haslinger W (2015) Implementation of a firebed cooling device and its influence on emissions and combustion parameters at a residential wood pellet boiler. Appl Energy 159:310–316. https://doi.org/10.1016/j.apenergy.2015.08.133
24. Pollex A, Zeng T, Khalsa J, Erler U, Schmersahl R, Schön C, Kuptz D, Lenz V, Nelles M (2018) Content of potassium and other aerosol forming elements in commercially available wood pellet batches. Fuel 232:384–394. https://doi.org/10.1016/j.fuel.2018.06.001
25. Jiao J, Zheng Y (2007) A multi-region model for determining the cyclone efficiency. Sep Purif Technol 53(3):266–273
26. Strassl M, Edelbauer J, Tischler F (2018) Hackschnitzel und Pelletfeuerung von 20kW bis 80kW mit integrierbarem Elektroabscheider. In: Thomas Nussbaumer (ed) 15. Holzenergie-Symposium: Netzintegration, Vorschriften und Feuerungstechnik, pp 111–122
27. Huang S-H, Chen C-C (2002) Ultrafine aerosol penetration through electrostatic precipitators. Environ Sci Technol 36(21):4625–4632. https://doi.org/10.1021/es011157
28. Li Y, Suriyawong A, Daukoru M, Zhuang Y, Biswas P (2009) Measurement and capture of fine and ultrafine particles from a pilot-scale pulverized coal combustor with an electrostatic precipitator. J Air Waste Manage Assoc 59(5):553–559. https://doi.org/10.3155/1047-3289.59.5.553
29. Jaworek A, Krupa A, Czech T (2007) Modern electrostatic devices and methods for exhaust gas cleaning: a brief review. J Electrost 65(3):133–155. https://doi.org/10.1016/j.elstat.2006.07.012
30. Dittler A (2001) Gasreinigung mit starren Oberflächenfiltern - Erscheinungsformen und Auswirkungen unvollständiger Filterregenerierung. Dissertation, Universität Fridericiana zu Karlsruhe
31. Hartmann H, Roßmann P, Turowski P et al. (2007) Getreidekörner als Brennstoff für Kleinfeuerungen: Technische Möglichkeiten und Umwelteffekte. Berichte aus dem TFZ, Straubing
32. Schwabl M, Scheibler M, Schmidl C (2012) Endbericht GoKRT: Experimentelle Entwicklung eines Metallgewebefilters

33. Schiller S, Schmid H-J (2015) Highly efficient filtration of ultrafine dust in baghouse filters using precoat materials. Powder Technol 279:96–105. https://doi.org/10.1016/j.powtec.2015.03.048
34. Struschka M, Goy J (2015) Entwicklung eines kompakten und kostengünstigen Gewebefilters für Biomassekessel. Institut für Feuerungs- und Kraftwerkstechnik (IFK), Universität Stuttgart
35. Yusof NSM, Babgi B, Alghamdi Y, Aksu M, Madhavan J, Ashokkumar M (2016) Physical and chemical effects of acoustic cavitation in selected ultrasonic cleaning applications. Ultrason Sonochem 29:568–576. https://doi.org/10.1016/j.ultsonch.2015.06.013
36. Chahine GL, Kapahi A, Choi J-K, Hsiao CT (2016) Modeling of surface cleaning by cavitation bubble dynamics and collapse. Ultrason Sonochem 29:528–549. https://doi.org/10.1016/j.ultsonch.2015.04.026
37. Lanzerstorfer C (2015) Chemical composition and physical properties of filter fly ashes from eight grate-fired biomass combustion plants. J Environ Sci (China) 30:191–197. https://doi.org/10.1016/j.jes.2014.08.021
38. Tejada J, Grammer P, Kappler A, Thorwarth H (2019) Trace element concentrations in firewood and corresponding stove ashes. Energy Fuel 33(3):2236–2247. https://doi.org/10.1021/acs.energyfuels.8b03732
39. Jaworek A, Czech T, Sobczyk AT, Krupa A (2013) Properties of biomass vs. coal fly ashes deposited in electrostatic precipitator. J Electrost 71(2):165–175. https://doi.org/10.1016/j.elstat.2013.01.009
40. DIN EN 14778:2011, Feste Biobrennstoffe – Probenahme
41. DIN EN 14780:2011, Feste Biobrennstoffe – Probenherstellung
42. DIN EN ISO 18122:2016-03, Biogene Festbrennstoffe_- Bestimmung des Aschegehaltes (ISO_18122:2015); Deutsche Fassung EN_ISO_18122:2015
43. DIN EN ISO 18134-2:2017-05, Biogene Festbrennstoffe_- Bestimmung des Wassergehaltes_-_Ofentrocknung_- Teil_2: Gesamtgehalt an Wasser_- Vereinfachtes Verfahren (ISO_18134-2:2017); Deutsche Fassung EN_ISO_18134-2:2017
44. DIN EN ISO 16994:2016-12, Biogene Festbrennstoffe_- Bestimmung des Gesamtgehaltes an Schwefel und Chlor (ISO_16994:2016); Deutsche Fassung EN_ISO_16994:2016
45. European Pellet Council ENplus Handbook, Version 3.0, 2015: Part 3: Pellet Quality
46. DIN SPEC 33999:2014-12, Emissionsminderung_- Kleine und mittlere Feuerungsanlagen (gemäß_1. BImSchV)_- Prüfverfahren zur Ermittlung der Wirksamkeit von nachgeschalteten Staubminderungseinrichtungen
47. VDI 2066 Blatt 1:2006: Messen von Partikeln - Staubmessungen in strömenden Gasen - Gravimetrische Bestimmung der Staubbeladung

A.1.2. Chemical Analysis

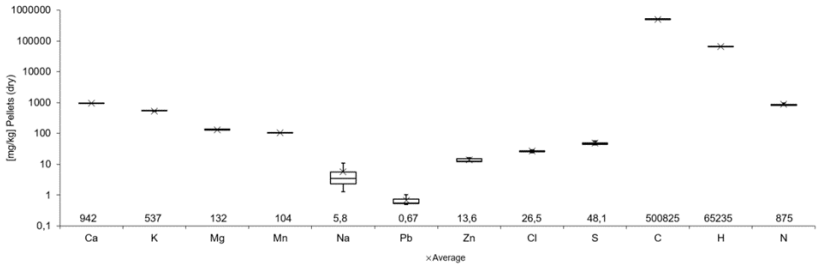

Figure A.1.: Analysis of Pellets, numbers equal the average

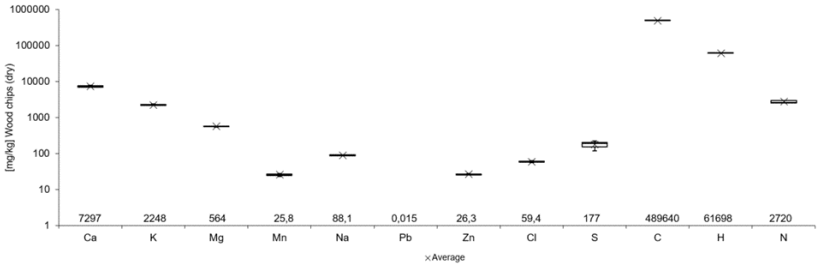

Figure A.2.: Analysis of Wood chips, numbers equal the average

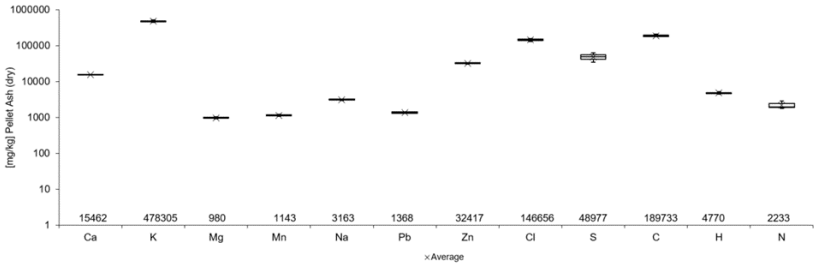

Figure A.3.: Analysis of Pellet ash, numbers equal the average

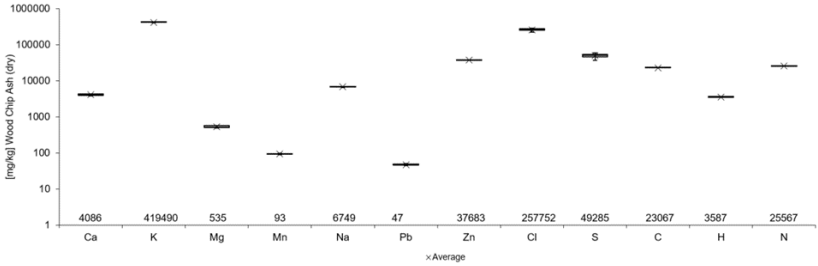

Figure A.4.: Analysis of Wood chip ash, numbers equal the average

A.1.3. Details of experimental runs

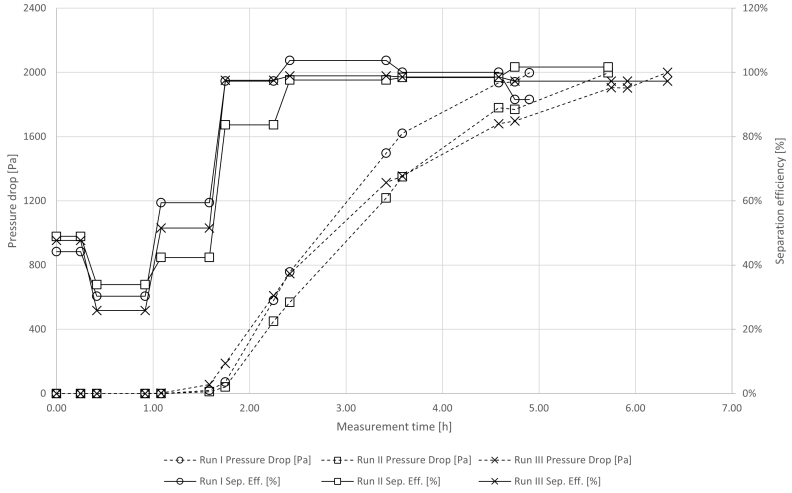

Figure A.5.: First Set of Experiments using Ultrasound cleaning: 3 Runs at 66.6 m/h, Pellets

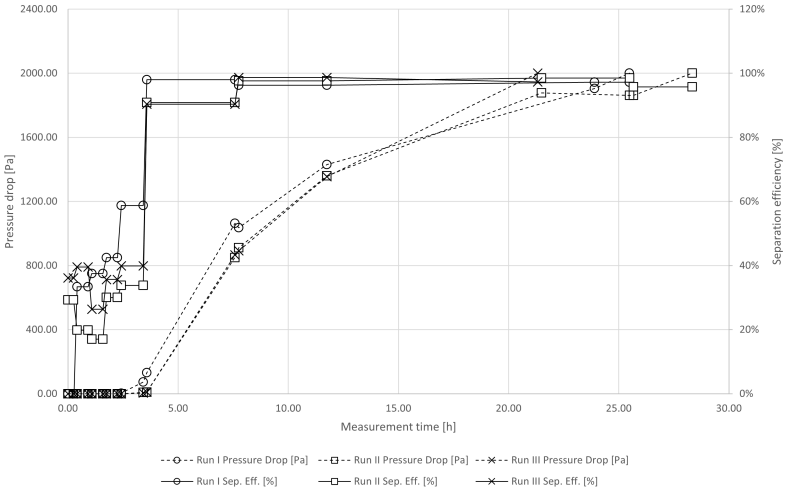

Figure A.6.: Second Set of Experiments using Ultrasound cleaning: 3 Runs at 50 m/h, Pellets

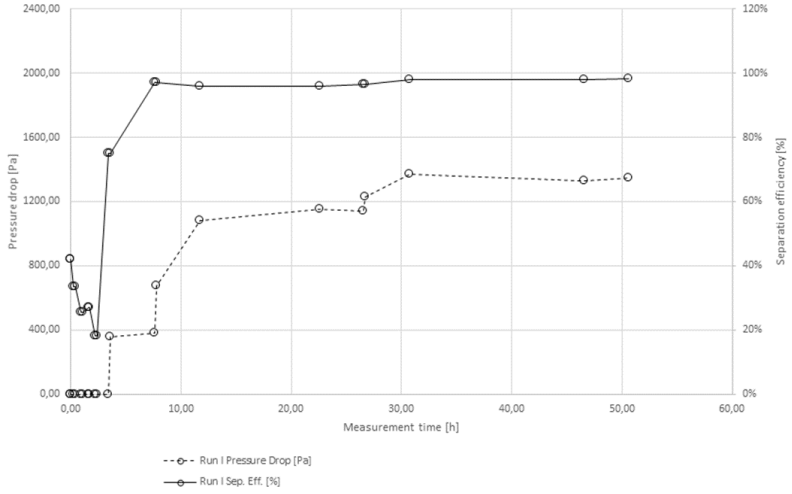

Figure A.7.: Third Set of Experiments using Ultrasound cleaning: 1 Run at 33.3 m/h, Pellets

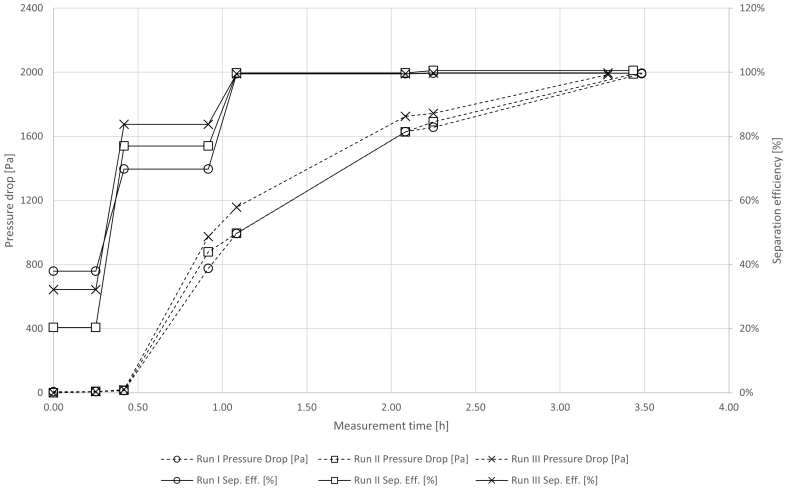

Figure A.8.: First Set of Experiments using Counter-current cleaning: 3 Runs at 66.6 m/h, Wood chips

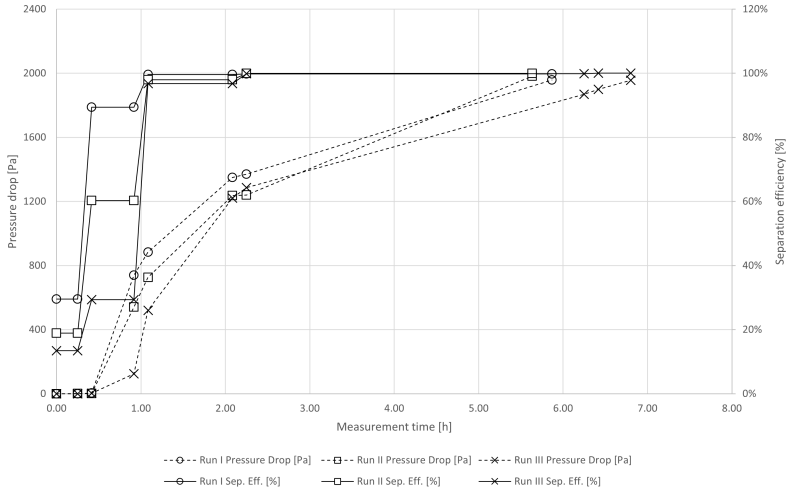

Figure A.9.: Second Set of Experiments using Counter-current cleaning: 3 Runs at 50 m/h, Wood chips

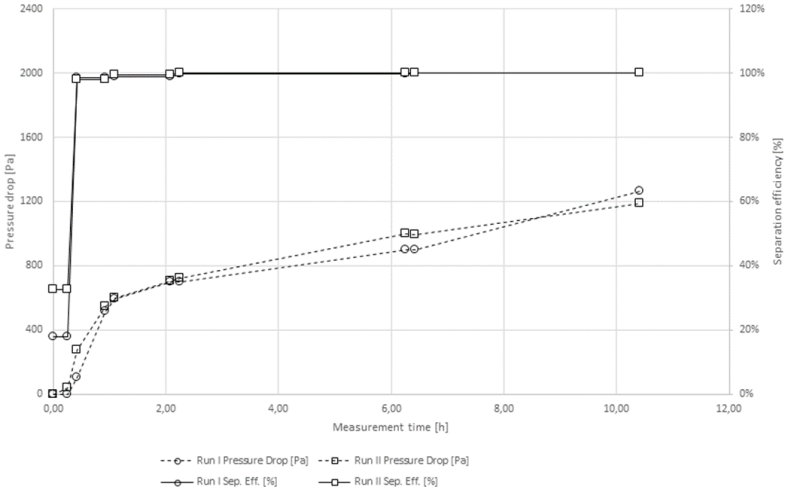

Figure A.10.: Third Set of Experiments using Counter-current cleaning: 2 Runs at 33.3 m/h, Wood chips

A.2. Evaluation of a filter prototype

A.2.1. Scientific publication

Biomass Conversion and Biorefinery
https://doi.org/10.1007/s13399-021-01716-2

ORIGINAL ARTICLE

Evaluation of a metal mesh filter prototype with wet regeneration

Björn Baumgarten[1] · Peter Grammer[1] · Ferdinand Ehard[2] · Oskar Winkel[3] · Ulrich Vogt[4] · Günter Baumbach[4] · Günter Scheffknecht[4] · Harald Thorwarth[1]

Received: 25 February 2021 / Revised: 17 June 2021 / Accepted: 28 June 2021

Abstract
Wood combustion is a major part of the current efforts to reduce CO_2 emissions. However, wood combustion leads to emissions of other pollutants like fine particulate matter. A new option to reduce particulate matter emissions is a metal mesh filter with counter current flushing. An automatic prototype was tested under realistic conditions including starts and stops of the boiler. For regeneration, the filter was flushed using water in opposite flow direction. The water was recycled multiple times to limit water consumption. The results are very promising. Regeneration was successful and no signs of decay could be observed over 419.5 h of operation and 234 regenerations. The filter can be operated during all phases of boiler operation, which is a major step forward compared to alternative secondary measures. Separation efficiency was high with 80–86%, even though the filter showed internal leakage, which reduced the separation efficiency. Additionally, waste products were examined. About 1000 l wastewater can be expected to be produced every month, which could be disposed using the communal waste water system, given the low heavy metal loading. A part of the fine particulate matter is unsoluble and has to be removed from the regeneration water before reuse. The unsoluble fraction contains the majority of heavy metals and has to be disposed as fly ash or used for urban mining. Generally spoken, the metal mesh filter is a new, promising option which can overcome limitations of current secondary measures without increasing costs given its simple and robust construction.

Keywords Biomass combustion · Particulate matter · Emission control · Baghouse filter · Metal mesh filter · Wet regeneration

1 Introduction

The climate change is one of the major challenges of the current time. It is important to limit the release of fossil CO_2 to an absolute minimum. For heating, wood combustion is an obvious and relatively easy to implement solution. Thus, it is a major part of the energy strategy of the European Union [1]. However, during combustion, certain pollutants are generated and can be emitted in comparably high concentrations [2].

One pollutant of special concern is particulate matter and here especially particulate matter with a diameter below 2.5 µm. It is known to be cancerogenic and cause cardiovascular diseases [3–6]. Therefore, the emissions must be limited.

The possibilities to further reduce particulate matter emissions are limited. One former major source, hydrocarbons from incomplete combustion, is mostly eliminated in modern boilers. Instead, the particulate matter mostly consists of the so-called aerosol-forming compounds [7–11].

Highlights
- Metal mesh filters can be regenerated by counter-current water flushing.
- 100% filter availability can be reached without the risk of clogging the filter mesh.
- Overall separation efficiencies between 80 and 86% were reached.

✉ Harald Thorwarth
thorwarth@hs-rottenburg.de

[1] University of Applied Sciences Rottenburg, Schadenweilerhof, 72108 Rottenburg am Neckar, Germany

[2] LK Metallwaren GmbH, Am Falbenholzweg 36, 91126 Schwabach, Germany

[3] Oskar Winkel Filtertechnik, Kaiser-Wilhelm-Ring 30, 92224 Amberg, Germany

[4] University of Stuttgart, Pfaffenwaldring 23, 70569 Stuttgart, Germany

Published online: 16 July 2021

The most important aerosol-forming substances are inorganic substances of potassium, zinc and sodium with chlorine and sulphur. During combustion, the aerosol-forming compounds are evaporated [12]. The aerosol-forming compounds are essential to the growth and for the metabolism of plants, thus their content is especially high in bark and branches [13]. Their content directly correlates with the amount of particulate matter generated [14–16].

A possible solution is to use fuel with low amounts of aerosol-forming compounds. Pollex et al. proposed a limit of 500 mg/kg if the emission limits should be met without the use of other measures [14].

Typically, fuels containing low amounts of aerosol-forming elements (e.g. pellets from sawdust) are relatively expensive. In January 2021, the price for pellets was 236 €/t, while the price for wood chips was between 79 and 123 €/t depending on the water content [17]. Thus, pellets are viable only if the fuel costs are relatively low compared to investments. Also, a possible solution in research is the addition of kaolin and other additives which bind aerosol-forming elements to the bottom ash by forming compounds which are stable at fuel bed temperatures [18–20].

Until now, no fuel with additives is available, due to additional costs involved, increased amount of ash which poses challenges for existing boilers, and nonconformity with current pellet standards [21, 22] (due to the higher ash amount).

Another option is to cool the fuel bed to avoid evaporation of the aerosol-forming compounds [23, 24]. While cooled grates are available for large boilers and for one type of small-scale biomass boiler (ÖKOTHERM [25]), it is still uncommon and associated with higher costs.

For large plants in excess of 1 MW, the usage of low-quality fuel and secondary measures is common. However, for plants between 50 kW and 1 MW, the situation is problematic. Usage of high-quality fuel has a relevant impact on costs, but also the investment for secondary measures is problematic. As theoretical option, the following secondary measures are possible:

Cyclones are currently available (and often in use in boilers exceeding 100 kW), but they only remove coarse particles with aerodynamic diameters above 10 µm [26].

Electrostatic precipitators are a second commercially available option [27]. Commercial electrostatic precipitators have a separation efficiency of 70–80% [28]; however, they are normally only operated once the exhaust gas reaches a sufficient temperature to avoid formation of condensate. Due to frequent start and stops during heat-based operation, this leads to low precipitator availability [29].

Filtering separators are a third option [30], and in wide use for many large-scale applications. For small-scale applications, a commercial option consisting of ceramic filter candles is available [31]. While they obtain very good separation efficiencies (according to the producer, < 3 mg/m^3 particulate matter in filtered gas), they again require a minimum exhaust gas temperature.

A solution using a metal mesh filter with similar restrictions was commercially available, but taken off the market. One reason for this was the required preheating of the filter before the furnace was started to avoid formation of dew [32]. Currently in research are filter solutions which incorporate SCR catalysts to reduce NOx emissions, but like the previous solution require electrical preheating to avoid condensation [33]. Brandelet et al. attempted to optimise the temperature window in which a fabric filter can be operated at a biomass boiler and showed that the current temperature limits are too high, but the issue remains [34].

The solutions mentioned before all have major drawbacks. Special focus for this work was put on cost-effectiveness, and the ability to filter the exhaust gas during all phases of boiler operation. A secondary goal was to construct a filter which shows no need to interact with the boiler, thereby allowing easy retrofitting of existing systems. One possible solution was the use of a metal mesh filter with water-based cleaning. Most of the particulate matter is water soluble, thus, water-based cleaning was expected to be very effective and reliable.

A proof of concept was achieved in a previous work [35]. There, it was shown that metal mesh filters can be an effective solution to limit the particulate matter emissions of wood boilers to a minimum. The main issues discussed above of other particulate matter filters can be avoided. In particular, higher separation efficiencies can be achieved compared to electrostatic separators. Depending on the gas velocity and fuel, separation efficiencies between 91 and 75% were reached. The filtering can be divided in two phases, first, surface filtration is the mode of filtration and separation efficiency is low. Second, after a filter cake has formed, depth filtration is the mode of filtration which results in a separation efficiency up to 99%. Thus, the overall separation efficiency over the entire filtering process must be measured, to correctly evaluate the separation efficiency.

A possible solution to further increase separation efficiency is to use a precoat as tested by Schiller and Schmid, which resulted in very high separation efficiencies. A precoat powder is applied to the filter surface after regeneration, thus, the time until a filter cake is formed is shortened. However, it also requires additional machinery and increases the amount of dust which has to be disposed considerably [36].

In the current work, the batch filter concept from the previous work was upscaled for a 180 kW boiler. Different to the previous filter, two pre-series filter units were constructed with extensive measuring equipment and automation to evaluate long-time operation.

The main purpose of this work is to evaluate the feasibility of the filtering concept under realistic conditions and to assess the waste materials produced. The main focus was

the reliability of the regeneration. Thus, an operation time of about 3–4 h at full load was aimed for. A pre-series model of the filtering system with two filter modules was built and the filter was subjected to a modulating 8 h load cycle including start and stop of the boiler as well as partial load. Theoretical possibilities to simplify the filter system were examined to reduce costs and improve reliability. Main simplifications tested are the removal of a prefiltering cyclone, and the removal of ultrasound assistance for cleaning. The boiler has an integrated multi-cyclone, and the influence of the multi-cyclone on separation efficiency and operation time was evaluated. While ultrasound cleaning was proven to be very effective in the earlier work, a cooling circuit is required to avoid decay of the piezoelectric compounds used to generate ultrasound, as well as an ultrasound transducer and a controller. Thus, it was tested if the ultrasound is required. To do so, one filtering module was equipped with an ultrasound transducer and one was limited to counter-current flushing. Another option is to use a larger mesh to reduce pressure drop caused by the mesh itself.

2 Methods and material

To evaluate the metal mesh filter system, a test rig according to DIN SPEC 33,999 [37] was designed and operated for a total of 419.5 h with 234 regenerations. For generation of the flue gas, a 180 kW boiler was used which burned wood chips obtained from a local distributor.

2.1 Filter prototype

The core of the new filter prototype is two filter cartridges made of metal mesh. The mesh is folded to increase the surface area without increasing required space as shown in Fig. 1. The filter surface of the cartridges is 5 m^2 each.

Two different plain weave meshes made of V2A (1.4301) were used, one with a pore size of 22 µm and one with a pore size of 60 µm.

The filter cartridges were integrated into two separate pre-series filter units, one with, one without ultrasound transducer (SONOPUSH® MONO HD, 2000 W, Weber Ultrasonics). A detailed view and operation scheme is shown in Fig. 2.

During filtering, the raw gas stream enters the filter module on top and passes the metal mesh filter from the inside to the outside (left part of Fig. 2). During regeneration, the module is flooded with water (right part of Fig. 2). Due to the counter current flow of the water from the outside to the inside, the filter cake on the inside of the filter module is removed. In case of the module containing an ultrasound transducer, the ultrasound transducer is also used for 5 min at 2000 W at 25 kHz (maximum power).

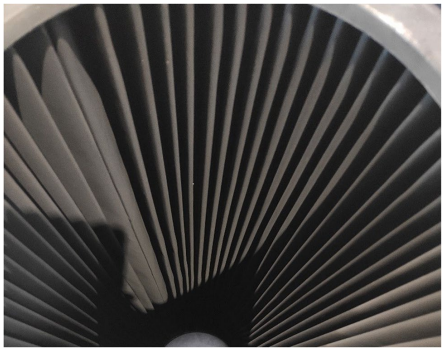

Fig. 1 Inner surface of a filter cartridge

2.2 Experimental setup

The experimental setup consists of a 180 kW boiler, two filter modules (one with, one without ultrasound emitter) with independent measuring sections before and after the respective filter module, a regeneration water reservoir, the required pumps and an additional flue gas fan to overcome the additional pressure drop. The P&ID diagram of the filter can be found in Fig. 3. For temperature measurements, the filter and the measuring sections were equipped with Type K thermocouples. Gas velocity was measured using two calorimetric flow meters (SEIKOM RLSW8AL). Pressure drop was measured using thermokon DPT 2500 differential pressure sensors. The measuring section was designed according to DIN SPEC 33,999 [37], with a diameter of 150 mm and distances between measuring openings as defined in the DIN SPEC to ensure reproducibility.

The filter was controlled using an industrial PLC and all data relevant for operation (temperatures, volumetric flow, pressure drop) were logged by the PLC. In addition, all data were logged using LabView for scientific purposes.

As boiler, a 180 kW grate furnace (Schmid UTSR 180, retrofitted with additional measurement ports and flue gas recirculation) was used. The boiler is a modified commercial boiler with additional thermocouples and exhaust gas recirculation with primary, secondary and tertiary air supply. The boiler was set to an exhaust oxygen concentration of 8.5% at full load and 10% at 30% load. Primary air was set to a fixed amount depending on the thermal output. Secondary and tertiary air was controlled by a lambda sensor. The primary air was diluted with exhaust gas at an approximate ratio of 80:20. Secondary and tertiary air was not diluted. As fuel, wood chips were used during the tests. The boiler is connected to the infrastructure of the University of Applied Sciences Rottenburg, which

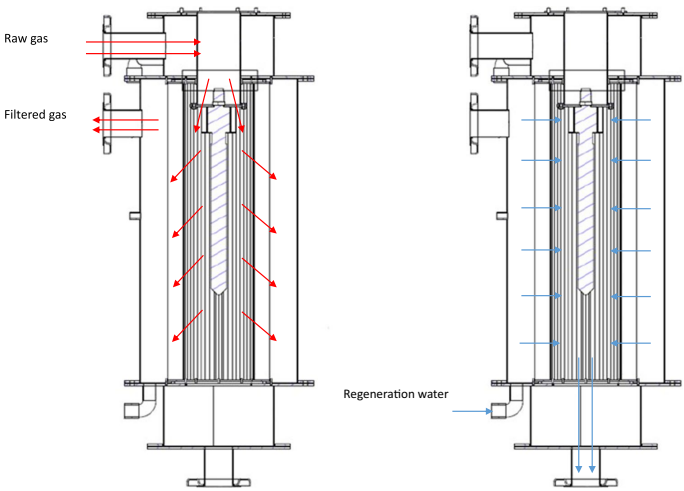

Fig. 2 Scheme and operation of the pre-series filter units

provides cooling water for the boiler at 75 °C and measurement of the thermal output.

2.3 Gaseous analysis

During the test runs, particulate matter concentration of the raw and filtered gas streams were measured according to VDI 2066 [38] under isokinetic conditions. For the measurement, plane quartz fiber filters (Munktell MG 160, diameter: 47 mm) and plugged extra-fine glass wool for prefiltration were used. Filters and glass wool were pre-treated at 200 °C for 1 h and at 180 °C for 1 h after measurement. Cooldown was performed in a desiccator overnight. Measurement of the loading was performed in a climate-controlled room with a lab scale (Sartorius CPA 124S, readability 0.1 mg). Measurement started once a volumetric flow could be detected after regeneration and stopped when the flue gas ventilator stopped (the first step of the automatic regeneration). Also, flue gas composition was logged using a modular measuring tower from ABB (CO, NO, CO_2, SO_2: Uras 26, O_2: Magnos 206, VOC: FIDAS 24). The units were calibrated as specified by ABB before experiments. Before measurement, water was removed from the flue gas by a condenser (ABB). All values given are corrected to standard temperature and pressure (STP).

2.4 Chemical analysis of the fuel, ashes and regeneration water

Fuel and ash samples were taken and prepared according to DIN EN 18,135:2017–08 [39] and 14,780:2020–02 [40]. Sampling of the fuel was achieved by taking 16 samples from the container using a sample scoop which were then mixed and reduced using sample dividers. From the regeneration water, 5 l samples were taking after stirring the reservoir. While replacing the regeneration water, the solid residue formed a slurry which could be removed. The slurry was filtered to remove regeneration water and subsequently dried and mixed.

Moisture content was analysed by drying of 300 g wood chips at 105 °C for 24 h as described in EN ISO 18,134–2:2017 [41].

The dried wood chips were milled to 0.25 mm for further analysis.

Calorific value was obtained according to EN ISO 18,125:2017 [42] by combustion in a calorimeter (C6000, IKA) after pressing a pellet of 1 g. The other solid samples (ashes and the insoluble fraction from regeneration) were also combusted as pre-treatment for IC (Ion chromatography) with the aid of a combustion bag and 250 mg paraffin oil in addition to 100 mg of sample.

After dilution with 50 ml using bi-distilled water, the chloride and sulphur content was analysed using a 883 Basic IC plus (Metrohm) in accordance to EN ISO 16,994:2016–12 [43].

Ultimate analysis was performed using a vario MACRO cube (Elementar) after pressing 40 mg milled fuel sample or 20 mg solid sample and 60 mg of WO_3 and zinc foil into a tablet. Oxygen content was calculated by difference.

Trace elements were analysed using a ICP-OES (inductively coupled plasma atomic emission spectroscopy,

Fig. 3 P&ID diagram

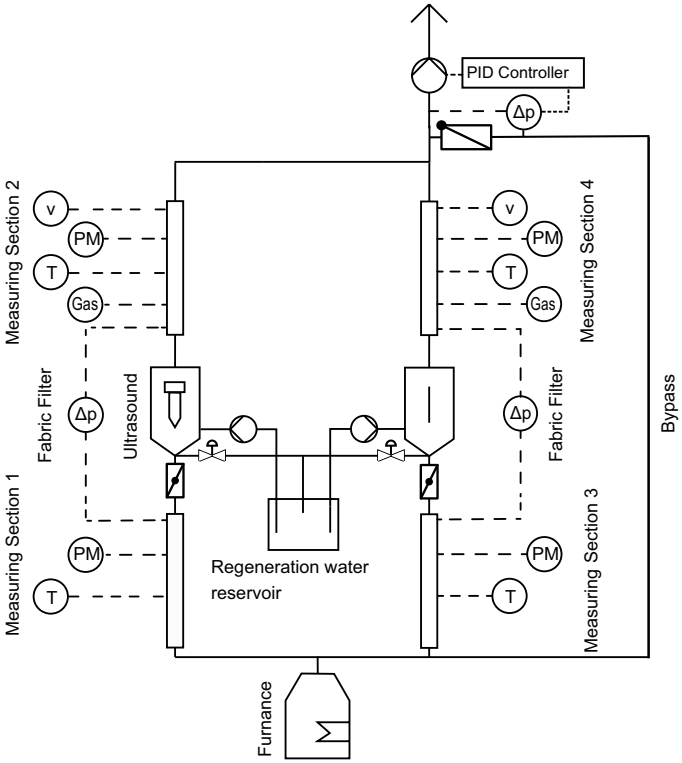

Spectroblue FMX 26, Spectro) after microwave digestion using HCl, HNO_3 and H_2O_2 as described by Tejada et al. in [44].

When disposing the used regeneration water, samples were taken for analysis of both the insoluble, solid fraction and the liquid fraction. The regeneration water was first filtered. The trace elements were measured using the same ICP-OES and IC methods as for the solid samples, but without digestion. Additionally, pH was measured using a pH-meter (Mettler Toleda FE20) and COD (chemical oxygen demand) was measured using a test kit (Macherey–Nagel, Nanocolor CSB 160 and Nanocolor CSB 40).

2.5 Filter testing

Testing of the filter can be separated into two categories:

- First, operation testing was conducted to prove long-time durability of the regeneration method.
- Second, an evaluation of multiple options to reduce costs was done.

2.6 Operation testing

During operation of a boiler, modulating load and start and stops are common, also when a buffer is used [45]. During operation testing, realistic operation of the boiler was simulated by modulating the power output according to 8-h cycles repeated during the day as shown in Fig. 4. The thermal output varied between 30 and 100% and included a stop of the boiler for 1 h during each 8-h cycle. The filter was set to treat the entire exhaust gas stream, also during start and stop phases.

Using the Labview programme which was also used to record data, the desired thermal output was transferred to the boiler using a MODBUS interface.

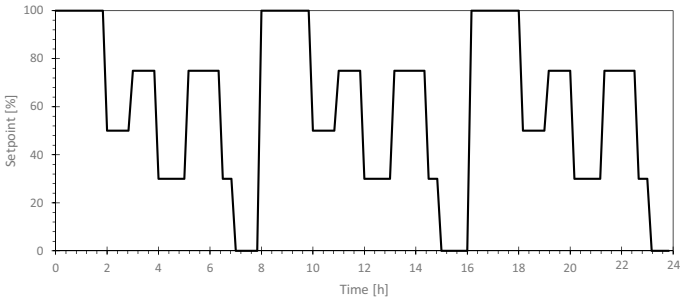

Fig. 4 Thermal output setpoint during operation testing

2.7 Design simplification

For reducing costs of a later series filter, the following options were tested:

- Usage of different metal mesh width
- Usage of ultrasound cleaning
- Usage of a cyclone as pre-filter

Thus, the filter cartridge in the ultrasound module was replaced by a finer mesh (22 µm). For evaluation, test runs as listed in Table 1 were conducted. The first 6 runs were to evaluate the influence of the metal mesh on the separation efficiency and on the operation time, the next two runs for evaluation of ultrasound usage, and the last two runs for evaluation of the cyclone.

Also, the internal construction of the filter was optimised to reduce internal leaks. However, as a side effect, this meant that the filter modules did not dry after cleaning. To avoid the usage of electrical heating, the filters were dried using exhaust gas. The exhaust gas was passed through the inside of the wet filter and filtered in the second filter as shown in Fig. 5.

3 Results

3.1 Fuel properties and raw gas quality

For the investigation, low-quality wood chips from a local supplier were used. Three batches were used during the experiments; their composition can be found in Table 2.

There was a spread in the wood chip quality. First, the water content of the second batch is lower. Second, the amount of aerosol-forming compounds (K, Na, Zn) is lower in batch 3 compared to batch 1 and 2. Batch 3 showed low amounts of which resulted in the lower amounts of trace elements. This results in different raw gas particulate matter concentrations as shown in Fig. 6.

As described earlier, the boiler is set to modulate its thermal output in 8-h cycles as shown in Fig. 4. The boiler automatically limits the rate of change of the thermal output to limit emissions due to rapid changes in output. In Fig. 7, the internal setpoint after smoothening by the boiler PLC and the recorded thermal output is shown, as well as the flue gas temperature before the filter. The change in thermal output is slower than the change in setpoint due

Table 1 Economic optimisation of the filter

Volumetric flow (m^3/h)	Mesh size (µm)	Repetitions	Cyclone	Ultrasound	Fuel	Boiler load
250	60	3	Yes	No	Batch II	100%
250	22	3	Yes	Yes	Batch II	100%
200	60	3	Yes	No	Batch II	100%
200	22	3	Yes	Yes	Batch III	100%
150	60	3	Yes	No	Batch III	100%
150	22	3	Yes	Yes	Batch III	100%
200	22	6	Yes	No	Batch III	100%
200	22	1	Yes	Yes	Batch III	100%
200	60	3	Yes	No	Batch III	100%
200	60	3	No	No	Batch III	100%

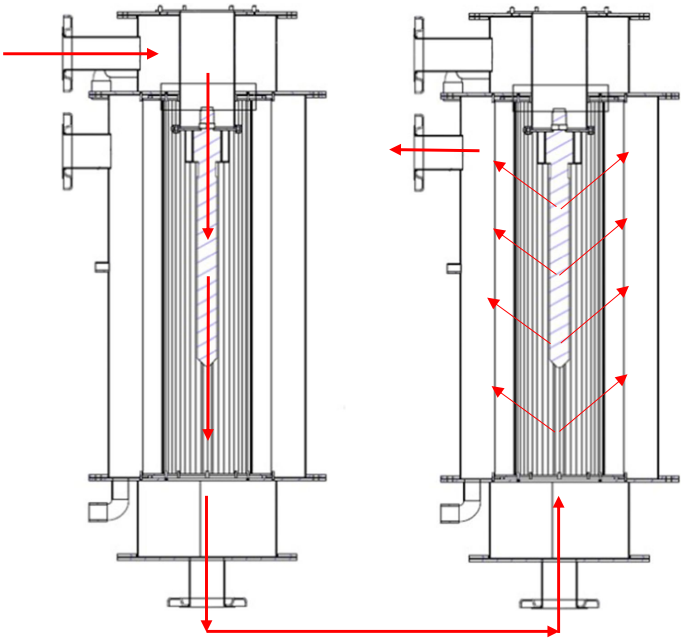

Fig. 5 Drying of the pre-series filter units

Table 2 Composition of the wood chips

Wood chips	Batch I		Batch II		Batch III	
Water content [b]	38.7	wt%	29.03	wt%	35.07	wt%
Lower heating value [b]	18,482 ± 32	J/g d.b	18,600 ± 14	J/g	18,516 ± 15	J/g
Ash content [b]	1.41 ± 0.1	% d.b	1.99 ± 0.2	% d.b	0.70 ± 0.1	% d.b
C [b]	491 ± 3	g/kg d.b	496 ± 3	g/kg d.b	485 ± 3	g/kg d.b
H [b]	64.4 ± 0.9	g/kg d.b	64.8 ± 0.6	g/kg d.b	64.1 ± 0.9	g/kg d.b
N [b]	2.2 ± 0.1	g/kg d.b	2.7 ± 0.2	g/kg d.b	0.9 ± 0.2	g/kg d.b
O	437.2	g/kg d.b	430.3	g/kg d.b	446.9	g/kg d.b
Cl [b]	58.6 ± 1.1	mg/kg d.b	52.3 ± 1.9	mg/kg d.b	57.7 ± 2.3	mg/kg d.b
S [b]	33.5 ± 12	mg/kg d.b	94.6 ± 47.4	mg/kg d.b	38.4 ± 13.0	mg/kg d.b
Ca [a]	3488 ± 71	mg/kg d.b	4479 ± 93	mg/kg d.b	2048 ± 21	mg/kg d.b
K [a]	1785 ± 14	mg/kg d.b	1814 ± 28	mg/kg d.b	1115 ± 4	mg/kg d.b
Na [a]	29 ± 3	mg/kg d.b	46 ± 1	mg/kg d.b	188 ± 10	mg/kg d.b
Zn [a]	12 ± 2	mg/kg d.b	30 ± 2	mg/kg d.b	18 ± 4	mg/kg d.b
Pb [a]	Below limit	mg/kg d.b	6.9 ± 6.1	mg/kg d.b	0.7 ± 0.11	mg/kg d.b

d.b, dry basis. Average ± standard deviation. [a]6 repetitions. [b]3 repetitions

to the large thermal mass of the boiler, but modulating output is achieved which was the main goal. Also, the flue gas temperature decreases to 70 °C when the boiler is shut off, which should be sufficiently low to cause formation of condensate. The short decreases in temperature (e.g. at 3:15) occur during regeneration, while the gas is stagnant in the measuring section.

The gas composition during the cycle is displayed in Fig. 8. The concentrations of CO are dependent on the load. Start, stop and change of the thermal output led to

elevated CO concentrations. The highest measured value was 2022 mg/m^3 during a stop of the boiler (average: 391 mg/m^3). Also, during ignition of the boiler, VOC emissions were measured. Oxygen content is higher as expected, especially during lower loads. In contrast, operation at stable load leads to CO emissions below 400 mg/m^3 and an average of 94 mg/m^3 as shown in Fig. 9. The oxygen concentration is close to the setpoint. VOC emissions could not be detected during operation at 100% load.

3.2 Operation testing

In Fig. 10, the pressure drop and the thermal output of the boiler is displayed for a full day of simulated operation.

During the first and third 8-h cycle, two regenerations were necessary, while during the second cycle, 4 were necessary. After each regeneration, the filters were still wet. While wet, no flue gas can pass through the filters, resulting in a spike in recorded pressure drop of up to 2500 Pa. Minimal pressure drop depended on the gas velocity and

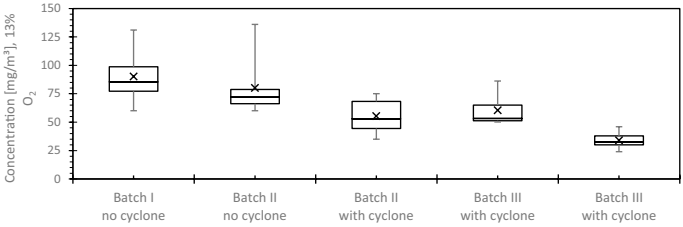

Fig. 6 Raw gas particulate matter concentration. X: average. Whiskers: minimum/maximum value. Box: first quartile, median and third quartile

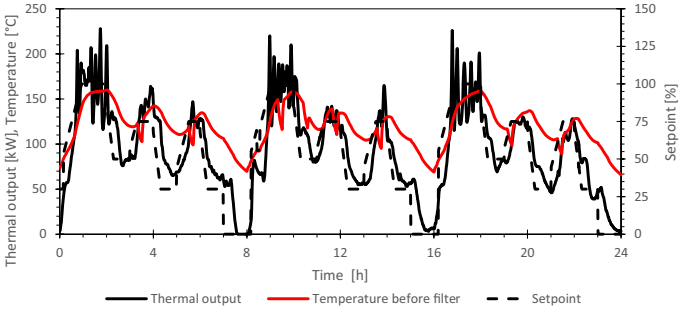

Fig. 7 Thermal output and flue gas temperature during modulating load. 8.4.2020, fuel: batch I

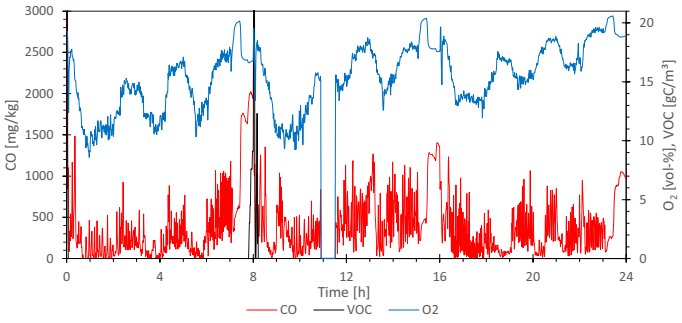

Fig. 8 Flue gas composition during modulating load. 8.4.2020, fuel: batch I

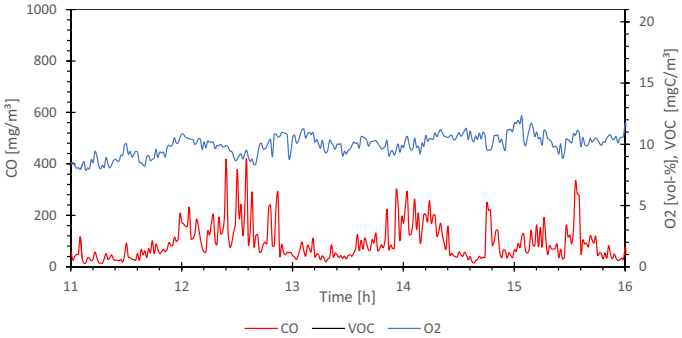

Fig. 9 Flue gas composition at full load. 19.08.2020, fuel: batch III

was around 700 and 1000 Pa. At a medium gas velocity (200 m^3/h), about 300 Pa of the residual pressure drop was caused by the piping, with the rest being caused by the metal mesh.

Regenerations were successful, up to a point where the particle load in the regeneration water reached a certain concentration. After operation for 2 weeks without replacing the regeneration water, the particles suspended in the regeneration water formed a secondary filter cake layer on the outside of the metal mesh, leading to more frequent regenerations as shown in Fig. 11. Estimated from the amount of dust in solution, about 1.35 kg/m^3 solid residue were present in the regeneration water.

Replacement of the regeneration water removed the filter cake and the previous, lower frequency of regeneration could be observed again, without the need for manual cleaning.

While the regeneration itself caused no problems, the separation efficiencies were unexpectedly low as shown in Table 3. This was caused by a significant internal leakage which increased over time during the tests, caused by an inappropriate gasket concept.

Separation efficiency in one of the filter modules decreased below 50%. The filter cartridge was mounted between the top and bottom covers, and the seals used only allowed 2–3 mm of clearance for thermal expansion. This led to compression and deformation of the cartridges. Instead of clamping, a sleeve with a radial seal was used on one side, so that there was sufficient room for thermal expansion.

Before starting the trials for economic optimisation, the construction of the filter was improved to reduce leakages. Also, one of the cartridges with 60 µm mesh openings was removed and replaced with a cartridge with 22 µm mesh openings. The results of these changes are shown in Table 4. Separation efficiency was increased up to 87% and no significant differences between the different mesh sizes could be measured.

However, especially during the later experiments with lower gas velocities, a leakage of about 50 m^3/h could be recorded and separation efficiency decreased.

The leakage becomes apparent when looking at the drying stage. Theoretically, while the metal mesh is still

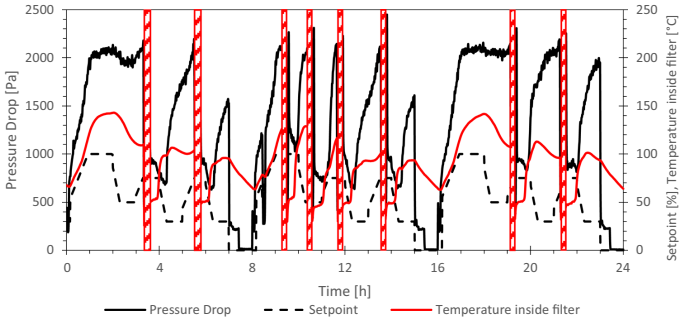

Fig. 10 Long-time measurements of 8.4.2020. Red boxes: regeneration. Fuel: batch I

wet, no gas flow should be registered. Directly after optimisation, the gaskets were tight and no leakage could be detected. However, after several experiments, the gaskets started to leak with the new configuration. In Fig. 12, the leakage flow after optimisation is shown. At approximately 10.52 h, regeneration was complete and the filter automatically started the drying process by setting fan speed to 100%, opening both water valves and closing the raw gas valve of the dry filter module in order to dry the filter as described in Fig. 5. Different from the expected behaviour, at the beginning of the process, about 50 m^3/h passed through the wet module (marked with arrows). This means that at full power of the fan (resulting in a recorded pressure drop of about 2500 Pa), 50 m^3/h pass the filter unfiltered. As drying progresses, the volumetric flow increases. Once it surpasses the set volumetric flow

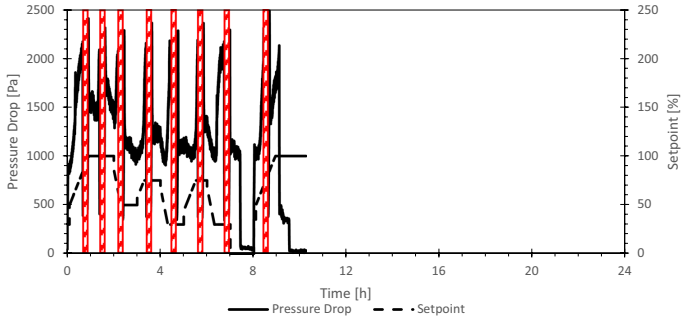

Fig. 11 Effect of particle enrichment in the regeneration water. Operation of the filter was stopped at 9:45 due to short regeneration intervals. Same scale as Fig. 7 for illustration. Red boxes: regeneration. Measured on 26.2.2020. Fuel: batch I

Table 3 Separation efficiencies during commissioning and long-time operation

		Fuel	Raw gas concentration (mg/m^3)[a]	Filtered gas concentration (mg/m^3)[a]	Separation efficiency (%)	Operation time (h)	Repetitions
Commissioning	12.2	Batch I	170 ± 17	35.8 ± 8.3	79	0.9	2
Commissioning	13.2	Batch I	123	22.7	82	0.9	1
Full load	17.2	Batch I	111 ± 13	30.1 ± 6	73	1.2	3
Full load	24.2	Batch I	77.9 ± 44	32.5 ± 22	58	1.6	3
Full load	11.3	Batch I	83.9 ± 25	31.3 ± 5	63	1.2	5
Full load	12.3	Batch I	90.0 ± 6.3	19.6 ± 4	78	1.2	4
Half load	13.3	Batch I	87.4 ± 17	23.9 ± 20	73	1.7	3
Modulating	9.4	Batch I	93.8 ± 15	27.9 ± 8	70	-	3

[a]Adjusted to standard conditions, 13% O_2, in mg/m^3. Repetitions of particulate matter measurements, the boiler and filter were in operation during the entire day

Table 4 Separation efficiency with improved gasket design and different mesh sizes

Volumetric flow (m^3/h)	Mesh size (µm)	Fuel	Raw gas concentration (mg/m^3) [a]	Filtered gas concentration (mg/m^3) [a]	Separation efficiency (%)	Operation time (h)
250	60	Batch II	51 ± 4	9 ± 1	82 ± 2	1.2
250	22	Batch II	46 ± 3	9 ± 2	81 ± 4	1.2
200	60	Batch II	53 ± 15	6 ± 1	87 ± 4	3.5
200	22	Batch III	32 ± 5	4 ± 1	86 ± 5	1.2
150	60	Batch III	39 ± 6	7 ± 1	81 ± 3	3.2
150	22	Batch III	31 ± 1	6 ± 1	80 ± 3	3.2

[a]Adjusted to standard conditions, 13% O_2, in mg/m^3. 3 repetitions per measurement

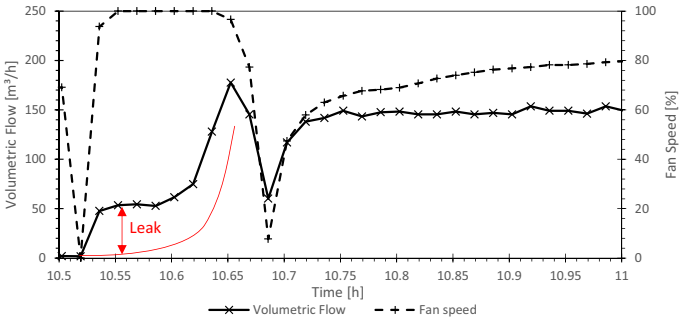

Fig. 12 Leakage during drying, 6.8.2020, 150 m^3/h, red line: expected behaviour without leak, module: 22 µm, fuel: batch III

(here: 150 m^3/h), drying ends and the filter enters normal filtering operation.

Still, given the relatively similar behaviour of both modules, the measurements are still comparable.

3.3 Design simplification

3.3.1 Usage of ultrasound

To examine the effect of the ultrasound transducer, six subsequent runs were performed without the use of the ultrasound transducer, followed by a seventh run after ultrasound cleaning as shown in Table 1. The results are presented in Table 5; the operation time was stable during the runs which indicate consistent, successful cleaning without an accumulation of not-removed filter cake.

3.3.2 Pre-separation by a cyclone-separator

Without cyclone, the raw gas concentration is considerably higher. As the separation efficiency remains unchanged, this results in an equally higher particulate matter concentration in the filtered gas. The operation time is slightly reduced.

3.4 Waste products

As last part of the evaluation, analyses of the waste products were performed. During regeneration, the filter cake is partly dissolved, leading to the formation of both a liquid and solid waste fraction. Analysis was performed on both waste products. During operation, 1000 l of wastewater were disposed per week of operation. Five samples of the regeneration water were analysed (Table 6).

Given the legal limits must be met at all times, the highest concentrations of contaminants measured are given in Table 7 as well as the German limits [46] for heavy metals.

Trace element concentrations for the solid fraction are displayed in Table 6. Three samples were taken and analysed.

4 Discussion

4.1 Fuel properties and raw gas quality

For economic reasons, most boiler operators use the cheapest fuel available. Thus, the fuel chosen for these experiments was also the cheapest fuel available. As expected, the quality of the fuel was rather low, which becomes apparent both during analysis and the emission measurements. The amount of potassium in the fuel is 2–4 times higher than

Table 5 Use of ultrasound transducer and cyclone

	Raw gas concentration (mg/m^3) [a]	Filtered gas concentration (mg/m^3) [a]	Separation efficiency (%)	Operation time (h)
No ultrasound [b]	28 ± 4	5 ± 3	84 ± 12	2.0 ± 0.15
Ultrasound	28	6	78	2.0
Cyclone[c]	34 ± 3	4 ± 1	87 ± 1	2.3 ± 0.03
No cyclone[c]	62 ± 17	8 ± 1	86 ± 3	1.97 ± 0.22

Average ± standard deviation. [a]Adjusted to standard conditions, 13% O_2, in mg/m^3. Operation at full load, fuel: batch III. [b]6 measurements. 22 µm module. [c]3 measurements, 60 µm module

Table 6 Regeneration water composition

	pH	*CSB (mg O_2/l)*	*Potassium (mg/l)*	*Sulfates (mg/l)*	*Chlorides (mg/l)*
Water	6.4–7.6	< 83	< 1210	< 989	< 169
	Cr (mg/l)	*Cu (mg/l)*	*Ni (mg/l)*	*Pb (mg/l)*	*Zn (mg/l)*
Water	< 0.095	< 0.0552	< 0.0225	< 0.0015	< 0.69
Limit (max.)	0.5	0.5	0.5	0.1	1

Highest values from five samples

Table 7 Composition of the insoluble fraction

	C (g/kg)	*H (g/kg)*	*N (g/kg)*	*Cl (g/kg)*	*S (g/kg)*
Insolubles	269 ± 48	16.6 ± 2.7	10.2 ± 2.3	0.2 ± 0.06	1.49 ± 0.1
	Ca (g/kg)	*Fe (g/kg)*	*K (g/kg)*	*Al (g/kg)*	*Mg (g/kg)*
Insolubles	169.4 ± 10	26.7 ± 7.5	12.9 ± 1.1	11.2 ± 1.7	8.9 ± 0.5
	Zn (g/kg)	*Cu (g/kg)*	*Mn (g/kg)*	*Pb (g/kg)*	*Cr (g/kg)*
Insolubles	8.7 ± 0.5	2.2 ± 1.4	2.9 ± 0.1	0.4 ± 0.05	0.3 ± 0.08

Average ± standard deviation. 6 measurements per sample, 3 samples

what would allow operation without secondary measurements according to Pollex et al. [14]. As expected, without secondary measures, the emissions were higher than German legal limits allow. Still, the quality of the fuel must be expected in real operation and thus the filter should be tested in these conditions to reflect real operation.

As shown in Sect. 3.1, gaseous emissions are 4 times higher during modulating operation than during stable load. This is in agreement with literature, which also reports high emissions during start and stop. This behaviour was expected, and given the filter must be reliable under all circumstances, it is important that the filter was operated while the burnout was not optimal and partially unburned hydrocarbons were present in the flue gas.

4.2 Operation testing

Both proposed cleaning methods resulted in reliable, sufficient cleaning over the test period. Based on the previous work, a time span of around 12 h between regenerations was considered the best compromise between cost and separation efficiency. Since the focus was on the reliability of the cleaning, the filter was dimensioned smaller. In total, 234 regenerations were done without problems. If the filter would have been dimensioned with 12 h operating time between regenerations as suggested, this would resemble 2808 h of operation instead of the 419.5 h the filter was operated. Also, the filter was always operated whenever the furnace was used, including ignition and warm-up of the furnace before the trials for evaluation of the mesh size, use of ultrasound, and cyclone. Thus, the conditions the filter was operated in should be close to real operation conditions. In other works, an increase in residual pressure could be recorded after few regenerations (e.g. Schiller and Schmid [47]: 18 regenerations). Still, further trials with longer total operation time should be conducted to proof long-time stability over multiple heating periods.

The most important improvement compared to other particle filters is the ability to operate at all times, even during challenging phases like start-up or stop of the boiler. The filter was generally operated whenever the boiler's exhaust gas ventilator was running, without any regard for exhaust gas temperature. A particularly problematic situation was ignition of the boiler. As shown in Sect. 3.1, high concentrations of CO and VOC were measured during ignition, and the exhaust gas temperature had decreased to 70 °C. Under these circumstances, condensation of both water and partially burned hydrocarbons must be expected.

During regeneration, the filter was regenerated with cold water, which also lead to low surface temperatures and thereby the risk of condensation. Still, cleaning was reliable.

However, it is important to limit the particle load of the regeneration water. Particles in the regeneration water formed a secondary filter cake on the filtered gas side of the metal mesh during regeneration. While it is easily removed once the particle load is reduced to normal levels, measures have to be introduced to remove particles from the regeneration water.

For the test unit, the particles were supposed to be separated using a tank as simple gravity separator. As proven, this is not efficient enough. As intermediate solution, the water was replaced once per week, but the insoluble fraction had to be removed by hand from the bottom of the tank. Thus, this is not an option for continuous use and involves a water consumption of 1 m^3 per week which can and should be avoided.

Thus, a more advanced particle separator like a band filter or a hydro cyclone is required, which enables continuous and automatic operation.

4.3 Separation efficiency

Determination of the separation efficiency over the metal mesh was problematic due to internal leakages of the filter during the operation test. Given a considerable amount of flue gas bypassed the filter, the measured separation efficiency was lower. According to the previous work on

a smaller scale [35], a separation of around 80–90% was expected. As the deformation of the filters progressed and the amount of bypassed gas increased, the separation efficiency decreased to less than 70%.

Before investigating possibilities to reduce costs, the gasket concept was changed as described in Sect. 3.2. Thus, higher separation efficiencies up to 87% were achieved during the later runs, independent on the mesh size. These results are more in line with the previous experiments.

Different to the previous measurements during commissioning and long-time operation testing, the influence of the mesh size was tested using the furnace's cyclone as pre-separator. Thus, and due to the different fuel, the measured raw gas concentration was lower. From literature, it also must be assumed that the particle size distribution changed as cyclones only remove coarse particles measuring multiple µm. However, as shown in the next chapter when discussing the influence of a cyclone, this has no influence on the separation efficiency. Thus, the improved separation efficiency is caused by the improved gasket design and not by using a pre-separator.

The different mesh sizes had no effect on separation efficiency, while the operation time increased due to the lower pressure drop caused by the wider mesh. In general, the operation time is lower than it was expected from the previous work. This is caused by an additional pressure drop of 300 Pa caused by the piping and 300 Pa caused by the filter mesh. In a commercial filter without the need for measuring sections, the pressure drop in the pipes should be lower, but the pressure drop caused by the mesh must be considered during design.

The operation time has a direct influence on the separation efficiency as discussed during the earlier work [35]. Depending on the selected values for gas velocity, a higher separation efficiency can be achieved, for example if this is required to fulfil the requirements for subventions.

4.4 Design simplification

One of the major obstacles when introducing flue gas cleaning technologies, are additional costs. Thus, much emphasis was put on identifying options to reduce costs without reducing the precipitation efficiency of the filter.

The first possible option is using a higher mesh size. Metal meshes with higher pore size have a lower pressure drop, thus requiring less energy and enabling longer operation times. Thus, 22 µm and 60 µm meshes were tested. During the testing, the fuel had to be changed from batch II to III, which caused a decrease in raw gas particulate matter concentration during the 200 m^3/h runs. Still, operation time was longer using the 60 µm mesh (at higher particulate matter concentration) compared to the operation time with 22 µm mesh. At the same time, the operation times in the other cases, where the same fuel was burned for both mesh sizes, are nearly identical. This is a strong indication that not only the concentration but also the composition of the particulate matter influences the operation time. This was also shown in the previous work, where a filter cake of the same weight from pellet combustion proved to cause a higher pressure drop then a filter cake from wood chip combustion. The separation efficiencies of both meshes were nearly identical, thus, the mesh size has a small influence on the filter. Due to the lower inherent pressure drop, a mesh size of 60 µm would be a better option.

While ultrasound cleaning is a cleaning technique which is easy to implement in an automatic system and yields good results, it also involves additional costs and required additional construction and maintenance efforts. The complexity of the filter increases, as an ultrasound transducer and ultrasound generator have to be integrated into the filter. Also, an additional cooling loop is required to avoid decay of the piezoelectric compounds used. However, no benefit of the ultrasound cleaning could be detected compared to counter-current flushing. During the operation test, one of the modules was using ultrasound while the second was not equipped with an ultrasound transducer. No differences could be measured between the modules. Additionally, the module with the mounted ultrasound transducer was operated without ultrasound cleaning for six runs followed by a run with ultrasound cleaning, again with no notable difference. Thus, it can be assumed that ultrasound cleaning has no benefit. Removing it and the cooling circuit for the transducer greatly simplifies the design of the filter and reduces the investment and maintenance efforts.

A third option is prefiltering using a cyclone. Many boilers with a thermal output above 100 kW are equipped with a cyclone, including the 180-kW boiler used for the tests. During the runs, the cyclone reduced the raw gas concentration by nearly half. On the other hand, cyclones only remove coarse particulate matter with a diameter exceeding 10 µm, and cause a significant pressure drop. According to Gaderer et al. [26], up to 1500 Pa pressure drop must be expected. The tested boiler produces about 700 m^3/h flue gas, so over 1.05 kW electrical power (assuming a maximum of 100% efficiency of the fan) is required to overcome the pressure drop of the cyclone, and 1.4 kW for the fabric filter (assuming a maximum of 100% efficiency). As was shown in the previous paper, the operation time and separation efficiency of a metal mesh filter can be improved by increasing the filter surface. Thus, it is recommended to remove existing cyclones or, in case of new boilers, order none to reduce electric power usage and investment costs. Instead, the required filter surface of a metal mesh filter should be based on the raw gas concentration without a cyclone.

4.5 Waste products

Ash from wood combustion contains various toxic elements. Thus, disposal of ash is problematic. In the ash produced during this process, notable amounts of chromium, copper, manganese, lead, iron and nickel were detected.

Most of the toxic compounds form oxides, salts or carbonates with low solubility, resulting in a low concentration of toxic elements in the liquid fraction. Thus, according to the measurements, the liquid fraction can be disposed into the municipal wastewater system. This might be different if contaminated fuels are used, and a measurement should be done to evaluate the regeneration water in these cases.

The solid fraction contains trace elements and heavy metals in high concentrations, thus it has to be disposed like fly ash. Still, the amount of ash is significantly lower compared to conventional precipitation methods, as the soluble part is disposed with the water. Given the high concentrations of valuable metals in the solid fraction, different applications should be evaluated.

5 Conclusion

In total, the metal mesh filter with wet regeneration is a new possibility to reduce fine particulate matter emissions while overcoming limitations of other secondary measures.

Regeneration of the pre-series filter units worked reliable during the entire testing period.

Most importantly, the filter does not require high exhaust gas temperatures to avoid the forming of condensates. Thus, it can be operated at all times, even during start-up at low exhaust gas temperatures. This is a major advantage compared to other secondary measures.

Separation efficiencies of up to 87% could be measured in experiments with stable load and gas velocity. Unfortunately, due to issues with internal leakages, the separation efficiency could not be determined during operation with variable loads, as a significant portion of the gas was bypassed and passed the filter unfiltered.

It could be proven that ultrasound assistance is not required to clean the filter mesh. Thus, the filter only requires ventilation, water pumps and valves which are relatively cheap, simple and reliable equipment. A further possibility to reduce costs is to construct boilers without a cyclone.

A full economic evaluation is not possible using the current knowledge. Given the results from this work, a commercial version would include no ultrasound and no cyclone (or the removal of an existing cyclone). Thus, the required power for ventilation can be assumed to be about 30% higher compared to a conventional boiler with a cyclone. Water costs were negligible from an economic point of view as the consumption was 4000 l/month. With water purification, water consumption should be further reduced. However, a realistic estimate of the construction costs is not possible. The biggest cost factor is the working time, which depends on the final design and the conditions on site. Therefore, a direct comparison with electrostatic precipitators or filtering separators is not possible, also because there is no reliable data for the cost of these.

As next step in the development process, an appropriate measure to remove the solid fraction from the regeneration water has to be integrated into the filter. Also, the gasket design of the pre-series filter units has to be optimized in order to avoid leakages. The current prototype was designed as an experimental setup—the piping and general construction were designed accordingly. For the series version, this must be improved. Instead of the current, spacious construction with large measuring sections, the construction must be as compact as possible while minimising any pressure drop caused by the piping. The series version is intended to consist of multiple modules with a filter unit similar to the pre-series one tested during this work, so the necessary scaling to the boiler output is easy. Regeneration should be performed sequentially, while the other modules still filter the exhaust gas. For very small boilers, a single filter unit might be an option with a different operation concept.

Supplementary Information The online version contains supplementary material available at https://doi.org/10.1007/s13399-021-01716-2.

CRediT author statement Björn Baumgarten: investigation, methodology, validation, conceptualization, writing
Peter Grammer: resources
Ferdinand Ehard: resources, funding acquisition, conceptualization
Oskar Winkel: conceptualization
Ulrich Vogt: conceptualisation, project administration, funding acquisition
Günter Baumbach: conceptualisation, funding acquisition
Günter Scheffknecht: supervision, writing–review and editing
Harald Thorwarth: supervision, writing–review and editing, project administration, funding acquisition

Funding Open Access funding enabled and organized by Projekt DEAL. The Fachagentur Nachwachsende Rohstoffe (FNR), fund grant number 22019417, funds the project.

References

1. Scarlat N, Dallemand J-F, Monforti-Ferrario F et al (2015) Renewable energy policy framework and bioenergy contribution in the European Union–an overview from National Renewable Energy Action Plans and Progress Reports. Renew Sustain Energy Rev 51:969–985. https://doi.org/10.1016/j.rser.2015.06.062
2. Vicente ED, Alves CA (2018) An overview of particulate emissions from residential biomass combustion. Atmos Res 199:159–185. https://doi.org/10.1016/j.atmosres.2017.08.027
3. Lewtas J (2007) Air pollution combustion emissions: characterization of causative agents and mechanisms associated with cancer, reproductive, and cardiovascular effects. Mutat Res 636:95–133. https://doi.org/10.1016/j.mrrev.2007.08.003
4. Torres-Duque C, Maldonado D, Pérez-Padilla R et al (2008) Biomass fuels and respiratory diseases: a review of the evidence. Proc Am Thorac Soc 5:577–590. https://doi.org/10.1513/pats.200707-100RP
5. Arif AT, Maschowski C, Garra P et al (1994) (2017) Cytotoxic and genotoxic responses of human lung cells to combustion smoke particles of Miscanthus straw, softwood and beech wood chips. Atmos Environ 163:138–154. https://doi.org/10.1016/j.atmosenv.2017.05.019
6. Ki-Hyun Kim, Ehsanul Kabir, Shamin Kabir (2015) A review on the human health impact of airborne particulate matter. Environ Int 36–143. https://doi.org/10.1016/j.envint.2014.10.005
7. Nussbaumer T (2003) Combustion and co-combustion of biomass: fundamentals, technologies, and primary measures for emission reduction †. Energy Fuels 17:1510–1521. https://doi.org/10.1021/ef030031q
8. Baumbach G, Winter F, Lenz V et al (2016) Stoffe aus unvollständiger Verbrennung der Hauptbrennstoffbestandteile. In: Kaltschmitt M, Hartmann H, Hofbauer H (eds) Energie aus Biomasse, 3., aktualisierte Aufl. 2016. Springer Berlin Heidelberg; Imprint: Springer Vieweg, Berlin, pp 732–756
9. Carroll JP, Finnan JM, Biedermann F et al (2015) Air staging to reduce emissions from energy crop combustion in small scale applications. Fuel 155:37–43. https://doi.org/10.1016/j.fuel.2015.04.008
10. Kelz J, Brunner T, Obernberger I (2012) Emission factors and chemical characterisation of fine particulate emissions from modern and old residential biomass heating systems determined for typical load cycles. Environ Sci Eur 24:11. https://doi.org/10.1186/2190-4715-24-11
11. Johansson LS, Leckner B, Gustavsson L et al (2004) Emission characteristics of modern and old-type residential boilers fired with wood logs and wood pellets. Atmos Environ 38:4183–4195. https://doi.org/10.1016/j.atmosenv.2004.04.020
12. Knudsen JN, Jensen PA, Dam-Johansen K (2004) Transformation and release to the gas phase of Cl, K, and S during combustion of annual biomass. Energy Fuels 18:1385–1399
13. Thorwarth H, Gerlach H, Rieger L et al (2018) Natürliche Einflüsse auf die Qualität von Holzbrennstoffen und deren Auswirkungen auf den Betrieb von Holz-Heizkraftwerken. VGB Powertech:41–49
14. Pollex A, Zeng T, Khalsa J et al (2018) Content of potassium and other aerosol forming elements in commercially available wood pellet batches. Fuel 232:384–394. https://doi.org/10.1016/j.fuel.2018.06.001
15. Anca-Couce A, Sommersacher P, Hochenauer C et al (2020) Multi-stage model for the release of potassium in single particle biomass combustion. Fuel 280:118569. https://doi.org/10.1016/j.fuel.2020.118569
16. Fatehi H, Li ZS, Bai XS et al (2017) Modeling of alkali metal release during biomass pyrolysis. Proc Combust Inst 36:2243–2251. https://doi.org/10.1016/j.proci.2016.06.079
17. Bruhn K (2021) Entwicklung der Brennstoffpreise von 2011 bis 2021. TFZ-Merkblatt: 21WBr002. Technologie- und Förderzentrum (TFZ)
18. Höfer I, Kaltschmitt M (2017) Effect of additives on particulate matter formation of solid biofuel blends from wood and straw. Biomass Conv Bioref 7:101–116. https://doi.org/10.1007/s13399-016-0217-7
19. Gollmer C, Höfer I, Harms D et al (2019) Potential additives for small-scale wood chip combustion–laboratory-scale estimation of the possible inorganic particulate matter reduction potential. Fuel 254:115695. https://doi.org/10.1016/j.fuel.2019.115695
20. Gehrig M, Wöhler M, Pelz S et al (2019) Kaolin as additive in wood pellet combustion with several mixtures of spruce and short-rotation-coppice willow and its influence on emissions and ashes. Fuel 235:610–616. https://doi.org/10.1016/j.fuel.2018.08.028
21. EUROPÄISCHES KOMITEE FÜR NORMUNG Feste Biobrennstoffe – Brennstoffspezifikationen und -klassen – Teil 2: Holzpellets für nichtindustrielle Verwendung(DIN EN 14961–2:2011)
22. International Organization of Standards (2014) ISO 17225–2:2014: Solid biofuels—fuel specifications and classes—part 2: graded wood pellets 75.160.10
23. Gehrig M, Pelz S, Jaeger D et al (2015) Implementation of a firebed cooling device and its influence on emissions and combustion parameters at a residential wood pellet boiler. Appl Energy 159:310–316. https://doi.org/10.1016/j.apenergy.2015.08.133
24. Pérez-Orozco R, Patiño D, Porteiro J et al (2020) Novel test bench for the active reduction of biomass particulate matter emissions. Sustainability 12:422. https://doi.org/10.3390/su12010422
25. A.P. Bioenergietechnik GmbH (2021) ÖKOTHERM – Compact Biomasse-Heizanlagen. https://oeko-therm.net/de/produkte-service-oekotherm/compact-biomasse-heizanlagen. Accessed 16 Jun 2021
26. Gaderer M (2016) Abgasreinigung. In: Kaltschmitt M, Hartmann H, Hofbauer H (eds) Energie aus Biomasse, 3., aktualisierte Aufl. 2016. Springer Berlin Heidelberg; Imprint: Springer Vieweg, Berlin, pp 936–972
27. Jaworek A, Krupa A, Czech T (2007) Modern electrostatic devices and methods for exhaust gas cleaning: a brief review. J Electrostat 65:133–155. https://doi.org/10.1016/j.elstat.2006.07.012
28. Strassl M, Edelbauer J, Tischler F (2018) Hackschnitzel und Pelletfeuerung von 20kW bis 80kW mit integrierbarem Elektroabscheider. In: Thomas Nussbaumer (ed) 15. Holzenergie-Symposium: Netzintegration, Vorschriften und Feuerungstechnik, pp 111–122
29. Nussbaumer T, Lauber A (2016) Monitoring the availability of electrostatic precipitators (ESP) in automated biomass combustion plants. Biomass Bioenerg 89:24–30. https://doi.org/10.1016/j.biombioe.2016.02.027
30. Singh R, Shukla A (2014) A review on methods of flue gas cleaning from combustion of biomass. Renew Sustain Energy Rev 29:854–864. https://doi.org/10.1016/j.rser.2013.09.005
31. Glosfume Technologies Limited (2021) Glosfume Website. http://www.glosfume.com/biomass-wood-fired-boilers/. Accessed 16 June 2021
32. Schwabl M, Scheibler M, Schmidl C (2012) Endbericht GoKRT: Experimentelle Entwicklung eines Metallgewebefilters. BIOENERGY 2020+. https://energieforschung.at/wp-content/uploads/sites/11/2020/12/GoKRT-Publizierbarer-Endbericht-Final.pdf
33. König M, Eisinger K, Hartmann I et al (2019) Combined removal of particulate matter and nitrogen oxides from the exhaust gas of small-scale biomass combustion. Biomass Conv Bioref 9:201–212. https://doi.org/10.1007/s13399-018-0303-0

34. Brandelet B, Pascual C, Debal M et al (2020) A cleaner biomass energy production by optimization of the operational range of a fabric filter. J Clean Prod 253:119906. https://doi.org/10.1016/j.jclepro.2019.119906
35. Baumgarten B, Grammer P, Ehard F et al (2020) Novel metal mesh filter using water-based regeneration for small-scale biomass boilers. Biomass Conv Bioref. https://doi.org/10.1007/s13399-020-00959-9
36. Schiller S, Schmid H-J (2015) Highly efficient filtration of ultrafine dust in baghouse filters using precoat materials. Powder Technol 279:96–105. https://doi.org/10.1016/j.powtec.2015.03.048
37. DIN SPEC 33999:2014–12, Emissionsminderung_- Kleine und mittlere Feuerungsanlagen (gemäß_1. BImSchV)_- Prüfverfahren zur Ermittlung der Wirksamkeit von nachgeschalteten Staubminderungseinrichtungen
38. VDI 2066 Blatt 1:2006: Messen von Partikeln - Staubmessungen in strömenden Gasen - Gravimetrische Bestimmung der Staubbeladung
39. DIN EN ISO 18135:2017–08, Biogene Festbrennstoffe_- Probenahme (ISO_18135:2017); Deutsche Fassung EN_ISO_18135:2017
40. DIN EN ISO 14780:2020–02, Biogene Festbrennstoffe_- Probenherstellung (ISO_14780:2017_+ Amd_1:2019); Deutsche Fassung EN_ISO_14780:2017_+ A1:2019
41. DIN EN ISO 18134–2:2017–05, Biogene Festbrennstoffe_- Bestimmung des Wassergehaltes_-_Ofentrocknung_- Teil_2: Gesamtgehalt an Wasser_- Vereinfachtes Verfahren (ISO_18134–2:2017); Deutsche Fassung EN_ISO_18134–2:2017
42. DIN EN ISO 18125:2017–08, Biogene Festbrennstoffe_- Bestimmung des Heizwertes (ISO_18125:2017); Deutsche Fassung EN_ISO_18125:2017
43. DIN EN ISO 16994:2016–12, Biogene Festbrennstoffe_- Bestimmung des Gesamtgehaltes an Schwefel und Chlor (ISO_16994:2016); Deutsche Fassung EN_ISO_16994:2016
44. Tejada J, Grammer P, Kappler A et al (2019) Trace element concentrations in firewood and corresponding stove ashes. Energy Fuels 33:2236–2247. https://doi.org/10.1021/acs.energyfuels.8b03732
45. Schön C, Roßmann P, Hartmann H (2019) NOx-Emissionen bei Hackschnitzelwerken in Abhängigkeit von der Brennstoffqualität, 19th edn. Fachkongress für Holzenergie, Würzburg
46. (2020) Federal Republic of Germany, Federal Ministry of Justice and Consumer Protection: Waste Water Ordinance. http://www.gesetze-im-internet.de/abwv/index.html
47. Schiller S, Schmidt H-J (2013) Hocheffiziente Feinstaubabscheidung aus Kleinfeuerungsanlagen mit einem Schlauchfilter. Chem Ing Tec 85:1324–1328. https://doi.org/10.1002/cite.201200114

A.2.2. Chemical Analysis

Table A.1.: Full chemical analysis wood

		Batch I	±	Batch II	±	Batch III	±
LHV	J/kg	18482.55	32.20	18600.05	13.89	18516.80	15.00
Water content	wt-%	38.70	0.37	29.03	0.55	35.07	0.17
C	wt-%	49.19	0.28	49.66	0.24	48.54	0.22
H	wt-%	6.44	0.09	6.48	0.06	6.41	0.09
N	wt-%	0.22	0.01	0.27	0.02	0.09	0.01
Cl	mg/kg	58.63	1.13	52.28	1.91	57.68	2.30
S	mg/kg	33.46	12.07	94.56	47.41	38.43	13.06
Al	mg/kg	71.98	2.67	157.74	6.54	32.28	5.73
B	mg/kg	2.41	0.26	4.44	1.71	< DL	
Ba	mg/kg	17.69	0.30	30.12	0.72	32.27	0.30
Ca	mg/kg	3488.99	71.34	4479.93	93.00	2047.75	21.30
Cr	mg/kg	0.85	0.31	4.92	1.83	0.95	0.04
Cu	mg/kg	0.92	0.12	1.77	0.16	4.25	0.27
Fe	mg/kg	73.62	10.08	177.99	19.10	32.89	4.50
K	mg/kg	1785.00	13.88	1814.17	27.67	1114.74	3.49
Li	mg/kg	3.70	1.71	7.59	1.73	0.77	0.14
Mg	mg/kg	326.70	2.18	643.33	8.37	304.30	2.75
Mn	mg/kg	155.06	2.81	132.69	2.93	42.78	0.43
Mo	mg/kg	0.01	0.01	0.12	0.09	0.04	0.02
Na	mg/kg	28.67	2.60	45.63	1.26	188.38	9.14
Ni	mg/kg	< DL		1.05	0.44	0.36	0.03
Pb	mg/kg	< DL		6.88	6.02	0.69	0.11
Sb	mg/kg	0.02	0.02	0.04	0.03	< DL	
Se	mg/kg	0.59	0.20	1.00	0.48	< DL	
Sr	mg/kg	7.91	0.23	10.89	0.32	10.00	0.35
Ti	mg/kg	2.58	0.47	7.02	0.85	1.44	0.29
V	mg/kg	0.18	0.07	0.35	0.10	0.15	0.12
Zn	mg/kg	12.24	1.48	29.99	1.52	17.51	3.66

< DL: below detection limit

Table A.2.: Full chemical analysis waste water

		24.2.	26.2.	20.07.	17.08.	25.08.
pH		7.57	7.51	7.29	6.44	6.93
CSB	g O_2 / kg	56.00	83.00	14.67	7.00	15.67
Al	mg/kg	< DL	< DL	< DL	< DL	< DL
B	mg/kg	0.94	1.75	0.13	< DL	0.06
Ba	mg/kg	0.11	0.15	0.08	0.10	0.11
Ca	mg/kg	175.40	214.40	76.46	74.87	80.30
Cr	mg/kg	0.06	0.09	0.01	0.01	0.01
Cu	mg/kg	0.06	0.03	< DL	0.01	0.03
Fe	mg/kg	0.01	0.01	< DL	< DL	< DL
K	mg/kg	732.90	1210.00	65.29	58.58	85.64
Li	mg/kg	0.03	0.04	0.03	0.03	0.03
Mg	mg/kg	37.25	45.19	24.30	24.74	25.05
Mn	mg/kg	0.50	0.88	0.39	0.11	0.48
Mo	mg/kg	0.07	0.09	< DL	< DL	< DL
Na	mg/kg	25.73	31.60	19.33	19.48	19.02
Ni	mg/kg	0.01	0.01	0.02	0.02	0.02
Pb	mg/kg	0.001	0.002	< DL	< DL	< DL
Sb	mg/kg	0.006	0.010	< DL	< DL	< DL
Se	mg/kg	0.006	0.011	< DL	< DL	< DL
Sr	mg/kg	0.35	0.40	0.20	0.20	0.20
Ti	mg/kg	0.0008	< DL	< DL	< DL	< DL
V	mg/kg	0.0015	0.0026	< DL	< DL	< DL
Zn	mg/kg	0.49	0.62	0.37	0.70	0.66
Flouride	mg/kg	0.36	0.52	0.26	0.24	0.29
Chloride	mg/kg	113.80	169.23	47.27	43.09	23.38
Nitrite	mg/kg	36.93	68.98	0.41	< DL	< DL
Nitrate	mg/kg	4.52	10.58	50.43	39.18	32.27
Phosphate	mg/kg	4.42	2.96	0.80	< DL	1.20
Sulfate	mg/kg	615.34	989.37	116.02	76.50	127.57

Table A.3.: Full chemical analysis solid residues

		20.07.	±	17.08.	±	25.08.	±
C	wt-%	22.68	0.27	24.61	0.47	33.66	0.75
H	wt-%	1.39	0.19	1.57	0.25	2.03	0.29
N	wt-%	0.75	0.09	1.00	0.01	1.31	0.16
Cl	mg/kg	244.58	30.48	377.92	48.52	260.67	51.70
S	mg/kg	1659.31	342.90	1465.27	323.53	1338.38	233.31
Al	mg/kg	11864.98	292.60	12845.80	201.58	8965.99	323.50
B	mg/kg	223.18	5.71	129.29	5.46	327.70	22.90
Ba	mg/kg	886.99	25.61	913.77	12.90	1010.20	34.70
Ca	mg/kg	181784.28	4994.92	158726.00	2212.00	167594.00	3719.00
Cr	mg/kg	412.37	20.15	442.62	39.97	256.40	19.60
Cu	mg/kg	503.15	14.99	2204.00	20.00	3939.00	159.00
Fe	mg/kg	28511.49	1046.68	34959.95	807.67	16842.77	671.40
K	mg/kg	13880.75	330.84	13418.24	199.36	11352.75	298.00
Li	mg/kg	83.24	13.29	46.11	4.45	61.20	7.77
Mg	mg/kg	9468.50	158.74	9134.00	31.00	8229.50	288.69
Mn	mg/kg	2842.35	31.66	2847.70	34.00	3115.00	110.00
Mo	mg/kg	< DL		< DL		< DL	
Na	mg/kg	1122.02	72.14	1513.00	55.00	1306.00	43.10
Ni	mg/kg	178.76	8.82	182.49	16.80	108.46	5.32
Pb	mg/kg	306.59	8.90	421.70	3.13	396.57	17.00
Sb	mg/kg	< DL		< DL		< DL	
Se	mg/kg	< DL		< DL		< DL	
Sr	mg/kg	463.57	438.43	392.09	1.43	494.90	29.72
Ti	mg/kg	< DL		< DL		< DL	
V	mg/kg	< DL		< DL		< DL	
Zn	mg/kg	9287.94	211.70	8738.00	31.00	8142.75	562.00

Table A.4.: Chemical analysis bottom and filter ash (sampled before regeneration)

		Bottom Ash 17.08.	±	Filter Ash 25.08.	±
C	wt-%	1.76	0.03	13.18	0.19
H	wt-%	0.31	0.05	0.55	0.10
N	wt-%	0.03	0.03	0.27	0.02
Cl	mg/kg	23.04	15.13	5899.53	592.29
S	mg/kg	706.39	125.30	5725.27	1063.89
Al	mg/kg	12387.64	400.49	7214.39	429.78
B	mg/kg	93.55	21.90	327.77	22.90
Ba	mg/kg	1230.35	34.24	954.99	49.50
Ca	mg/kg	331646.31	9203.02	236875.20	12812.00
Cr	mg/kg	53.97	2.75	146.49	10.50
Cu	mg/kg	29.64	4.00	1272.19	85.44
Fe	mg/kg	7473.24	209.24	8294.73	459.95
K	mg/kg	87399.33	2519.62	31354.24	2218.00
Li	mg/kg	188.20	55.66	61.20	7.77
Mg	mg/kg	37665.80	1075.29	17079.25	939.00
Mn	mg/kg	3551.99	82.40	4303.96	219.00
Na	mg/kg	4963.78	179.00	2312.60	155.00
Ni	mg/kg	92.44	5.58	66.59	5.30
Pb	mg/kg	< DL		357.00	15.00
Sr	mg/kg	968.90	33.80	494.90	29.70
Zn	mg/kg	76.09	13.48	11286.00	645.00

A.2.3. List of experimental runs

Table A.5.: Experimental Runs of the 180 kW filter

Date	Operation Time	Regenerations	Fuel	Operation mode
10.02.2020	5.4 h	6	other	(Comissioning) full load
12.02.2020	5.2 h	9	Batch I	(Comissioning) full load
13.02.2020	5.6 h	4	Batch I	(Comissioning) full load
17.02.2020	6.6 h	6	Batch I	full load
18.02.2020	3.5 h	0	Batch I	Furnace malfunction
24.02.2020	14 h	6	Batch I	full load, 30% load
25.02.2020	24 h	12	Batch I	30% load, modulating load
26.02.2020	9.5 h	9	Batch I	modulating load
11.03.2020	5.7 h	4	Batch I	full load
12.03.2020	6.5 h	5	Batch I	full load
13.03.2020	5.6 h	4	Batch I	full load
07.04.2020	13.5 h	5	Batch I	modulating load
08.04.2020	24 h	8	Batch I	modulating load
09.04.2020	11.6 h	5	Batch I	modulating load
	Filter cartridge replacement			
16.04.2020	13 h	15	Batch II	full load
17.04.2020	11.5 h	16	Batch II	full load
21.04.2020	11.2 h	6	Batch II	full load
22.04.2020	24 h	16	Batch II	full load
23.04.2020	13.2 h	8	Batch II	modulating
24.04.2020	12.2 h	5	Batch II	modulating
27.04.2020	7 h	3	Batch II	250 m^3/h
28.04.2020	18 h	10	Batch II	modulating
29.04.2020	15 h	10	Batch II	modulating
04.05.2020	8.3 h	6	Batch II	modulating

Table A.5.: Experimental Runs of the 180 kW filter, Continuation

Date	Operation Time	Regenerations	Fuel	Operation mode
05.05.2020	6.6 h	2	Batch II	200 m³/h
12.05.2020	6.7 h	4	Batch II	250 m³/h
15.05.2020	9.1 h	6	Batch II	150 + 200 m³/h
19.05.2020	6.9 h	2	Batch II	150 + 200 m³/h
29.05.2020	9.4 h	5	Batch II	150 + 200 m³/h
	Gasket replacement			
18.06.2020	2.5 h	2	Batch II	full load
22.06.2020	5.9 h	3	Batch II	250 m³/h
23.06.2020	8.1 h	4	Batch II	200 + 250 m³/h
24.06.2020	19.1 h	3	Batch II	200 m³/h
04.08.2020	7.3 h	3	Batch III	150 m³/h
05.08.2020	7.9 h	4	Batch III	150 + 200 m³/h
06.08.2020	8.2 h	3	Batch III	200 m³/h
11.08.2020	5.7 h	4	Batch III	150 m³/h
12.08.2020	7.4 h	3	Batch III	Ultrasound
13.08.2020	8.9 h	4	Batch III	Ultrasound
18.08.2020	6.3 h	3	Batch III	Cyclone
19.08.2020	7.1 h	3	Batch III	Cyclone
20.08.2020	8.5 h	4	Batch III	Cyclone

Bibliography

[1] J. Gupta. 'A history of international climate change policy'. In: *WIREs Climate Change* 1.5 (2010), pp. 636–653. DOI: https://doi.org/10.1002/wcc.67 (cit. on p. 2).

[2] R. Tschötschel, A. Schuck, A. Wonneberger. 'Patterns of controversy and consensus in German, Canadian, and US online news on climate change'. In: *Global Environmental Change* 60 (2020), p. 101957. DOI: 10.1016/j.gloenvcha.2019.101957 (cit. on p. 2).

[3] T. Rayner, A. Jordan. 'Climate Change Policy in the European Union'. In: *Oxford Research Encyclopedia of Climate Science* (Aug. 2016). DOI: 10.1093/acrefore/9780190228620.013.47 (cit. on p. 2).

[4] S. Proskurina, R. Sikkema, J. Heinimö, E. Vakkilainen. 'Five years left – How are the EU member states contributing to the 20% target for EU's renewable energy consumption; the role of woody biomass'. In: *Biomass and Bioenergy* 95 (2016), pp. 64–77. DOI: https://doi.org/10.1016/j.biombioe.2016.09.016 (cit. on p. 2).

[5] N. Scarlat, J.-F. Dallemand, F. Monforti-Ferrario, M. Banja, V. Motola. 'Renewable energy policy framework and bioenergy contribution in the

European Union – An overview from National Renewable Energy Action Plans and Progress Reports'. In: *Renewable and Sustainable Energy Reviews* 51 (2015), pp. 969–985. DOI: 10.1016/j.rser.2015.06.062 (cit. on p. 2).

[6] M. A. Bari, G. Baumbach, B. Kuch, G. Scheffknecht. 'Wood smoke as a source of particle-phase organic compounds in residential areas'. In: *Atmospheric Environment* 43.31 (2009), pp. 4722–4732. DOI: 10.1016/j.atmosenv.2008.09.006 (cit. on p. 2).

[7] *Gesetz zur Einsparung von Energie und zur Nutzung erneuerbarer Energien zur Wärme- und Kälteerzeugung in Gebäuden (Gebäudeenergiegesetz - GEG)*. Law. Aug. 2020 (cit. on p. 3).

[8] *Erstes Gesetz zur Änderung des Bundes-Klimaschutzgesetzes, Bundesgesetzblatt Teil I Nr. 59 vom 30. August 2021*. Law. Aug. 2021 (cit. on p. 3).

[9] *Erste Verordnung zur Durchführung des Bundes-Immissionsschutzgesetzes. Verordnung über kleine und mittlere Feuerungsanlagen - 1. BImSchV (Germany)*. Law. June 2020 (cit. on pp. 3, 4, 36).

[10] *Richtlinie für die Bundesförderung für effiziente Gebäude – Wohngebäude (BEG WG)*. Law. Sept. 2021 (cit. on p. 4).

[11] *Richtlinie für die Bundesförderung für effiziente Gebäude - Einzelmaßnahmen (BEG EM)*. Law. Sept. 2021 (cit. on p. 4).

[12] L. Rector, P. J. Miller, S. Snook, M. Ahmadi. 'Comparative emissions characterization of a small-scale wood chip-fired boiler and an oil-fired boiler in a school setting'. In: *Biomass and Bioenergy* 107 (2017), pp. 254–260. DOI: https://doi.org/10.1016/j.biombioe.2017.10.017 (cit. on p. 5).

[13] N. Nakićenović. ‘Greenhouse Gas Emissions Scenarios’. In: *Technological Forecasting and Social Change* 65.2 (2000), pp. 149–166. DOI: 10.1016/S0040-1625(00)00094-9 (cit. on p. 5).

[14] A. Cincinelli, C. Guerranti, T. Martellini, R. Scodellini. ‘Residential wood combustion and its impact on urban air quality in Europe’. In: *Current Opinion in Environmental Science & Health* 8 (2019), pp. 10–14. DOI: 10.1016/j.coesh.2018.12.007 (cit. on p. 5).

[15] I. Haberle, Ø. Skreiberg, J. Łazar, N. E. L. Haugen. ‘Numerical models for thermochemical degradation of thermally thick woody biomass, and their application in domestic wood heating appliances and grate furnaces’. In: *Progress in Energy and Combustion Science* 63 (2017), pp. 204–252. DOI: 10.1016/j.pecs.2017.07.004 (cit. on pp. 6, 7).

[16] A. Anca-Couce, P. Sommersacher, C. Hochenauer, R. Scharler. ‘Multi-stage model for the release of potassium in single particle biomass combustion’. In: *Fuel* 280 (2020), p. 118569. DOI: 10.1016/j.fuel.2020.118569 (cit. on pp. 6, 9).

[17] A. Boriouchkine, V. Sharifi, J. Swithenbank, S.-L. Jämsä-Jounela. ‘A study on the dynamic combustion behavior of a biomass fuel bed’. In: *Fuel* 135 (2014), pp. 468–481. DOI: 10.1016/j.fuel.2014.07.015 (cit. on p. 7).

[18] M. A. Gómez, J. Porteiro, D. Patiño, J. L. Míguez. ‘CFD modelling of thermal conversion and packed bed compaction in biomass combustion’. In: *Fuel* 117 (2014), pp. 716–732. DOI: 10.1016/j.fuel.2013.08.078 (cit. on p. 7).

[19] M. A. Gómez, J. Porteiro, D. de La Cuesta, D. Patiño, J. L. Míguez. 'Numerical simulation of the combustion process of a pellet-drop-feed boiler'. In: *Fuel* 184 (2016), pp. 987–999. DOI: 10.1016/j.fuel.2015.11.082 (cit. on p. 7).

[20] G. Baumbach, F. Winter, V. Lenz, I. Höfer, M. Kaltschmitt, T. Nussbaumer. 'Stoffe aus unvollständiger Verbrennung der Hauptbrennstoffbestandteile'. In: *Energie aus Biomasse*. Ed. by M. Kaltschmitt, H. Hartmann, H. Hofbauer. Berlin, Heidelberg: Springer Berlin Heidelberg and Imprint: Springer Vieweg, 2016, pp. 732–756 (cit. on p. 7).

[21] M. Mladenović, M. Paprika, A. Marinković. 'Denitrification techniques for biomass combustion'. In: *Renewable and Sustainable Energy Reviews* 82 (2018), pp. 3350–3364. DOI: 10.1016/j.rser.2017.10.054 (cit. on p. 7).

[22] J. P. Carroll, J. M. Finnan, F. Biedermann, T. Brunner, I. Obernberger. 'Air staging to reduce emissions from energy crop combustion in small scale applications'. In: *Fuel* 155 (2015), pp. 37–43. DOI: 10.1016/j.fuel.2015.04.008 (cit. on p. 8).

[23] L. S. Johansson, B. Leckner, L. Gustavsson, D. Cooper, C. Tullin, A. Potter. 'Emission characteristics of modern and old-type residential boilers fired with wood logs and wood pellets'. In: *Atmospheric Environment* 38.25 (2004), pp. 4183–4195. DOI: 10.1016/j.atmosenv.2004.04.020 (cit. on p. 8).

[24] T. Nussbaumer. 'Combustion and Co-combustion of Biomass: Fundamentals, Technologies, and Primary Measures for Emission Reduction'. In: *Energy & Fuels* 17.6 (2003), pp. 1510–1521. DOI: 10.1021/ef030031q (cit. on p. 8).

[25] J. P. Carroll, J. M. Finnan, F. Biedermann, T. Brunner, I. Obernberger. 'Air staging to reduce emissions from energy crop combustion in small scale applications'. In: *Fuel* 155 (2015), pp. 37–43. DOI: 10.1016/j.fuel.2015.04.008 (cit. on p. 8).

[26] J. Kelz, T. Brunner, I. Obernberger. 'Emission factors and chemical characterisation of fine particulate emissions from modern and old residential biomass heating systems determined for typical load cycles'. In: *Environmental Sciences Europe* 24.1 (2012), p. 11. DOI: 10.1186/2190-4715-24-11 (cit. on p. 8).

[27] J. Lewtas. 'Air pollution combustion emissions: characterization of causative agents and mechanisms associated with cancer, reproductive, and cardiovascular effects'. In: *Mutation research* 636.1-3 (2007), pp. 95–133. DOI: 10.1016/j.mrrev.2007.08.003 (cit. on p. 8).

[28] C. Torres-Duque, D. Maldonado, R. Pérez-Padilla, M. Ezzati, G. Viegi. 'Biomass fuels and respiratory diseases: a review of the evidence'. In: *Proceedings of the American Thoracic Society* 5.5 (2008), pp. 577–590. DOI: 10.1513/pats.200707-100RP (cit. on p. 8).

[29] A. T. Arif, C. Maschowski, P. Garra, M. Garcia-Käufer, T. Petithory, G. Trouvé, A. Dieterlen, V. Mersch-Sundermann, P. Khanaqa, I. Nazarenko, R. Gminski, R. Gieré. 'Cytotoxic and genotoxic responses of human lung cells to combustion smoke particles of Miscanthus straw, softwood and beech wood chips'. In: *Atmospheric environment* 163 (2017), pp. 138–154. DOI: 10.1016/j.atmosenv.2017.05.019 (cit. on p. 8).

[30] H. Thorwarth, H. Gerlach, L. Rieger, M. Schroth, R. Kirchhof, J. Tejada. 'Natürliche Einflüsse auf die Qualität von Holzbrennstoffen und deren

Auswirkungen auf den Betrieb von Holz-Heizkraftwerken'. In: *VGB Powertech* 2018.11 (2014), pp. 41–49 (cit. on p. 9).

[31] H. Fatehi, Z. S. Li, X. S. Bai, M. Aldén. 'Modeling of alkali metal release during biomass pyrolysis'. In: *Proceedings of the Combustion Institute* 36.2 (2017), pp. 2243–2251. DOI: 10.1016/j.proci.2016.06.079 (cit. on p. 9).

[32] T. Torvela, J. Tissari, O. Sippula, T. Kaivosoja, J. Leskinen, A. Virén, A. Lähde, J. Jokiniemi. 'Effect of wood combustion conditions on the morphology of freshly emitted fine particles'. In: *Atmospheric Environment* 87 (2014), pp. 65–76. DOI: 10.1016/j.atmosenv.2014.01.028 (cit. on p. 9).

[33] R. J. Olave, E. Forbes, C. R. Johnston, J. Relf. 'Particulate and gaseous emissions from different wood fuels during combustion in a small-scale biomass heating system'. In: *Atmospheric Environment* 157 (2017), pp. 49–58. DOI: 10.1016/j.atmosenv.2017.03.003 (cit. on p. 10).

[34] P. Sommersacher, T. Brunner, I. Obernberger, N. Kienzl, W. Kanzian. 'Application of Novel and Advanced Fuel Characterization Tools for the Combustion Related Characterization of Different Wood/Kaolin and Straw/Kaolin Mixtures'. In: *Energy & Fuels* 27.9 (2013), pp. 5192–5206. DOI: 10.1021/ef400400n (cit. on p. 10).

[35] O. Sippula, K. Hytönen, J. Tissari, T. Raunemaa, J. Jokiniemi. 'Effect of Wood Fuel on the Emissions from a Top-Feed Pellet Stove'. In: *Energy & Fuels* 21.2 (2007), pp. 1151–1160. DOI: 10.1021/ef060286e (cit. on p. 10).

[36] H. Lamberg, J. Tissari, J. Jokiniemi, O. Sippula. 'Fine Particle and Gaseous Emissions from a Small-Scale Boiler Fueled by Pellets of Various Raw Materials'. In: *Energy & Fuels* 27.11 (2013), pp. 7044–7053. DOI: 10.1021/ef401267t (cit. on p. 10).

[37] A. Pollex, T. Zeng, J. Khalsa, U. Erler, R. Schmersahl, C. Schön, D. Kuptz, V. Lenz, M. Nelles. 'Content of potassium and other aerosol forming elements in commercially available wood pellet batches'. In: *Fuel* 232 (2018), pp. 384–394. DOI: 10.1016/j.fuel.2018.06.001 (cit. on pp. 10, 79).

[38] A. Shiehnejadhesar, R. Mehrabian, C. Hochenauer, R. Scharler. 'The virtual biomass grate furnace - an overall CFD model for biomass combustion plants'. In: *Energy Procedia* 120 (2017), pp. 516–523. DOI: 10.1016/j.egypro.2017.07.189 (cit. on p. 10).

[39] J. Silva, J. Teixeira, S. Teixeira, S. Preziati, J. Cassiano. 'CFD Modeling of Combustion in Biomass Furnace'. In: *Energy Procedia* 120 (2017), pp. 665–672. DOI: 10.1016/j.egypro.2017.07.179 (cit. on p. 10).

[40] M. Obaidullah, S. Bram, V. K. Verma, J. de Ruyck. 'A Review on Particle Emissions from Small Scale Biomass Combustion'. In: *International Journal of Renewable Energy Research* 2012.2 (2012). DOI: 10.20508/IJRER.15633 (cit. on p. 10).

[41] C. Schmidl, M. Luisser, E. Padouvas, L. Lasselsberger, M. Rzaca, C. Ramirez-Santa Cruz, M. Handler, G. Peng, H. Bauer, H. Puxbaum. 'Particulate and gaseous emissions from manually and automatically fired small scale combustion systems'. In: *Atmospheric Environment* 45.39 (2011), pp. 7443–7454. DOI: 10.1016/j.atmosenv.2011.05.006 (cit. on p. 10).

[42] *Solid biofuels - Fuel specifications and classes - Part 1: General requirements (ISO 17225-1:2021); German version EN ISO 17225-1:2021*. Norm. 2021 (cit. on pp. 11, 12).

[43] S. Lesche. *Entwicklung der Brennstoffpreise von 2012 bis 2022. TFZ-Merkblatt: 22WLs002*. Ed. by Technologie- und Förderzentrum. 2022. URL: https://www.tfz.bayern.de/mam/cms08/festbrennstoffe/dateien/merkblatt_entwicklung_der_brennstoffpreise.pdf (visited on 01/01/2023) (cit. on p. 11).

[44] C. Gollmer, I. Höfer, D. Harms, M. Kaltschmitt. 'Potential additives for small-scale wood chip combustion – Laboratory-scale estimation of the possible inorganic particulate matter reduction potential'. In: *Fuel* 254 (2019), p. 115695. DOI: 10.1016/j.fuel.2019.115695 (cit. on p. 11).

[45] K.-Q. Tran, K. Iisa, B.-M. Steenari, O. Lindqvist. 'A kinetic study of gaseous alkali capture by kaolin in the fixed bed reactor equipped with an alkali detector'. In: *Fuel* 84.2 (2005), pp. 169–175. DOI: https://doi.org/10.1016/j.fuel.2004.08.019 (cit. on p. 11).

[46] B.-M. Steenari, O. Lindqvist. 'High-temperature reactions of straw ash and the anti-sintering additives kaolin and dolomite'. In: *Biomass and Bioenergy* 14.1 (1998), pp. 67–76. DOI: 10.1016/S0961-9534(97)00035-4 (cit. on p. 11).

[47] E. Lindström, M. Sandström, D. Boström, M. Öhman. 'Slagging Characteristics during Combustion of Cereal Grains Rich in Phosphorus'. In: *Energy & Fuels* 21.2 (2007), pp. 710–717. DOI: 10.1021/ef060429x (cit. on p. 11).

[48] C. Gilbe, M. Öhman, E. Lindström, D. Boström, R. Backman, R. Samuelsson, J. Burvall. 'Slagging Characteristics during Residential Combustion of Biomass Pellets'. In: *Energy & Fuels* 22.5 (2008), pp. 3536–3543. DOI: 10.1021/ef800087x (cit. on p. 11).

[49] L. Wang, J. E. Hustad, Ø. Skreiberg, G. Skjevrak, M. Grønli. 'A Critical Review on Additives to Reduce Ash Related Operation Problems in Biomass Combustion Applications'. In: *Energy Procedia* 20 (2012). Technoport 2012 - Sharing Possibilities and 2nd Renewable Energy Research Conference (RERC2012), pp. 20–29. DOI: https://doi.org/10.1016/j.egypro.2012.03.004 (cit. on p. 12).

[50] M. Gehrig, S. Pelz, D. Jaeger, G. Hofmeister, A. Groll, H. Thorwarth, W. Haslinger. 'Implementation of a firebed cooling device and its influence on emissions and combustion parameters at a residential wood pellet boiler'. In: *Applied Energy* 159 (2015), pp. 310–316. DOI: 10.1016/j.apenergy.2015.08.133 (cit. on p. 12).

[51] M. Gehrig, D. Jaeger, S. K. Pelz, A. Weissinger, A. Groll, H. Thorwarth, W. Haslinger. 'Influence of firebed temperature on inorganic particle emissions in a residential wood pellet boiler'. In: *Atmospheric Environment* 136 (2016), pp. 61–67. DOI: 10.1016/j.atmosenv.2016.04.018 (cit. on p. 12).

[52] M. Gehrig, M. Wöhler, S. Pelz, J. Steinbrink, H. Thorwarth. 'Kaolin as additive in wood pellet combustion with several mixtures of spruce and short-rotation-coppice willow and its influence on emissions and ashes'. In: *Fuel* 235 (2019), pp. 610–616. DOI: 10.1016/j.fuel.2018.08.028 (cit. on p. 12).

[53] R. Pérez-Orozco, D. Patiño, J. Porteiro, J. L. Míguez. 'Novel Test Bench for the Active Reduction of Biomass Particulate Matter Emissions'. In: *Sustainability* 12.1 (2020), p. 422. DOI: 10.3390/su12010422 (cit. on p. 12).

[54] M. Gaderer. 'Abgasreinigung'. In: *Energie aus Biomasse*. Ed. by M. Kaltschmitt, H. Hartmann, H. Hofbauer. Berlin, Heidelberg: Springer Berlin Heidelberg and Imprint: Springer Vieweg, 2016, pp. 936–972 (cit. on pp. 13, 14, 84).

[55] A. Jaworek, T. Czech, A. T. Sobczyk, A. Krupa. 'Properties of biomass vs. coal fly ashes deposited in electrostatic precipitator'. In: *Journal of Electrostatics* 71.2 (2013), pp. 165–175. DOI: 10.1016/j.elstat.2013.01.009 (cit. on p. 13).

[56] M. Strassl, J. Edelbauer, F. Tischler. 'Hackschnitzel und Pelletfeuerung von 20kW bis 80kW mit integrierbarem Elektroabscheider'. In: *15. Holzenergie-Symposium*. Ed. by Thomas Nussbaumer. 2018, pp. 111–122 (cit. on p. 13).

[57] T. Nussbaumer, F. Winter. 'Stickstoffoxide'. In: *Energie aus Biomasse*. Ed. by M. Kaltschmitt, H. Hartmann, H. Hofbauer. Berlin, Heidelberg: Springer Berlin Heidelberg and Imprint: Springer Vieweg, 2016, pp. 705–716 (cit. on p. 13).

[58] R. Singh, A. Shukla. 'A review on methods of flue gas cleaning from combustion of biomass'. In: *Renewable and Sustainable Energy Reviews* 29 (2014), pp. 854–864. DOI: 10.1016/j.rser.2013.09.005 (cit. on p. 13).

[59] H. Hartmann, P. Roßmann, P. Turowski, F. Ellner-Schuberth, N. Hopf, A. Bimüller. *TFZ Bericht 13. Getreidekörner als Brennstoff für Kleinfeuerungen: Technische Möglichkeiten und Umwelteffekte*. Straubing, 2007. URL: https://www.tfz.bayern.de/publikationen/berichte/234565/index.php (visited on 01/01/2023) (cit. on p. 14).

[60] M. Schwabl, M. Scheibler, C. Schmidl. *Endbericht GoKRT: Experimentelle Entwicklung eines Metallgewebefilters*. Ed. by BIOENERGY 2020+ GmbH. URL: https://energieforschung.at/wp-content/uploads/sites/11/2020/12/GoKRT-Publizierbarer-Endbericht-Final.pdf (visited on 01/01/2023) (cit. on p. 14).

[61] S. Schiller, H.-J. Schmid. 'Highly efficient filtration of ultrafine dust in baghouse filters using precoat materials'. In: *Powder Technology* 279 (2015), pp. 96–105. DOI: 10.1016/j.powtec.2015.03.048 (cit. on pp. 14, 81).

[62] B. Brandelet, C. Pascual, M. Debal, Y. Rogaume. 'A cleaner biomass energy production by optimization of the operational range of a fabric filter'. In: *Journal of Cleaner Production* 253 (2020), p. 119906. DOI: 10.1016/j.jclepro.2019.119906 (cit. on p. 14).

[63] M. König, K. Eisinger, I. Hartmann, M. Müller. 'Combined removal of particulate matter and nitrogen oxides from the exhaust gas of small-scale biomass combustion'. In: *Biomass Conversion and Biorefinery* 9.1 (2019), pp. 201–212. DOI: 10.1007/s13399-018-0303-0 (cit. on p. 14).

[64] M. Struschka, J. Goy. *Schlussbericht zum Vorhaben: Entwicklung eines kompakten und kostengünstigen Gewebefilters für Biomassekessel*. Universität Stuttgart: Institut für Feuerungs- und Kraftwerkstechnik (IFK),

2015. URL: https://heizen.fnr.de/index.php?id=11409&fkz=22031611%22 (visited on 01/01/2023) (cit. on p. 14).

[65] Institut für Feuerungs- und Kraftwerkstechnik (IFK), Hochschule für Fortwirtschaft Rottenburg (HFR), LK Metallwaren GmbH. *Schlussbericht zum Verbundvorhaben: Entwicklung eines kompakten und kostengünstigen Gewebefilters für Biomassekessel – Stufe 2*. URL: https://www.fnr.de/projektfoerderung/projektdatenbank-der-fnr/projektverzeichnis-details?fkz=22019417&cHash=9def05b6d113aa7b2e03d07da935f16e (visited on 12/09/2022) (cit. on pp. 15, 16).

[66] B. Baumgarten, P. Grammer, F. Ehard, O. Winkel, U. Vogt, G. Baumbach, G. Scheffknecht, H. Thorwarth. 'Novel metal mesh filter using water-based regeneration for small-scale biomass boilers'. In: *Biomass Conversion and Biorefinery* (2020), pp. 1–13. DOI: https://doi.org/10.1007/s13399-020-00959-9 (cit. on p. 16).

[67] B. Baumgarten, P. Grammer, F. Ehard, O. Winkel, U. Vogt, G. Baumbach, G. Scheffknecht, H. Thorwarth. 'Evaluation of a metal mesh filter prototype with wet regeneration'. In: *Biomass Conversion and Biorefinery* (2021), pp. 1–16. DOI: 10.1007/s13399-021-01716-2 (cit. on p. 16).

[68] N. S. M. Yusof, B. Babgi, Y. Alghamdi, M. Aksu, J. Madhavan, M. Ashokkumar. 'Physical and chemical effects of acoustic cavitation in selected ultrasonic cleaning applications'. In: *Ultrasonics sonochemistry* 29 (2016), pp. 568–576. DOI: 10.1016/j.ultsonch.2015.06.013 (cit. on p. 17).

[69] G. L. Chahine, A. Kapahi, J.-K. Choi, C.-T. Hsiao. 'Modeling of surface cleaning by cavitation bubble dynamics and collapse'. In: *Ultrasonics sonochemistry* 29 (2016), pp. 528–549. DOI: 10.1016/j.ultsonch.2015.04.026 (cit. on p. 18).

[70] *DIN SPEC 33999. Emission control - Small and medium-sized firing systems (according to 1. BImSchV) - Test method for the determination of the efficiency of downstream dust separators*. Norm. Dec. 2014 (cit. on pp. 28, 29, 61).

[71] *VDI 2066 Page 1. Particulate matter measurement - Dust measurement in flowing gases - Gravimetric determination of dust load*. Norm. May 2021 (cit. on p. 29).

[72] *DIN EN 14778:2011-09 Solid biofuels - Sampling*. Norm. Sept. 2011 (cit. on p. 31).

[73] *DIN EN 14780:2011 Solid biofuels - Sample preparation*. Norm. Sept. 2011 (cit. on p. 31).

[74] *ISO 18125:2017 Solid biofuels — Determination of calorific value*. Norm. Apr. 2017 (cit. on p. 31).

[75] *ISO 16994:2016 Solid biofuels — Determination of total content of sulfur and chlorine*. Norm. Dec. 2016 (cit. on p. 31).

[76] *ENplus Handbook. Part 3: Pellet Quality Requirements. Version 3.0*. Norm. Aug. 2015. URL: https://www.enplus-pellets.eu/en-in/resources-en-in/technical-documentation-en-in.html#handbook (visited on 12/09/2022) (cit. on p. 34).

[77] *Certification Scheme Wood Pellets class A1 in accordance with DIN EN ISO 17225-2 (A1)*. Norm. Nov. 2021. URL: https://www.dincertco.de/din-certco/en/main-navigation/products-and-services/certification-of-products/fuels/wood-pellets-for-central-heating-boilers/ (visited on 12/09/2022) (cit. on p. 34).

[78] *Federal Republic of Germany, Federal Ministry of Justice and Consumer Protection: Waste Water Ordinance.* Law. June 2020. URL: http://www.gesetze-im-internet.de/abwv/index.html (visited on 12/09/2022) (cit. on p. 78).

[79] E. Mayer, J. Eichermüller, F. Endriss, B. Baumgarten, R. Kirchhof, J. Tejada, A. Kappler, H. Thorwarth. 'Utilization and recycling of wood ashes from industrial heat and power plants regarding fertilizer use'. In: *Waste Management* 141 (2022), pp. 92–103. DOI: https://doi.org/10.1016/j.wasman.2022.01.027 (cit. on p. 85).